Degradation Phenomenon of Cementitious Materials under Sulphuric Acid Attack

Lei Gu
M.E. Civil and Structural Engineering

Thesis submitted in fulfilment of the requirements for the degree of Doctor of Philosophy

The University of Adelaide
Faculty of Engineering, Computer and Mathematical Sciences
School of Civil, Environmental and Mining Engineering

September, 2018

This thesis is dedicated to my beloved wife and parents.

Degradation Phenomenon of Cementitious Materials under Sulphuric Acid Attack

By:
Lei Gu

Supervised by:
Terry Bennett, *Ph.D., Senior Lecturer,*
School of Civil, Environmental & Mining Engineering,
The University of Adelaide

Phillip Visintin, *Ph.D., Senior Lecturer,*
School of Civil, Environmental & Mining Engineering,
The University of Adelaide

Thesis submitted in fulfilment of the requirements for the degree of
Doctor of Philosophy

School of Civil, Environmental & Mining Engineering
Faculty of Engineering, Computer and Mathematical Sciences
The University of Adelaide
North Terrace, Adelaide, SA 5005, Australia
Tel: +61(8) 8313 4183
Fax: +61(8) 8313 4359
Email: lei.gu@adelaide.edu.au

Copyright© Lei Gu, September, 2018

Contents

Abstract ii
Statement of Originality iv
Declaration v
List of Publication vi
Acknowledgments vii
Chapter 1. Introduction and General Overview 1
Objectives of research 2
Outline of the thesis 3
Chapter 2. Journal Paper 1 – The Behaviour of Concretes with Different Exposure Regimes and Chemical Concentrations 5
Introduction 5
List of manuscripts 5
Evaluation of accelerated degradation test methods for cementitious composites subject to sulfuric acid attack; application to conventional and alkali-activated concretes 7
Chapter 3. Journal Paper 2 – Long-term Behaviour of Concretes and Evaluation of Measurement Technique 48
Introduction 48
List of manuscripts 48
Sulphuric acid exposure of conventional concrete and alkali-activated concrete: assessment of test methodologies 50
Chapter 4. Journal Paper 3 – Degradation Mechanism of Chemical Reaction and Scale of Manufacture 77
Introduction 77
List of manuscripts 77
A multiscale approach to investigating the resistance of cementitious materials to the sulphuric acid exposure: the degradation mechanism of chemical reaction and scale of manufacture 79
Chapter 5 – Conclusions and Future Work 117
Thesis outcomes 117
Scope for future work 118

Abstract

Sulphuric acid corrosion of Ordinary Portland Cement (OPC) based materials has attracted significant attention in recent decades, both as a result of its widespread occurrence in aggressive environments and the substantial economic impact of the resulting damage.

At the same time, the development of alkali-activated (AA) cementitious materials that have been reported to have considerably improved durability-related properties has significantly increased. Alkali-activated cementitious materials are expected to have higher sulphuric acid resistance than that of OPC based materials and investigations on understanding the behaviour of OPC based and AA cementitious materials under sulphuric attack therefore of great research interest. The agglomeration of a global database of test results is complicated by the differing test methodologies employed in each study which makes it very difficult to compare the relative results of studies performed as part of septate experimental campaigns. To better utilise the results of existing and new experimental studies and to be able to compare the results across different types of material there is a need to assess and understand the results obtained from a range of test methodologies applies to for a range of cementitious composite materials. This thesis contains a series of journal papers in which the methodologies commonly applied in the literature have been further assessed and the degradation mechanisms under sulphuric acid attack of both OPC based and AA cementitious materials at the paste, mortar, and concrete levels have been investigated.

In the assessment of test methodologies of OPC and AA concrete under sulphuric acid attack, the behaviour of concretes with different exposure regimes (continuous immersion, brushing, and wetting and drying cycling) and chemical concentrations (1% and 3% w/w) have been investigated such that the influence of test methodology on degradation rate and microstructural performance can be identified. The results show that the OPC and AA concrete subjected to increased acid concentration displays the most rapid degradation. The indicators of susceptibility to corrosion (acid consumption, change of mass, length, compressive strength, and cross-section) are also discussed based on their potential advantages and limitations as well as application to both OPC based and AA cementitious materials. The results show that there is no single universal indicator of resistance to sulphuric acid that could be applied as a simple test technique for both materials. Through these assessments of the test methods and

measurement technique, it shows that a test procedure to indicate the susceptibility of concretes can be performed within a reasonable time frame for standard testing.

In the investigation of degradation mechanism of OPC based and AA cementitious materials under sulphuric acid attack, the physical, mechanical properties, and the chemical and microstructural characteristics of cementitious materials have been analysed over time. A multiscale approach has been established to understanding how cementitious materials respond to the external acidic environment in terms of scale of manufacture (paste to mortar to concrete) and in levels of observation from microscopic to macroscopic measurements. The investigation of paste behaviour shows a clear chemical response of OPC and AA paste exposed to sulphuric acid. The contradictory degradation mechanism of OPC and AA paste identified in the previous studies have been investigated. The investigation of mortar shows that the presence of fine aggregate and interfacial transition zone between the paste and fine aggregate causes change in porosity of the mortar, affecting the resistance of mortar to sulphuric acid. Finally, the investigation of concrete shows that the chemical composition of coarse aggregate has significant effects on the degradation mechanism.

Statement of Originality

I, **Lei Gu**, hereby declare that this work contains no material which has been accepted for the award of any other degree or diploma in any university or other tertiary institution in my name and, to the best of my knowledge and belief, contains no material previously published or written by another person, except where due reference has been made in the text. In addition, I certify that no part of this work will, in the future, be used in a submission in my name, for any other degree or diploma in any university or other tertiary institution without the prior approval of the University of Adelaide and, where applicable, any partner institution responsible for the joint award of this degree.

I give consent to this copy of my thesis when deposited in the University Library, being made available for loan and photocopying, subject to the provisions of the Copyright Act 1968.

The author acknowledges that copyright of published works contained within this thesis resides with the copyright holder(s) of those works.

I also give permission for the digital version of my thesis being made available on the web, via the University's digital research repository, the Library catalogue, the Australian Digital Thesis Program (ADTP) and also through web search engines, unless permission has been granted by the University to restrict access for a period of time.

..... 5/9/2018

Lei Gu Date

Declaration

I, **Lei Gu**, certify that this work contains no material which has been accepted for the award of any other degree or diploma in my name, in any university or other tertiary institution and, to the best of my knowledge and belief, contains no material previously published or written by another person, except where due reference has been made in the text. In addition, I certify that no part of this work will, in the future, be used in a submission in my name, for any other degree or diploma in any university or other tertiary institution without the prior approval of the University of Adelaide and where applicable, any partner institution responsible for the joint-award of this degree. I acknowledge that copyright of published works contained within this thesis resides with the copyright holder(s) of those works. I also give permission for the digital version of my thesis to be made available on the web, via the University's digital research repository, the Library Search and also through web search engines, unless permission has been granted by the University to restrict access for a period of time. I

..... 5/9/2018

Lei Gu Date

List of Publication

Gu, L., Visintin, P. and Bennett, T., 2018. Evaluation of accelerated degradation test methods for cementitious composites subject to sulfuric acid attack; application to conventional and alkali-activated concretes. *Cement and Concrete Composites, 87*, pp.187-204.

Gu, L., Bennett, T. and Visintin, P., 2018. Sulphuric acid exposure of conventional concrete and alkali-activated concrete: assessment of test methodologies. Submitted to *Construction and Building Materials.*

Gu, L., Visintin, P. and Bennett, T., 2018. A multiscale approach to investigating the resistance of cementitious materials to the sulphuric acid exposure: the degradation mechanism of chemical reaction and scale of manufacture. To be submitted to *Cement and Concrete Research.*

Acknowledgments

I would like to express my special appreciation and thanks to my supervisors Dr. Terry Bennett and Dr. Phillip Visintin. I would like to thank you for encouraging my research and for allowing me to grow as a research scientist. Your advice on both research as well as on my career have been priceless.

I would like to acknowledge the support of the technician team. Particular thanks are given to Mr. Jon Ayoub, Mr. Dale Hodson, Mr. Ian Ogier, Mr. Ian Cates, Mr. Gary Bowman and Mr. Simon Golding. Without your support, the experiment work in this presented thesis would not be possible.

Finally, I would like to acknowledge the support of my family. To my wife Zhiyun Liu for her love and continuous support. To my parents and parents-in-law for their support and encouragement.

Chapter 1. Introduction and General Overview

The rapid increase in the rate of industrialization and urbanization has led to a great worldwide demand for concrete. However, serious problems of concrete degradation have been caused due to the lack of understanding about the long-term performance of concrete and impacts of aggressive environments. One of the most rapid cases of Ordinary Portland Cement (OPC) concrete degradation occurs when the material is exposed to sulphuric acid attack, which generally occurs in various branches of industry, agriculture, and wastewater infrastructure. The increasing rehabilitation costs has resulted in enormous challenges for current OPC concrete structures in aggressive environments. Thus, cementitious materials with high resistance to sulphuric acid are needed to improve the service life of concrete.

As one of the alternative materials to OPC concrete, the development of alkali-activated (AA) concrete with considerably improved durability-related properties has significantly been increased recently. AA cementitious materials are expected to have higher sulphuric acid resistance than that of OPC based materials due to the different chemical composition of the matrix materials. Thus, there has been interest in using AA cementitious materials to resist the sulphuric acid attack.

During the past two decades, a series of studies have been undertaken to understand the behaviour of conventional OPC and AA concrete under sulphuric acid attack. However, in the previous studies, a wide range of test variables have been employed and it is very difficult to directly compare results with large scatter in variables, such as sample size, chemical concentration, exposure regime and the measurements performed. A reliable, yet simple measurement technique to indicate the level of degradation is desirable for a unified test methodology which may be applied to all types of cementitious materials. To accommodate this demand, the evaluation of the methodologies of sulfuric acid corrosion for a range of cementitious composite materials is therefore of great interest. It is envisaged that this work will provide the basis for further development of a unified test methodology to indicate the susceptibility of a wide range of cementitious materials to sulphuric acid attack.

The behaviour of cementitious materials, subject to sulphuric acid exposure, involves the complex interactions of chemical reactions, transport processes and response under applied stress, which is further complicated with scale issues as which can affect a materials efficacy

against degradation. In the previous studies, the results obtained from cementitious materials under sulphuric acid attack were not expected to be similar, and in some cases were even in direct contrast. Therefore a multiscale approach to understanding how cementitious materials respond to the external acidic environment is required, both in terms of scale of manufacture (paste to mortar to concrete) and in levels of observation from microscopic to macroscopic measurements. It is envisaged that this work will provide the basis for further development of a unified test methodology to understand the degradation mechanism of cementitious materials under sulphuric acid attack in paste, mortar and concrete levels.

In this work, the methodologies commonly applied in the previous studies have been further assessed, including the exposure regime, chemical concentration and the measurements performed. The physical, mechanical properties, and the chemical and microstructural characteristics of paste, mortar, and concrete were analysed over time to understand the degradation mechanism of OPC based and AA cementitious materials under sulphuric acid attack.

Objectives and scope of research

The four main objectives of this research are:
1. To access the influence of exposure regimes and chemical concentration on the different cementitious materials under sulphuric acid attack. The exposure regimes applied in this research include: continuous immersion, brushing, and wetting and drying cycling, which have all commonly been used exposure in the previous experimental investigations. These techniques are applied under two different chemical exposure concentrations (1% and 3% w/w) as these were also identified to be most commonly used in previous studies.

2. To access the measurements performed on the different cementitious materials under sulphuric acid attack. The measurements and indicators of durability have been selected as those most commonly applied in the previous studies. These include: acid consumption, change of mass, change of length, change in compressive strength, and change of cross-section.

3. *To understand the degradation mechanism of OPC and AA paste under sulphuric acid attack.* The degradation mechanism of OPC and AA paste investigated in this research mainly focuses on the contradictions identified when reviewing previous studies. A series of comprehensive

characterization tests, including inductively coupled plasma mass spectrometer (ICP-MS), scanning electron microscopy (SEM), energy dispersive x-ray (EDX), X-ray diffraction (XRD), Fourier transform infrared spectroscopy (FTIR) and micro-computed tomography (CT) are undertaken to understand the physical and chemical change in the OPC and AA paste over time. After addressing these contradictions, an improved degradation mechanism is provided.

4. *To understand the degradation mechanism of different cementitious materials under sulphuric acid attack in different scale of manufacture (paste to mortar to concrete).* The degradation mechanism in different scales of manufacture focuses on the influence of aggregate type and the interfacial transition zone on the sulphuric acid resistance of cementitious materials.

Outline of the thesis

This thesis contains a collection of manuscripts published, accepted or submitted to internationally recognised journals. Each of the chapters 2 - 4, which are titled according to the research objective, contain: an introduction explaining the aim of the chapter and how the work fits into the overall objective; a list of manuscripts contained within the chapter; and finally the presentation each manuscript.

Chapter 2 provide a comprehensive assessment of the behaviour of concretes with different exposure regimes (continuous immersion, brushing, and wetting and drying cycling) and chemical concentrations (1% and 3% w/w) to achieve Objective 1. OPC and AA concretes susceptible to corrosion are utilised in this study in order to ensure that degradation is observed. Importantly, the first paper points out that the OPC and AA concrete subjected to increased acid concentration displayed the most rapid degradation when compared to other accelerated degradation test methods.

Chapter 3 provide a comprehensive assessment of the indicators of susceptibility to corrosion (acid consumption, change of mass, length, compressive strength, and cross-section) based on their potential advantages and limitations as well as application to both OPC and AA concrete to achieve Objective 2. With a further assessment of the behaviour of concretes with chemical concentrations (1% and 3% w/w) in the longer term, it demonstrates that a test procedure to indicate the susceptibility of concretes can be performed within a reasonable time frame for

standard testing. In addition, the chemical composition of coarse aggregate has a significant influence on the degradation mechanism of concrete.

Chapter 4 then focused on the degradation mechanism of cementitious materials in terms of chemical reaction and scale of manufacture. A series of comprehensive characterization tests are undertaken to understand the physical and chemical change in the OPC and AA paste over time to achieve Objective 3. The physical and mechanical properties of paste and mortar are then discussed to investigate the different degradation mechanism influenced by scale of manufacture to achieve Objective 4.

Chapter 2. Journal Paper 1 – The Behaviour of Concretes with Different Exposure Regimes and Chemical Concentrations

Introduction

This chapter contains the paper "Evaluation of accelerated degradation test methods for cementitious composites subject to sulfuric acid attack; application to conventional and alkali-activated concretes" which focuses on the assessment of test methods commonly used to identify and measure susceptibility to sulphuric acid corrosion for a range of cementitious composite materials, rather than directly comparing the chemical resistance of OPC concrete with AA concrete. It should be noted that low strength OPC and AA concretes chosen to be susceptible to corrosion were utilised in this study in order to ensure that degradation was observed. The different exposure regimes, including the continuous immersion, brushing, and wetting and drying cycling, and different chemical concentrations (1% and 3% w/w) are applied to both OPC and AA concrete. The influence of each test method is investigated via a series of physical, mechanical and microstructural tests. The degradation mechanism of OPC and AA concrete with different test methodologies are discussed. Taking compressive strength as the baseline for comparing approaches, the results show that only the specimens subjected to increased acid concentration display significantly accelerated degradation compared to the standard test approach. Further it is shown that neither wetting and drying cycling nor brushing had a significant influence on the rate of strength change.

List of manuscripts

Gu, L., Visintin, P. and Bennett, T., 2018. Evaluation of accelerated degradation test methods for cementitious composites subject to sulfuric acid attack; application to conventional and alkali-activated concretes. *Cement and Concrete Composites*, *87*, pp.187-204.

Statement of Authorship

Title of Paper	Evaluation of accelerated degradation test methods for cementitious composites subject to sulfuric acid attack; application to conventional and alkali-activated concretes
Publication Status	☑ Published ☐ Accepted for Publication ☐ Submitted for Publication ☐ Unpublished and Unsubmitted w ork w ritten in manuscript style
Publication Details	Gu, L., Visintin, P. and Bennett, T., 2018. Evaluation of accelerated degradation test methods for cementitious composites subject to sulfuric acid attack; application to conventional and alkali-activated concretes. *Cement and Concrete Composites, 87*, pp.187-204.

Principal Author

Name of Principal Author (Candidate)	Lei Gu		
Contribution to the Paper	Developed the test methodologies, performed analysis on all samples, interpreted data, and wrote manuscript.		
Overall percentage (%)	70		
Certification:	This paper reports on original research I conducted during the period of my Higher Degree by Research candidature and is not subject to any obligations or contractual agreements with a third party that would constrain its inclusion in this thesis. I am the primary author of this paper.		
Signature		Date	5/9/2018

Co-Author Contributions

By signing the Statement of Authorship, each author certifies that:

i. the candidate's stated contribution to the publication is accurate (as detailed above);

ii. permission is granted for the candidate in include the publication in the thesis; and

iii. the sum of all co-author contributions is equal to 100% less the candidate's stated contribution.

Name of Co-Author	Phillip Visintin		
Contribution to the Paper	Supervised development of work, helped in data interpretation and manuscript evaluation.		
Signature		Date	05/09/2018

Name of Co-Author	Terry Bennett		
Contribution to the Paper	Supervised development of work, helped in data interpretation and manuscript evaluation.		
Signature		Date	5/9/2018

Evaluation of accelerated degradation test methods for cementitious composites subject to sulfuric acid attack; application to conventional and alkali-activated concretes

Lei Gu[1], Phillip Visintin[1] and Terry Bennett[1]
[1]School of Civil, Environmental and Mining Engineering, The University of Adelaide, SA 5005, Australia

Abstract:

The degradation of cementitious composite materials under chemical sulfuric acid attack has been widely investigated. The agglomeration of a global database of test results is complicated by the differing test methodologies employed in each study. As a result it is difficult to isolate the influence of individual test parameters and hence directly compare the relative performance of different cementitious material. In this study the existing accelerated test methodologies including: brushing, wetting and drying cycling, and increased concentration of sulfuric acid are investigated such that the influence of test methodology on degradation rate and microstructural performance can be identified. This approach is taken with the view of developing a common methodology for indicating the susceptibility of a given cementitious material in an aggressive environment. Rather than comparing the performance of individual materials this work aims to compare the influence of test methodology when applied to different materials.

Keywords: Conventional concrete; Alkali-activated concrete; concrete degradation; sulfuric acid corrosion; accelerated testing

1. Introduction

Cementitious materials are required for applications that are subject to chemically and biologically aggressive environments. The demands for durable materials are expected to increase with time as both the amount of infrastructure and the aggressiveness of the external environment, to which components are subject to, increases [1].

Particularly demanding environments for cementitious products occurs when the material is exposed to biological processes, for example those encountered in waste water systems. Biogenic degradation commonly occurs in sewage collection systems, dramatically reducing the infrastructure service life and leading to significant economic losses. For example, in the United States alone, it has been estimated that $390 billion will be needed to repair existing wastewater infrastructure over the period from 2002 to 2022 [2]. Biogenic sulfuric acid

corrosion occurs in environments with high hydrogen sulfide (H_2S) concentration, moisture, and atmospheric oxygen, and is one of the most rapid causes of concrete degradation [3].

Biogenic degradation of concrete can be directly studied by in-situ testing or the use of a biogenic simulation chamber [1, 3]. The biogenic activity gradually reduces the pH of environment until it stabilises at a pH 1-2 [4]. In a normal sewage collection system, this process takes several years, making in-situ testing an unfeasible option for rapidly developing a new material [5]. In a biogenic simulation chamber, bacterial process can be accelerated by a complex control system, reducing test periods to approximately 5 months [6, 7]. While capturing the mechanism of biogenic corrosion, the use of a biogenic chamber is largely infeasible in most civil engineering labs which do not have the ability to purchase, operate, or maintain complex biogenic chambers.

As an alternative to the long time periods and complexity of in-situ and simulation chamber tests, standard chemical tests (i.e. ASTM C 267 [8]) are easily conducted. Standard tests usually use realistic concentrations of sulfuric acid (i.e. sulfuric acid of pH 1) and subject the specimens to continuous sulfuric acid immersion. In general, specimens under standard conditions are able to withstand attack longer than the corresponding field exposure specimens [1]. This is because the field specimens are exposed to an environment with an almost constantly maintained sulfuric acid concentration and pH value while specimens in standard test conditions consume the sulfuric acid, leading to a decreased concentration and increased pH. Whilst standard chemical testing methods cannot be used to predict the service life of a given cementitious material, they can be employed to act as indicators of a materials susceptibility to biogenic attack.

In order to conduct relatively easy chemical tests to simulate the entire life of concrete under sulfuric acid attack within a short period, accelerated chemical tests with specific methodologies have been conducted in previous studies. Existing methodologies include: 1) regularly brushing the degraded layer of specimens; 2) subjecting the specimens into wetting and drying cycling and; 3) increasing the concentration of sulfuric acid.

1. **Brushing:** As sulfuric acid reacts with OPC concrete during the corrosion process, a soft gypsum layer is formed. The formation of this layer constitutes an extra barrier which the sulfuric acid must penetrate before it reaches the non-degraded concrete.

Brushing removes the soft surface layer of the concrete, which may allow the sulfuric acid to react directly with the non-degraded concrete, which in turn accelerates the corrosion process [3, 9].

2. **Wetting and drying cycling:** In wastewater infrastructure, cycles of wetting and drying may occur. During the drying process, expansive sulphate products crystallise in the pores, leading to micro-cracks which cause more rapid deterioration [10].
3. **Increased acid concentration:** In field conditions, concrete degrades more rapidly in a lower pH environment where high concentrations of H_2S can exist. In chemical corrosion tests this may be simulated by using a higher concentration of sulfuric acid which reduces the pH and increase the sulphate ion concentration of the environment [1]. The term increased acid concentration is used here to indicate exposure to pH levels below that suggested in standard tests (and used in both the brushing and wetting and drying cycles experiments).

In previous research De Belie et al. [11] designed an automatic apparatus to subject concrete specimens to both brushing and wetting and drying cycling. Tests could be conducted within a 2 month period after which a maximum corrosion depth of 0.4 mm was observed [12]. Herisson et al. [13] tested the sulfuric acid resistance of OPC mortar specimens in pH 1 and pH 2 solutions, and reported the corrosion of the specimens was more significant in pH 1 sulfuric acid. While studies [9, 12-18] have reported behaviour of OPC concrete under chemical sulfuric acid attack by standard and different accelerated methodologies, there is no study comparing these methodologies. Thus, before the results of individual studies can be compared it is necessary to understand the influence of existing test methodologies for both standard and accelerated tests.

Test methodologies used in previous studies are summarised in table 1. It is evident that a wide range of test variables have been employed and it is very difficult to directly compare results with large scatter in variables, such as sample size, chemical concentration, exposure regime and the measurements performed.

A reliable, yet simple measurement technique to indicate the level of degradation is desirable for a unified test methodology which may be applied to all types of cementitious materials. For example, the length change of a specimen is often used as a proxy measurement, instead of directly measuring physical properties such as compressive strength. In this paper simple to

conduct indirect measurement techniques commonly applied in the studies listed in Table 1 are performed on specimens subjected to a range of acceleration techniques and the results compared to those obtained from direct strength measurements.

Table 1. Summary of existing test approaches

Reference	Test method	Sample size	Sample type	W/C	Curing	Test details	Chemical type	Chemical concentration	Solution exchange	Measurements	Measuring time
ASTM C 267-01 (2012) [8]	Continuous Immersion	Ø25mm × 25mm; 50mm × 50mm × 50mm	Mortar specimens		24h in moulds at 23 ± 2 °C and over 98% relative humidity, demoulding, curing under this condition to 28 days	Immerse the specimens in the solution		Simulate the anticipated service conditions	Replace the solution after each inspection period	Visual inspection Mass change Length change Compressive strength	1,7,14,28,56, and 84 days
Attiogbe and Rizkalla (1988) [19]	Continuous Immersion	Ø152mm × 305mm	OPC concrete specimens	0.67	Moist-cure for 28 days	Immerse the specimens in the solution	Sulfuric acid	1%	Replenish the depleted acid when pH exceeded 1.1	Mass change Length change	5, 10, 18, 32, and 72 days
Fattuhi and Hughes (1988) [20]	Continuous Immersion	102mm × 102mm × 102mm	OPC concrete and mortar specimens	0.36, 0.40, 0.46, 0.50, 0.60, 0.70	24h in moulds in ambient environment, demoulding, curing in a water tank at 18 ± 2 °C for 27 to 34 days	Immerse the specimens in the solution at 22 to 26 °C	Sulfuric acid	1.03% and 3.03%	Replenish the depleted acid regularly	Mass loss	Once a week for 36, 48, 93 days in different groups
Herisson et al. (2013) [13]	In situ test; Continuous immersion	Ø60mm × 140mm; 20mm × 20mm × 20mm	OPC and calcium aluminate cement concrete specimens	0.37		In situ test: suspend in two sewer networks; Lab test: Immerse the specimens in the solution for 1 week	In situ test: biogenic corrosion; Lab test: sulfuric acid	Lab test: pH 1 and 2		Change of calcium and aluminium concentrations in acidic solution Mass loss	Twice a day

Xie et al. (2004) [21]	Periodic soaking; spraying	100mm × 100mm × 100mm	OPC and slag concrete specimens	0.5	Water-cure for 28 days	Periodic soaking: subject concrete specimens to a 6-day cycle, immerse 5 days and dry 1 day for 66 to 90 days Spraying: subject concrete specimens to a 6-day cycle spray 60 ml/h for 5 days and dry 1 day	Sulfuric acid and nitric acid	pH 5.6, 3.5, and 1.0	Every cycle	Corrosion depth Change of compressive strength Calcium Oxide loss Change of sulphate compounds	30, 74, 105, 135 days
Hewayde et al. (2007) [22]	Wetting and drying cycling	Ø100mm × 200mm; Ø75mm × 150mm; Ø50mm × 100mm	OPC concrete specimens	0.25, 0.30, 0.35, 0.40, 0.50	Moist-cure for 28 days at 23 ± 1 °C	Immerse the specimens in the solution, oven dry the specimens at 105°C every day, then re-immerse in the acid solution	Sulfuric acid	0.3%, 0.6%, 1.0%, 1.5%, 2.0%, 2.5%, 3.0%	Every day	Mass loss Corrosion depth	1, 2, 3, 4, 6, 8, and 13 weeks
Gao et al. (2013) [23]	Wetting and drying cycling	70mm × 70mm × 280mm	OPC, fly ash and GBFS concrete specimens	0.35	Moist-cure for 28 days at 20 ± 3 °C	Immerse the specimens in the solution for 21h, ambient dry the specimens for 3h every day, then re-immerse in the solution	Sodium sulphate	5%		Relative dynamic elastic modulus Pore size distribution	1, 2, 3, 4, 5, 7, 9, 11, 15, 19, 20, 25 weeks
Fattuhi and Hughes (1983) [24]	Brushing	102mm × 102mm × 102mm	OPC concrete specimens	0.47		Immerse the specimens in a hydraulic channel with continuous circulation of acid, lightly brush the specimens to remove debris from the surface before every weighting	Sulfuric acid	1%	Replenish the depleted acid regularly	Mass loss	1, 3, 7, 14, 21, 35, 56, 75, 104, 120, and 174 days
De Belie et al. (2002) [11]	Brushing; Wetting and drying cycling	Ø200mm × 70mm	High sulphate resistant Portland cement and OPC	0.4, 0.39		Rotate samples in acid solution at speed of 1.04 rev/h, keep 1/3 of sample immersing in the acid, after each cycle, air dry the samples, then brush the samples before measuring	Sulfuric acid and lactic/acetic acid	Sulfuric acid:0.5%; Lactic and acetic acid: 30 g/l	Every cycle	Change in radius Surface roughness	Sulfuric acid: Every cycle (12 days) 9 cycles Lactic and acetic acid:

			concrete specimens							Every cycle (6 days) 6 cycles
Mori et al. (1992) [7]	In situ test; Biogenic test	100mm thick core sample in pipe 40mm × 40mm × 160mm	Mortar specimens	0.65	Water-cure for 28 days at 20 to 22 ℃	In situ test: place mortar specimens in situ, measure the specimen after 8 months Biogenic chamber test: partial immerse the specimens in the medium, inoculate treatment plant on the surface of specimens every 2 week for the first 2 month	Hydrogen sulphide	400 ppm		Corrosion depth	Biogenic chamber test: 42, 72, 180 days
Jiang et al. (2014) [25]	Biogenic test	100mm × 70mm × 70mm	Concrete coupons prepared from corroded concrete sewer slabs			Partial immerse the specimens in domestic sewage in the simulation chamber for 45 months	Hydrogen sulphide	0 ppm,5 ppm, 10 ppm, 15 ppm, 25 ppm and 50 ppm		Surface pH Surface sulfate Corrosion rate	0, 6, 12, 18, 24, 33, and 45 weeks
Vincke et al. (2000) [26]	Biogenic test	20mm × 20mm × 50mm	OPC and blast furnace slag concrete specimens			Place the samples in H_2S chambers for 3 days, then incubate the samples in solution for 10 days, then rinse with Milli-Q water for 2 days, then dry the samples for 2 days, repeat this process for another 2 cycles	Hydrogen sulphide	250 ppm		pH of solution sulphate concentrations of solution Calcium release Mass loss	Every cycle (17 days)
De Belie et al. (2004) [12]	Brushing; Wetting and drying cycling;	Ø200mm × 60mm Ø200mm × 80mm	High sulphate resistant Portland cement	0.25, 0.36-0.40, 0.43-0.49		Chemical test: Rotate samples in acid solution at speed of 1 rev/h, keep 1/3 of sample immersing in the acid, after each cycle, air dry	Sulfuric acid Hydrogen sulphide	Sulfuric acid: 0.5% Hydrogen sulphide :250 ppm	Sulfuric acid: Every cycle	Length change Mass loss	Chemical test: Every cycle (5 days)

	Biogenic test	20mm × 20mm × 50mm	and blast furnace slag concrete specimens	the samples, then brush the samples before measuring Biogenic test: Place the samples in H_2S chambers for 3 days, then incubate the samples in solution for 10 days, then rinse with Milli-Q water for 2 days, then dry the samples for 2 days, repeat this process for another 3 cycles		Biogenic test: Every cycle (17 days)

In recent years, alkali-activated (AA) concrete has been suggested as a potentially more durable alternative to conventional ordinary Portland cement (OPC) concrete in aggressive environment [27, 28]. Several authors have reported observing a good resistance of AA concrete to sulfuric acid attack [27, 29-31]. In these studies, the sulfuric acid resistance of AA concrete has been tested using a similar approach [27, 29-31]. That is, concrete or mortar specimens were simply immersed in sulfuric acid solution for a period of time, and the physical and mechanical properties compared to those of a control group to quantify any change. While similar, each of these studies considers a different size of specimens, concentration of acid, and period of immersion, and hence it is difficult to compare results across studies.

The purpose of this paper, rather than comparing the chemical resistance of OPC concrete with AA concrete, is to assess the test methodologies of sulfuric acid corrosion for a range of cementitious composite materials. Here OPC and AA concretes are used to test the accelerated methodologies capacity to indicate susceptibility to biogenic corrosion. The investigation covers accelerated methodologies including: brushing, wetting and drying cycling, and concentrated sulfuric acid on the physical and mechanical properties of OPC and AA concrete under sulfuric acid attack. A control group using a non-accelerated methodology provides a baseline for comparison of the three accelerated methodologies. Microstructural analysis was conducted in order to glean insights into the physical mechanisms underlying the macrostructural observations. It is envisaged that this work will provide the basis for further development of a unified test methodology to indicate the susceptibility of a wide range of cementitious materials to sulfuric acid attack.

The paper initially provides a summary of the experimental program, including material properties, specimen properties, testing methodology and instrumentation, which is followed by the results of the experimental program. A detailed discussion of the results is then presented, where the different degradation mechanisms observed in non-accelerated test and the three accelerated test methodologies are discussed in term of changes to the microstructure of the concretes.

2. Materials and methodologies

In this section, the information regarding materials, specimen manufacture and the test methodology are presented.

2.1 Materials

General purpose cement and class F fly ash were used as binders in the OPC and AA concretes respectively. The chemical compositions of these binders are supplied in Table 2. Crushed limestone having specific gravity of 2.65 and fineness modulus of 5.4 was used as coarse aggregate. River sand having specific gravity of 2.61 and fineness modulus of 2.3 was used as fine aggregate. For all AA mixes, the alkaline solution phase consisted of a combination of sodium silicate (Na_2SiO_3) and 14 molar sodium hydroxide (NaOH), pre-mixed with a ratio of Na_2SiO_3:NaOH of 1.5:1.

Table 2. Chemical composition of binders

Oxide (wt%)	SiO_2	Al_2O_3	Fe_2O_3	CaO	MgO	Na_2O	K_2O	SO_3	TiO_2	P_2O_5	Mn_2O_3	LOI*
Cement	19.89	4.69	3.16	63.35	1.94	0.22	0.40	2.77	0.27	0.03	0.07	3.55
Fly ash	54.24	28.94	4.01	3.58	1.80	0.60	1.46	0.25	1.21	0.27	0.06	3.12

LOI: Loss on ignition

2.2 Test specimens

Two unique batches of specimens, including one batch of OPC concrete and one batch of AA concrete were manufactured. The mix proportions of the OPC concrete (CC) and AA concrete (AAC) used in this study are given in Table 3, in which the AA mix was designed according to Albitar et al. [32, 33]. The fly ash used in AA concrete mix had quite similar composition when compared with the work done by Albitar et al. [32, 33]. The OPC concrete specimens were kept in moulds at ambient temperature for approximately 24 hours to harden before being demolded and transferred to a fog room with a constant temperature of 22 °C for a curing period of 28 days. The AAC specimens were kept in moulds at ambient temperature for approximately 48 hours to harden before being demoulded. The AAC specimens were sealed in plastic bags and transferred to the fog room for a curing period of 28 days. The 28 days compressive strength of CC and AAC is 36.4 MPa and 22.2 MPa, respectively. It should be noted that low strength concretes were utilised in this study in order to observe degradation and as such the water to cement ratio of the OPC was 0.7. That is, the purpose of the paper is not to develop a highly durable concrete but rather to highlight and compare test methodologies commonly used to study degradation.

Table 3. Mix proportion of conventional and alkali-activated concrete

Mix ID	Cement	Fly ash	CA	FA	Water	SP	NaOH	Na_2SiO_3

	(kg/m^3)	(kg/m^3)	(kg/m^3)	(kg/m^3)	(kg/m^3)	(kg/m^3)	(kg/m^3)	(kg/m^3)
CC	280	0	1110	740	196	0	0	0
AAC	0	424.8	1176	576	16.8	48	63.4	95.0

CA: Coarse aggregate; FA: Fine aggregate; SP: Superplasticizer

2.3 Testing methods

Following 28 days of curing the specimens were laid on a plastic grid and subsequently immersed in sulfuric acid solution. The pH of the sulfuric acid solutions were monitored, by a portable digital pH meter, and adjusted twice a week. The following details show the experimental process of each test methodology:

1. **Non-accelerated test:** Specimens were immersed in 1% sulfuric acid solutions for up to 144 days. The pH levels was maintained to a target value of 1.0±0.05. As the corrosion speed was expected to be slower than accelerated methods, the immersion period of non-accelerated specimens was 1 month longer than those of accelerated methods.
2. **Brushing:** Specimens were immersed in 1% sulfuric acid solutions for up to 116 days. The pH level was maintained to a target value of 1.0±0.05. The test apparatus shown in figure 1 was manufactured to allow for consistent brushing. The apparatus consists of a nylon brush, installed via a threaded rod above the frame. A height adjustable compressed spring was employed to allow a constant force to be applied throughout the test series as the diameter of the specimens reduced. To rotate the specimen, the roller was connected with a hexagon socket screw to a motor running at a constant speed of 30 RPM. Before weekly brushing, the specimens were dried in ambient lab conditions for 12 hours.

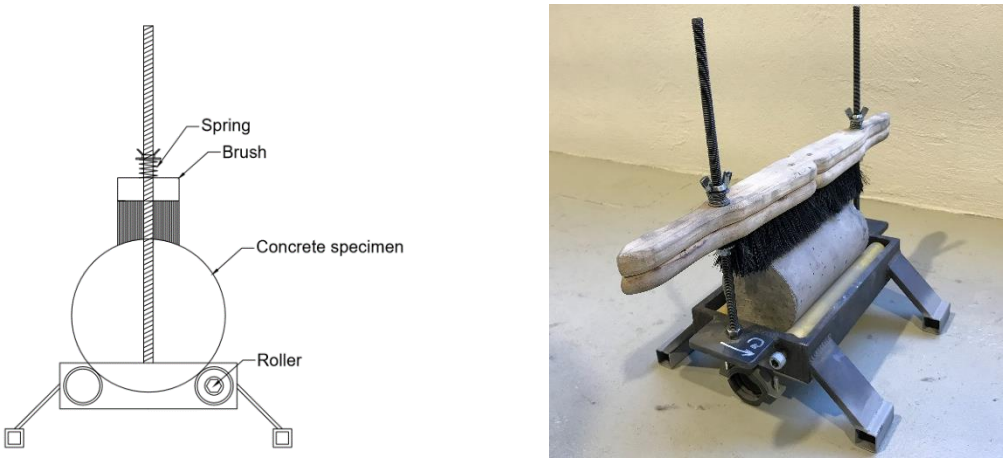

Figure1. The apparatus for brushing

3. **Wetting and drying cycling:** Specimens were immersed in 1% sulfuric acid solutions for up to 116 days. The pH level was maintained to a target value of 1.0±0.05. Two submersible pumps, with electronic timers, subjected the specimens to a 12 hour wetting and drying cycle. The choice of a 12 hour cycle time was made based on the findings of the test methodologies in Table 1.
4. **Increased acid concentration:** Specimens were immersed in 3% sulfuric acid solution for up to 116 days. The pH level was maintained to a target value of 0.5±0.05.

2.4 instrumentation

The mass change of specimens was determined by measuring a single specimen (3 replicates; 75 mm by 75 mm by 285 mm prism) which was dried under ambient lab conditions for 48 hours prior to weighing. The change in length of the specimens was determined by measuring prism specimens (3 replicates; 75 mm by 75 mm by 285 mm manufactured with DEMEC gauges embedded in both ends) via a digital micrometre. Tests were conducted after 4 hours of drying under ambient lab conditions.

The compressive strength change was determined from cylindrical specimens (3 replicates; 100 mm in diameter and 200 mm in height) via a universal test machine. A 10 mm thick piece which was cut from the test cylinders and sprayed with a 1% Phenolphthalein solution to identify the residual alkalinity of the cross-section. The change in corrosion depth was determined by subtracting the residual alkaline radius from the original specimen radius, both measured at nine locations using a digital microscope.

The degradation of specimens was examined by scanning electron microscopy (SEM), energy dispersive x-ray (EDX) and X-ray diffraction (XRD). For the SEM and EDX analysis, samples were cut from the surface (4~5mm depth) in the middle height of the specimens. The samples used in SEM and EDX were taken before sulfuric acid exposure and at the immersion ages of 2, 6 and 14 weeks, and coated with platinum prior to the analysis. SEM (Phillips XL 30) with EDX was performed at an accelerating voltage of 15 kV. For the XRD analysis, mortar was carefully removed from the surface (4~5mm depth) in the middle height of the specimens. Each mortar sample was finely ground prior to the XRD analysis. The samples used in XRD analysis were taken before sulfuric acid exposure and at the immersion ages of 6 and 14 weeks. XRD analysis was made using a Rigaku-Miniflex diffractometer with the following conditions: 40

kV, 15 mA, Cu–Kα radiation. The XRD patterns were obtained by scanning from 3° to 80° (2θ) at 10° (2θ) per min and in steps of 0.02° (2θ).

As a potential measure of degradation, the consumption of sulfuric acid was recorded. The increased percentage of sulfuric acid consumption is taken as the total amount of added sulfuric acid / the initial amount of sulfuric acid used before immersion.

3. Macroscopic performance indicators

In this section, the test results including visual appearance, acid consumption, change of cross-section, mass, length and compressive strength of both OPC and AA concretes are presented.

3.1 Conventional concrete

3.1.1 Visual appearance

Figure 2 shows the visual appearance of OPC concrete specimens after 14 weeks immersion in sulfuric acid subjected to brushing, wetting and drying cycling and increased acid concentration. It can be seen that the specimen subjected to brushing in figure 2(a) showed a rougher surface due to the removal of surface cement matrix and aggregates. A specimen subjected to wetting and drying cycling shown in figure 2(b) had no significant change in appearance after 14 weeks immersion. A specimen subjected to increased acid concentration in figure 2(c) showed severe corrosion after 6 weeks immersion, with the surface layer of specimen expanding during weeks 6-14.

(a) (b) (c)

Figure 2. Conventional concrete specimens after 14 weeks immersion in sulfuric acid: (a) Brushing; (b) Wetting and drying cycling; (c) Increased acid concentration

3.1.2 Change of cross-section

Figure 3 presents the change of cross-section area of OPC concrete specimens subjected to accelerated methodologies after 2, 6 and 14 weeks sulfuric acid immersion. Subsequent to spraying of the phenolphthalein solution on the cut surface of the specimens, the portion of the specimens in which there was residual alkalinity is indicated by a fuchsia colour, as shown in figure 3. It can be seen from the digital microscope image in figure 3(a) that the gypsum layer at surface of specimen subjected to brushing was not totally removed. The specimen subjected to wetting and drying cycling shown in figure 3(b) was seen to maintain its alkalinity during the 14 weeks of immersion. The specimen subjected to increased acid concentration shown in figure 3(c) had severe corrosion after 6 weeks of immersion, the digital microscope image shows a layer with porous structure as well as a weak bond between the aggregate and gypsum.

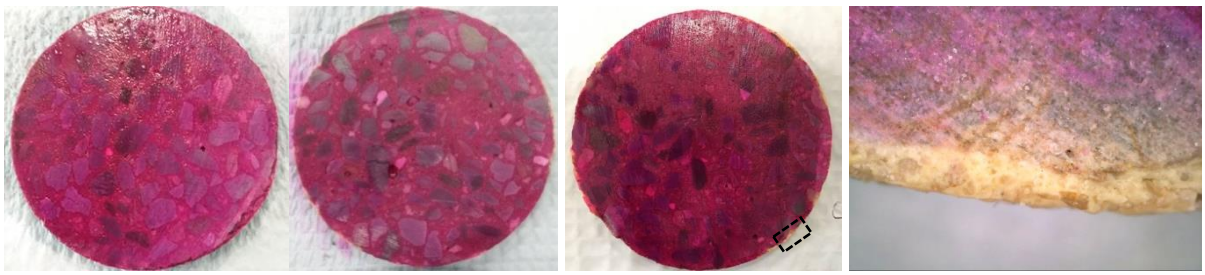

(a)： 2 weeks 6 weeks 14 weeks digital microscope image

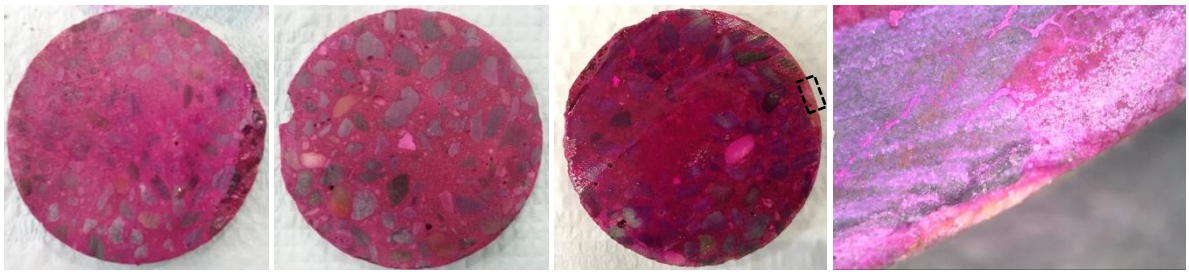

(b)： 2 weeks 6 weeks 14 weeks digital microscope image

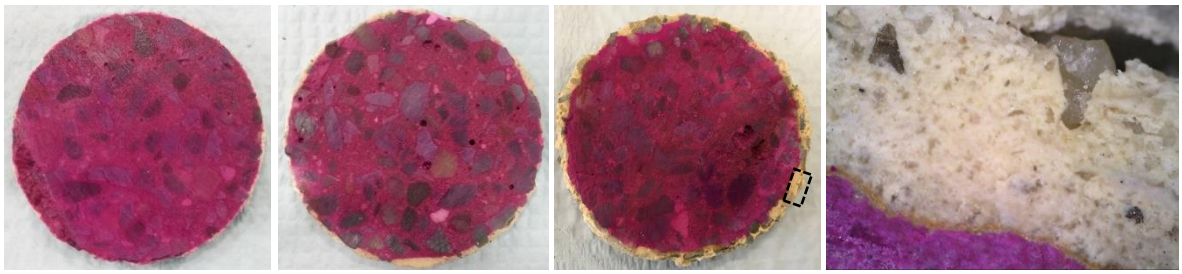

(c)： 2 weeks 6 weeks 14 weeks digital microscope image

Figure 3. Change of cross-section of conventional concrete specimens: (a) Brushing; (b) Wetting and drying cycling; (c) Increased acid concentration

3.1.3 Physical and mechanical properties change

Figure 4(a) presents the increased percentage of sulfuric acid consumption of OPC concrete specimens, compared to the initial dosage. It can be seen that for all tests the consumption of sulfuric acid of specimens varied approximately linearly with time. Among all the tests, the specimens subjected to wetting and drying cycling consumed much less sulfuric acid than those in other tests. This can be attributed to the fact that those specimens were only immersed for half of the time in sulfuric acid in comparison with the specimens in other tests.

Figure 4(b) presents the corrosion depth of OPC concrete specimens in all the tests. The average corrosion depth of the specimens in non-accelerated tests increased almost linearly with time. The specimens subjected to brushing showed little residual corrosion for the first two weeks before the residual corrosion depth gradually increased to 1.26 mm after 112 days immersion. The rough surface shown in figure 2(a) indicates that some aggregates were brushed off, from which it can be inferred that the bond between the matrix and aggregates was damaged. The gypsum layer shown in figure 3(a) indicates that the brushing did not remove the entire degraded layer. Therefore, it is difficult to determine a brushing force sufficient to clean all the degraded matrix without breaking the bond between the aggregate and matrix near the surface.

The specimens subjected to wetting and drying cycling showed no corrosion during the entire test period. However, as shown in figure 4(a), these specimens consumed 15% additional sulfuric acid compared to the initial dosage, which indicated that the OPC matrix was attacked by sulfuric acid. A large amount of solid precipitates were also found, indicating that the wetting and drying cycling eroded the surface layer of the specimens. The average corrosion depth of specimens subjected to increased concentration of sulfuric acid increased significantly during the first 6 weeks of immersion, and subsequently increased at a reduced rate to 5.06 mm after 112 days immersion. Therefore, the use of increased concentration of sulfuric acid improves the corrosion speed at early immersion times.

Figure 4(c) presents the mass change rate of OPC concrete specimens compared to the initial mass of specimens before immersion in all the tests. It can be seen that the mass of all the specimens decreased slowly during the initial 7 weeks with less than 0.4% mass loss observed and subsequently rapidly increased. The specimens exposed to increased acid concentration displayed a dramatic increase in mass loss, enhanced by the spalling of the aggregates and degraded matrix with increased corrosion depth, as shown in figure 2(c).

Figure 4(d) presents the length change of OPC concrete specimens in all the tests. It can be seen that the specimens subjected to wetting and drying cycling shrank while all other specimens expanded. The difference in behaviour with wet-dry specimens can be explained by the fact that the effect of drying shrinkage in the specimens subjected to periods of drying is more significant than that of the autogenous shrinkage of specimens cured in wet condition [34].

Figure 4(e) presents the rate of change of compressive strength for OPC concrete specimens in all the tests, compared to the initial strength before immersion. It can be seen that the compressive strength of specimens exposed to increased concentration of sulfuric acid decreased by up to 30% during the 114 days of immersion. However, the compressive strength of specimens in other tests increased slightly during the initial 6 weeks before decreasing. The increase of compressive strength at the early stage can be attributed to continued hydration of the OPC matrix, as the central part of the specimens remained under alkali conditions as shown in figure 3. The reduction of compressive strength will be discussed further in section 4 in conjunction with the microstructural analysis.

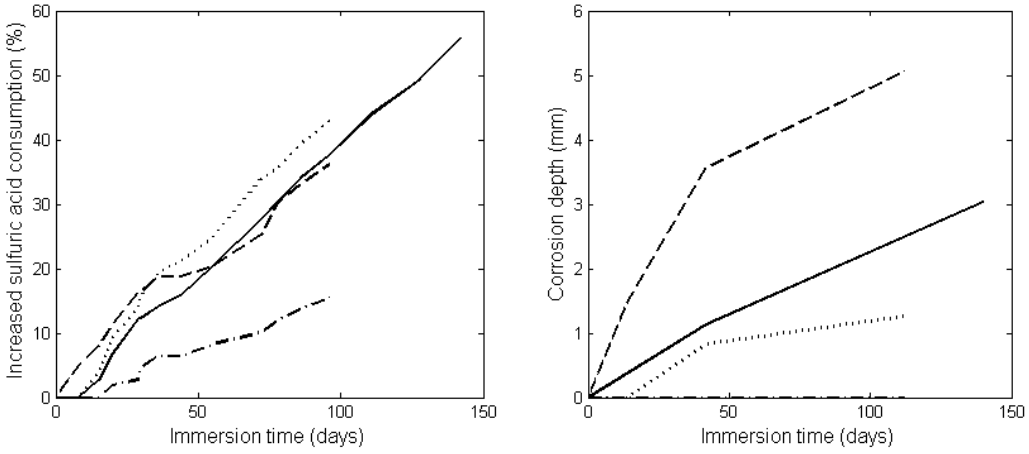

(a) (b)

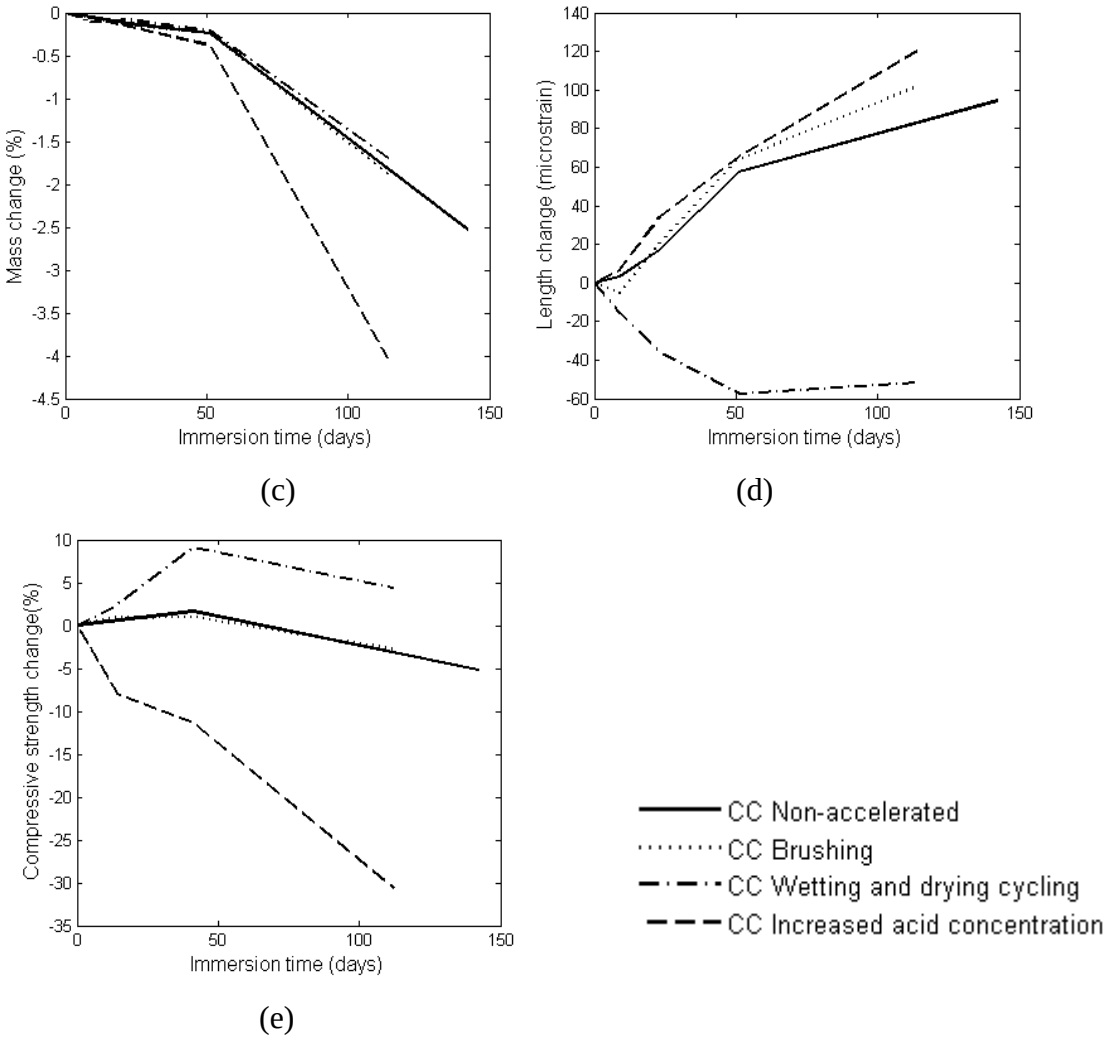

Figure 4. Physical and mechanical properties change of conventional concrete specimens under sulfuric acid attack: (a) sulfuric acid consumption; (b) corrosion depth; (c) mass change; (d) length change; (e) compressive strength change

3.2 Alkali-activated concrete

3.2.1 Visual appearance

Figure 5 shows the visual appearance of AA concrete specimens after 14 weeks of immersion in sulfuric acid subjected to the three accelerated methodologies. It can be seen that the specimen subjected to brushing showed a severely roughened surface in figure 5(a). The specimen subjected to wetting and drying cycling had no significant change in appearance (shown in figure 5(b)) after 14 weeks of immersion. The specimen subjected to increased acid concentration showed significant corrosion in figure 5(c).

During the initial weeks of immersion, it was observed that many bubbles were generated and attached to the surface of the specimens in the non-accelerated tests and those subjected to increased acid concentration. It can be inferred that the carbonate in the aggregate (i.e. calcium carbonate in limestone) and matrix (i.e. absorbed carbon dioxide during curing) reacted with the sulfuric acid, generating carbon dioxide gas. This phenomenon was also observed in OPC concrete specimens when initially placed into the acid. A more violent reaction, with a large amount of carbon dioxide gas generated within a short time, was observed with OPC specimens; however, less bubbles were attached to the surface of the specimen. However, as the porosity in AA concrete specimens was much lower than that in OPC concrete specimens [36], the carbon dioxide gas escaped at a slower rate from the pores of the matrix. The presence of carbon dioxide bubbles led to a slow corrosion rate during the initial stages of exposure as they acted as a barrier between the specimens and the sulfuric acid solution. During this period of exposure the specimens showed no significant change in appearance.

Both brushing and wetting and drying cycling avoided the formation of carbon dioxide bubbles. However, as the specimens were only brushed once per week, some carbon dioxide bubbles were observed before brushing during the initial 6 weeks. The carbon dioxide bubbles on the specimens subjected to increased acid concentration gradually disappeared, and cracks formed in the surface layer after 6 weeks immersion. The surface layer of those specimens continued to expand leading to the formation of further cracks and ultimately the spalling of the AA fly ash matrix over the following 8 weeks.

(a) (b) (c)

Figure 5. Alkali-activated concrete specimens after 14 weeks immersion in sulfuric acid: (a) Brushing; (b) Wetting and drying cycling; (c) Increased acid concentration

3.2.2 Change of cross-section

Figure 6 presents the change of cross-section area of AA concrete specimens subjected to accelerated methodologies after 2, 6 and 14 weeks of sulfuric acid immersion. It can be seen from figure 6(a) and (b) that in comparison with OPC concrete specimens (shown in figure 3(a) and (b)), a much larger area in the cross-section lost alkalinity with brushing and wetting and drying cycling. However, based on the digital microscope images shown in figure 6(a) and (b), unlike the soft gypsum layer observed in OPC concrete, the surface layer still retains a similar structure to that of the non-degraded area. The specimens subjected to increased acid concentration show that more than 60% of the cross-section lost alkalinity, shown in figure 6(c). Due to severe corrosion, part of the AA concrete matrix and aggregate spalled off during the cutting, and obvious cracks can be observed near the edge of the cross-section shown in figure 6(c). However, based on the microscope images, no significant difference can be observed between the AA concrete matrix in the degraded and non-degraded area in figure 6(c).

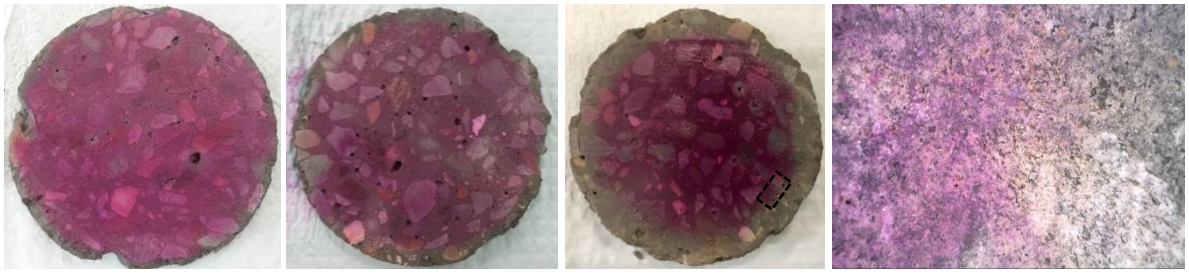

(a): 2 weeks 6 weeks 14 weeks digital microscope image

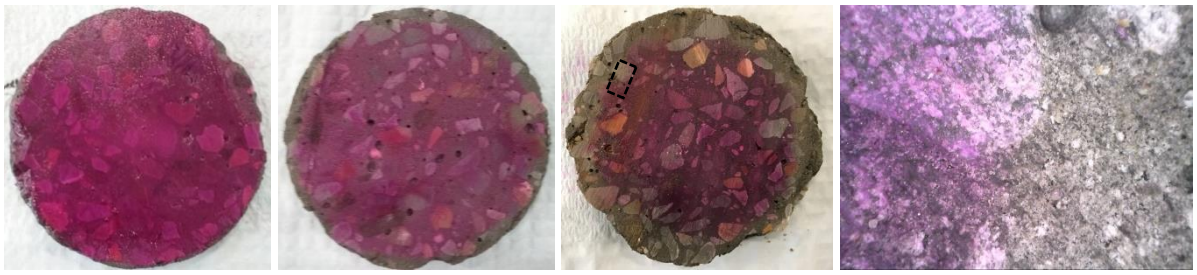

(b): 2 weeks 6 weeks 14 weeks digital microscope image

(c): 2 weeks 6 weeks 14 weeks digital microscope image

Figure 6. Change of cross-section of alkali-activated concrete specimens: (a) Brushing; (b) Wetting and drying cycling; (c) Increased acid concentration

3.2.3 Physical and mechanical properties change

Figure 7(a) presents the increased percentage of sulfuric acid consumption of AA concrete specimens, compared to the initial dosage. It can be seen that the consumption of sulfuric acid of specimens subjected to wetting and drying cycling increased almost linearly. However, the acid consumption of specimens in non-accelerated test and other two accelerated tests remained at 0 during an initial stage, (approximately 20 days), before increasing almost linearly. Again, this is attributed to the fact that the formation of carbon dioxide bubbles worked as a barrier between the specimens and sulfuric acid solution, leading to extremely low acid consumption during the initial stage.

Figure 7(b) presents the corrosion depth of AA concrete specimens in all the tests. The average corrosion depth of the specimens in non-accelerated test and subjected to wetting and drying cycling increased almost linearly. Figure 7(c) presents the mass change rate of AA concrete specimens compared to the initial mass of specimens before immersion in all the tests. It can be seen that the mass of all the specimens decreased slowly during the initial 7 weeks with less than 2.5% mass loss observed. Subsequently, mass loss of the specimens in non-accelerated test and subjected to brushing and wetting and drying cycling still decreased slowly with less than 4% final mass loss, while the mass loss of the specimens subjected to increased acid concentration accelerated significantly due to the spalling of AA fly ash matrix and aggregates shown in figure 5(c).

Figure 7(d) presents the length change of AA concrete specimens in all the tests. It can be seen that the specimens subjected to wetting and drying cycling shrank slightly while all other specimens expanded. The specimens subjected to increased acid concentration expanded significantly after 7 weeks of immersion. This dramatic change will be discussed in section 4 in conjunction with the microstructural analysis.

Figure 7(e) presents the compressive strength change rate of AA concrete specimens in all the tests, compared to the initial strength before immersion. It can be seen that the compressive strength of specimens subjected to increased acid concentration decreased by up to 23% during the 114 days of immersion. The compressive strength of specimens subjected to brushing

remained stable during the initial 6 weeks, then decreased by up to 7.8% during the 114 days of immersion. However, the compressive strength of specimens in non-accelerated test and subjected to wetting and drying cycling increased significantly during the initial 6 weeks before decreasing. The increase of compressive strength of AA concrete under sulfuric acid attack at the initial stage was also observed in the previous studies [27, 31, 37].

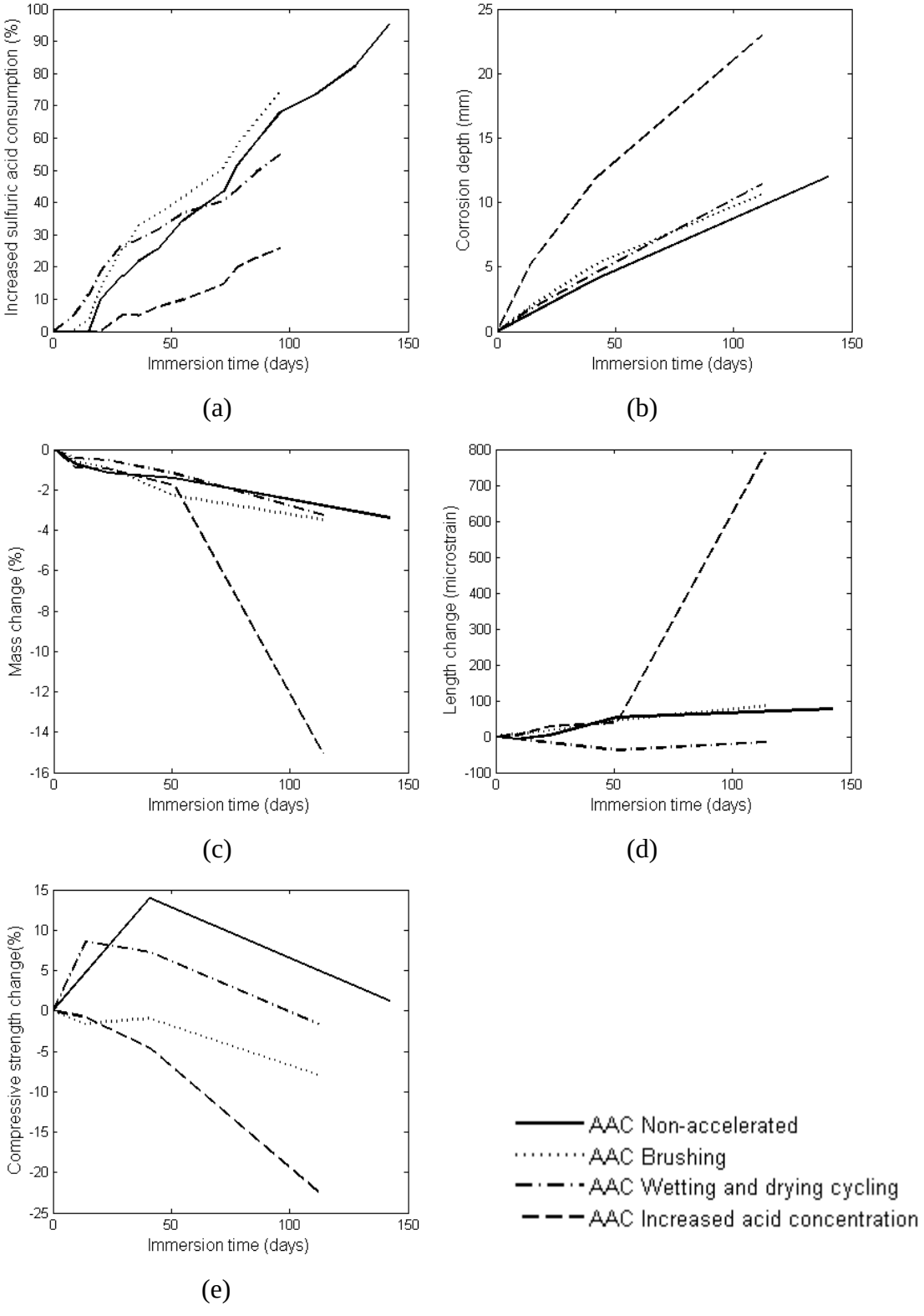

Figure 7. Physical and mechanical properties change of alkali-activated concrete specimens under sulfuric acid attack: (a) sulfuric acid consumption; (b) corrosion depth; (c) mass change; (d) length change; (e) compressive strength change

Comparing the rates of change of physical properties to the rates of change of the strength for OPC in figure 4 and those of AA in figure 7 reveals that a direct comparison of degradation measures for different materials is inappropriate. Moreover, even for a given material, the rate of change of length, mass loss, corrosion depth and acid consumption are not comparable and do not closely follow the same trend for the differing acceleration methods. A further comparison of the indicators of degradation under differing acceleration techniques will be considered in Section 5.

4. Microstructural performance indicators

In this section, the different degradation mechanisms observed in non-accelerated test and the three accelerated test methodologies are discussed in terms of changes to the microstructure.

4.1 OPC samples

Results of microstructural analyses of OPC samples are reported and discussed.

4.1.1 Non-accelerated test

Figure 8 shows the XRD pattern of OPC concrete samples before the test and after 6 weeks and 14 weeks immersion. According to the XRD analysis, crystalline quartz (main component of sand), portlandite and calcite was detected in the sample before the immersion. At 6 weeks immersion gypsum was detected and after 14 weeks immersion, the chemical composition of the OPC sample was changed significantly as shown with the traces dominated by gypsum and the peaks for calcite and portlandite phases significantly reduced.

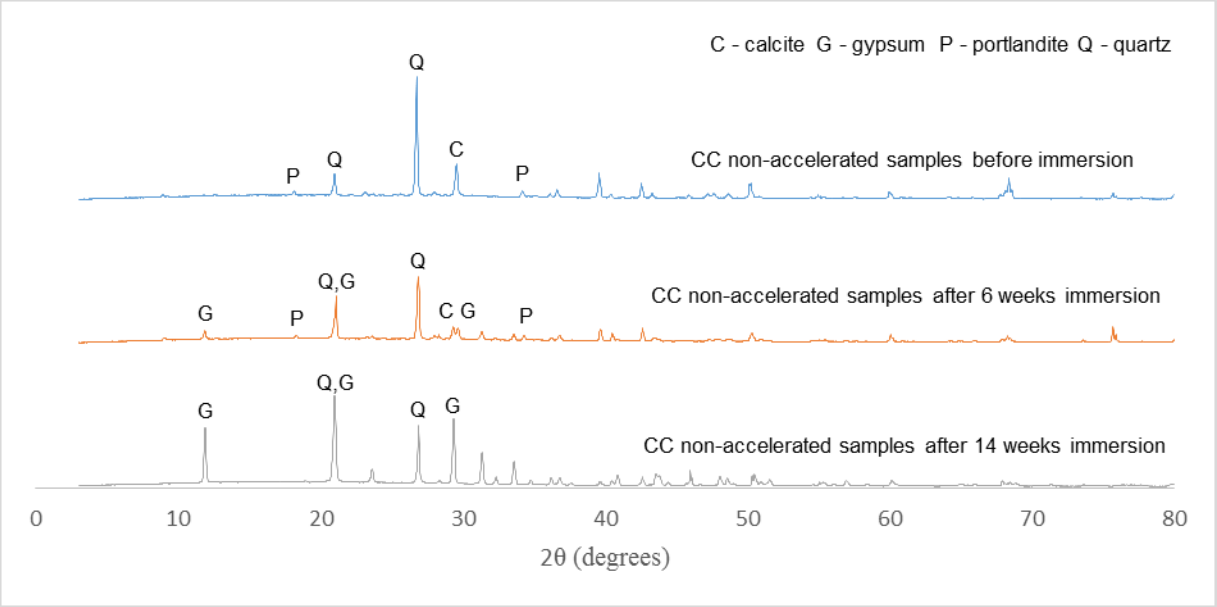

Figure 8. X-ray analysis of conventional concrete samples in non-accelerated test

Figure 9 presents the SEM images of OPC samples from a non-accelerated test before and after 142 days sulfuric acid immersion, and table 4 presents the surface element analysis by EDX of the marked area in figure 9. The OPC matrix in figure 9(a) is seen to have a dense structure of calcium silica hydrate (C-S-H) before immersion (see EDX results in Table 4 in which area A is shown to have a typical C-S-H chemical composition [34]). The OPC matrix in figure 9(b) exhibited a significant number of monoclinic crystals after 142 days immersion. From the surface element analysis of area B, it can be observed that the atomic ratio of calcium and sulfur is close to 1 and no silicon content is detected, from this it can be inferred that these monoclinic crystals are gypsum. In addition, it can be seen in figure 9(b) that the structure of the matrix after sulfuric attack is porous, which can be attributed to the dissolving of calcium hydroxide (C-H) and C-S-H due to the reaction with sulfuric acid. As C-S-H in the matrix of OPC contributes most to the strength [34], dissolving of C-S-H results in the reduction of compressive strength of specimens shown in figure 4(e).

The development of expansive products creates internal stresses that result in the change in length measured at the macro-scale shown in figure 4(d), and lead to the increase in the porosity at the microscale in figure 9(b). The expansive products are presumed to be gypsum rather than ettringite due to the pH level according to the findings of Gabrisova et al. [35] who suggest that ettringite is only stable above pH 10.7. Expansion of specimens submerged in sulfuric acid has also been also observed by Monteny et al. [11].

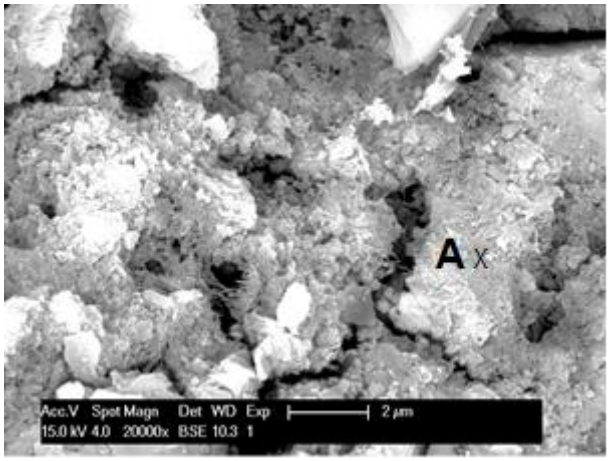

(a) before immersion

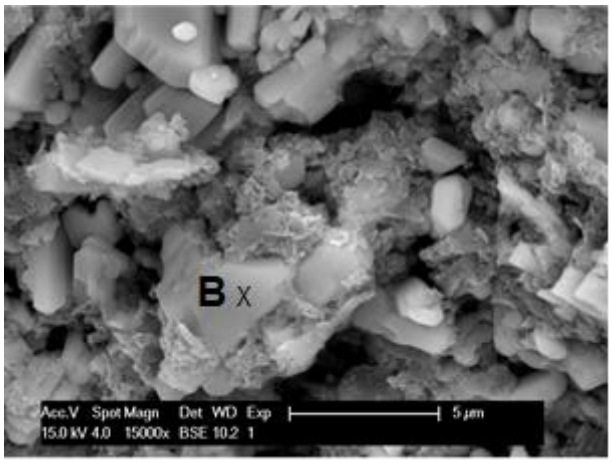

(b) after 142 days immersion

Figure 9. SEM images of OPC concrete sample in non-accelerated test

Table 4. Surface element analysis of OPC concrete sample in non-accelerated test

	Element	Oxygen	Sodium	Aluminium	Silicon	Sulfur	Potassium	Calcium
Area A	Wt.%	45.6	-	3.8	11.9	-	-	38.7
	At.%	65.0	-	3.3	9.7	-	-	22.0
Area B	Wt.%	58.3	2.4	-	-	17.4	1.0	20.9
	At.%	75.7	1.8	-	-	11.2	0.5	10.8

Wt. %: Weight percentage; At. %: Atom percentage

Figure 10 presents the SEM images of the interfacial transition zone (ITZ) change of OPC concrete samples from a non-accelerated test. It can be seen from figure 10(a) that the ITZ of an OPC sample before the immersion showed a very firm connection between the aggregate and matrix. After 142 days of immersion in sulfuric acid, gypsum crystals have developed near the ITZ, shown in figure 10(b). The porous and soft structure of gypsum resulted in a weak

ITZ, leading to significant reduction in the strength of the specimens, as shown in figure 4(e). This observation was in agreement with those reported in the previous studies [1, 38].

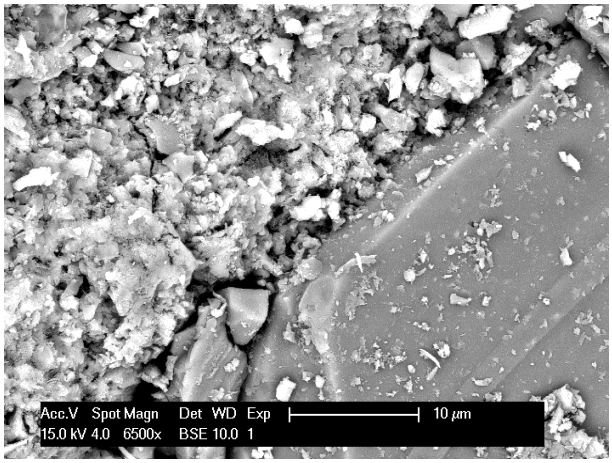

(a) before immersion

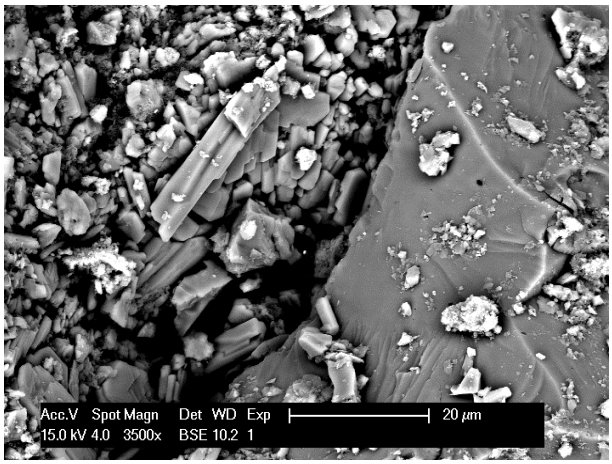

(b) after 142 days immersion

Figure 10. Interfacial transition zone change of OPC concrete sample in non-accelerated test

4.1.2 Brushing

The OPC samples subjected to brushing showed no significant difference in SEM and EDX analysis with those in non-accelerated test. However, as discussed in section 3.1, brushing potentially damages the bond between the aggregate and non-degraded matrix when removing the gypsum layer. In general, brushing can simulate field conditions of the sewage pipe with high speed water flow or solid wastes.

4.1.3 Wetting and drying cycling

Figure 11 presents the SEM images of OPC samples subjected to wetting and drying cycling after 114 days sulfuric acid immersion, and table 5 presents the surface element analysis by EDX of the marked area in figure 11. The rod like structures in figure 11 are ettringite, as identified by their high aluminium and sulfur concentrations. Specimens subjected to wetting and drying cycles show a reduced presence of gypsum and an increased presence of ettringite, than the samples subjected to non-accelerated conditions. The process of drying replaces the acidic pore solution with air and the residual sulfuric acid inside the surface of specimens reacts with the C-H and C-S-H in the OPC matrix consuming hydrogen ions, leading to a pH of the environment where sulphate ions are more likely to form ettringite than gypsum [38].

A large amount of solid precipitates were also found at the bottom of the immersion tanks, which was mainly composed of sand and gypsum, indicating that the wetting and drying cycling can mimic tidal area effects and erode the surface layer of the specimens.

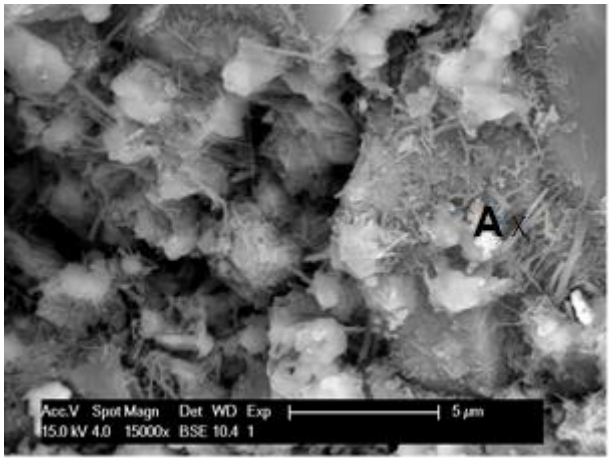

Figure 11. SEM images of OPC concrete sample subjected to wetting and drying cycling

Table 5. Surface element analysis of OPC concrete sample subjected to wetting and drying cycling

	Element	Oxygen	Magnesium	Aluminium	Silicon	Sulfur	Calcium	Ferrum
Area A	Wt.%	25.7	1.7	4.7	3.2	13.1	46.0	5.6
	At.%	44.4	2.0	4.8	3.1	11.3	31.7	2.8

Wt. %: Weight percentage; At. %: Atom percentage

4.1.4 Increased acid concentration

Figure 12 presents the SEM images of OPC samples subjected to increased acid concentration after 114 days of sulfuric acid immersion. It can be seen from figure 12(a) that the OPC matrix

has almost dissolved and a large amount of gypsum has formed in the area where residual alkalinity is lost. The OPC matrix in the area retaining alkalinity in figure 12(b) shows a different morphology from that in non-accelerated tests. The SEM image of the sample after immersion in non-accelerated tests shows almost no difference in OPC matrix in the area retaining alkalinity from that before immersion. However in figure 12(b), the crystalline gypsum grows from the large pores in the OPC matrix retaining alkalinity. Higher concentration sulfuric acid reduces the pH value and increases the sulphate ion concentration of the environment, changing the equilibrium in the chemical reaction, leading to the generation of more gypsum in the OPC matrix. This process further increases the diffusion of sulfuric acid, leading to a more rapid chemical reaction between sulfuric acid and the concrete specimens [1]. Meanwhile, as the area retaining alkalinity was affected by higher concentration sulfuric acid, the compressive strength of the specimens decreased more significantly than that of other methodologies shown in figure 4(e). Therefore, the specimens subjected to increased acid concentration have the most rapid degradation, approximating the field condition of very high concentration of H_2S in the atmosphere.

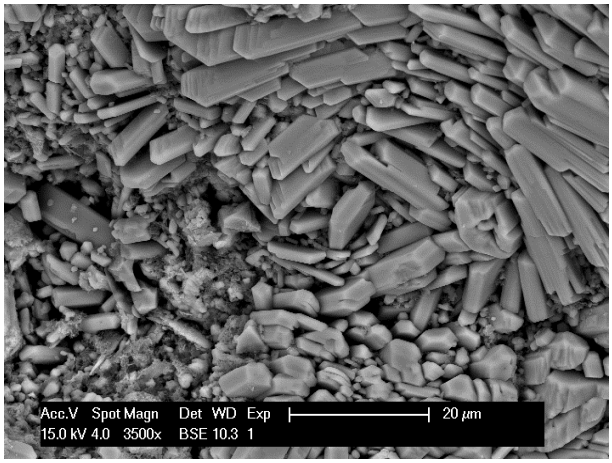

(a) area losing alkalinity

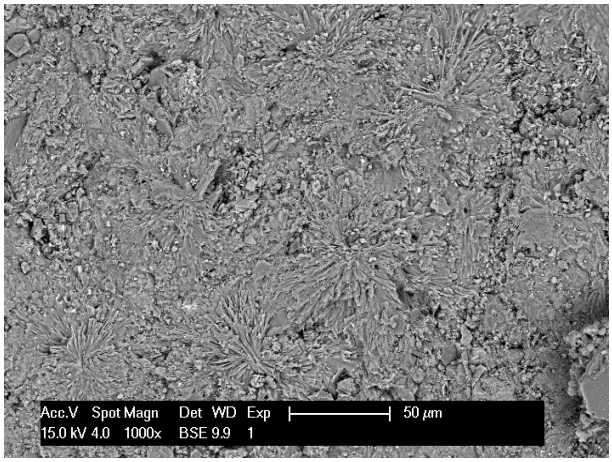

(b) area retaining alkalinity

Figure 12. SEM images of OPC concrete sample subjected to increased acid concentration

4.2 Analysis of alkali-activated concrete samples and discussion

In this section, the different degradation mechanisms observed in non-accelerated test and the three accelerated test methodologies is discussed in term of changes to the microstructure of the alkali-activated concrete samples.

4.2.1 Non-accelerated test

Figure 13 shows the XRD pattern of AA concrete samples before the test and after 6 weeks and 14 weeks immersion. According to the XRD analysis, crystalline quartz (main component of sand) and mullite was detected in the sample before the immersion. After 6 weeks immersion, the XRD traces was similar to that of a non-degraded sample, indicating that the degradation process was quite slow at the initial stage. After 14 week immersion, crystalline gypsum was detected. Owing to the very low amount of calcium in class F fly ash, reported in Table 2, the formation of gypsum was therefore most likely due to the calcium carbonate in limestone coarse aggregate reacting with sulfuric acid.

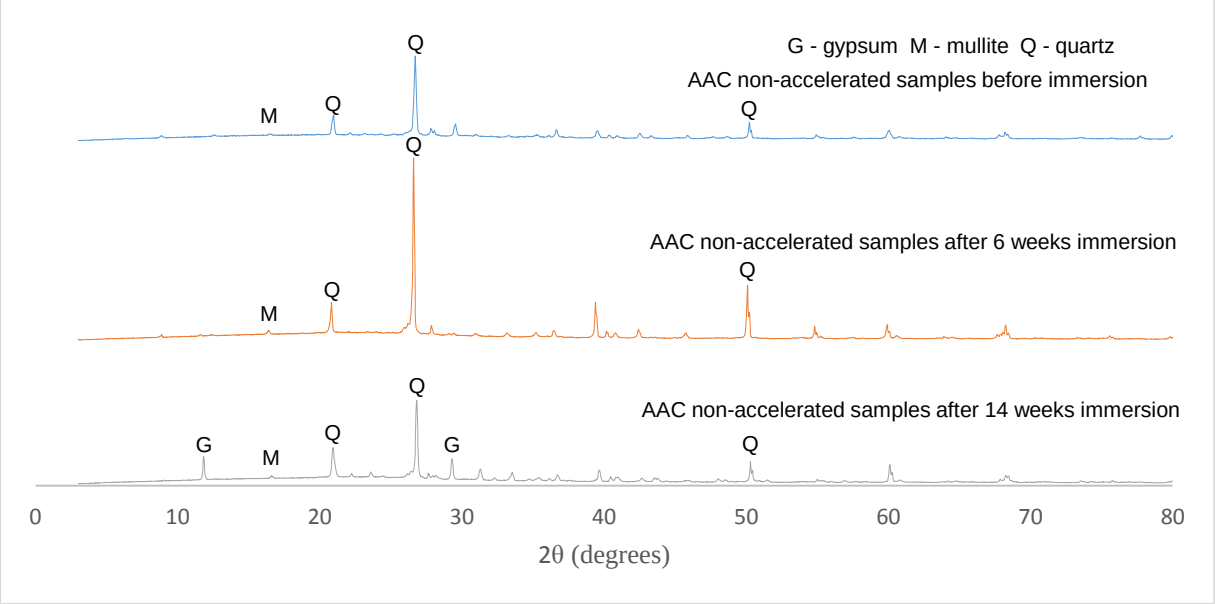

Figure 13. X-ray analysis of alkali-activated concrete samples in non-accelerated test

Figure 14 presents the SEM images of AA concrete samples from a non-accelerated test before and after 142 days sulfuric acid immersion, and table 6 presents the surface element analysis by EDX of the marked areas. The AA fly ash matrix in figure 14(a) showed a dense structure of sodium aluminosilicate hydrate (N-A-S-H) before immersion. The surface element analysis of area A showed a typical N-A-S-H chemical composition [36], the atomic ratio of silicon and aluminium was 1.5 which is close that atomic ratio (i.e. 1.58) of raw material measured by XRF in table 2. The sphere like structure shown in figure 14(a) is unreacted fly ash. The AA fly ash matrix in figure 14(b) displayed no significant difference in morphology from that in figure 14(a). In general, the AA fly ash matrix after sulfuric acid attack, shown in figure 14(b), still remained as a dense structure but with the presence of some micro-cracks. However, the surface element analysis of area B showed that the atomic ratio of silicon and aluminium increased to 2.3, which can be attributed to the dissolving of N-A-S-H due to the reaction with sulfuric acid. This phenomenon was also observed by the study of Bakharev [29]. When AA fly ash matrix is attacked by sulfuric acid, the Si-O-Al bond in N-A-S-H is dissolved by the hydrogen ions, resulting in the ejection of aluminium from the N-A-S-H framework. The framework vacancies are re-occupied by silicon atoms, and part of the ejected aluminium accumulates in the intra-framework space [36]. As a result, although the AA concrete was attacked by sulfuric acid, the framework still remains in good form, and no expansive products are generated.

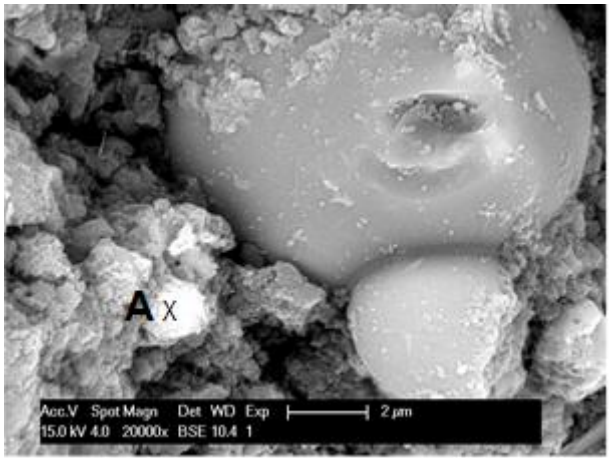

(a) before immersion

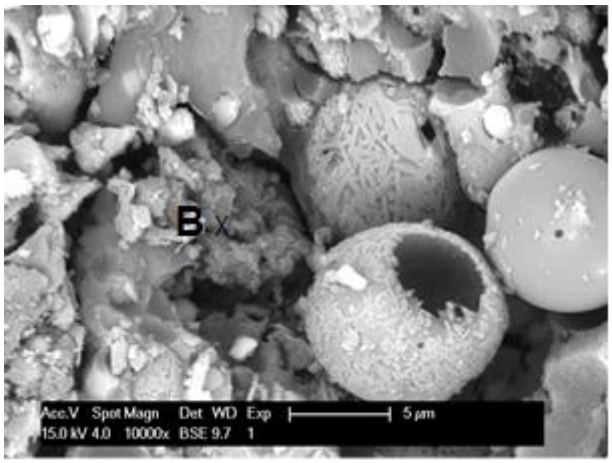

(b) after 142 days immersion

Figure 14. SEM images of AA concrete sample in non-accelerated test

Table 6. Surface element analysis of AA concrete sample in non-accelerated test

	Element	Oxygen	Sodium	Aluminium	Silicon	Calcium	Ferrum
Area A	Wt.%	43.8	6.1	17.6	27.2	5.3	-
	At.%	57.5	5.6	13.7	20.4	2.8	-
Area B	Wt.%	34.7	-	16.2	39.4	1.4	8.3
	At.%	49.7	-	13.8	32.3	0.8	3.4

Wt. %: Weight percentage; At. %: Atom percentage

Figure 15 presents the SEM images of the ITZ change of AA concrete samples from a non-accelerated test. It can be seen from figure 15(a) that the ITZ of AA concrete samples before immersion show a very firm connection between the aggregate and matrix. The ITZ of AA concrete samples after sulfuric acid immersion in figure 15(b) do not show a significant difference in morphology from that before immersion in figure 15(a) suggesting the ITX in AA

concrete is less susceptible to sulfuric acid attack than the ITZ in OPC. This phenomenon was also observed by the study of Provis and van Deventer [36].

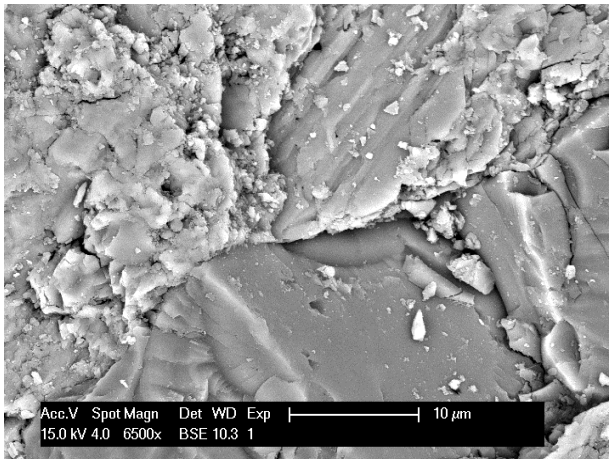

(a) before immersion

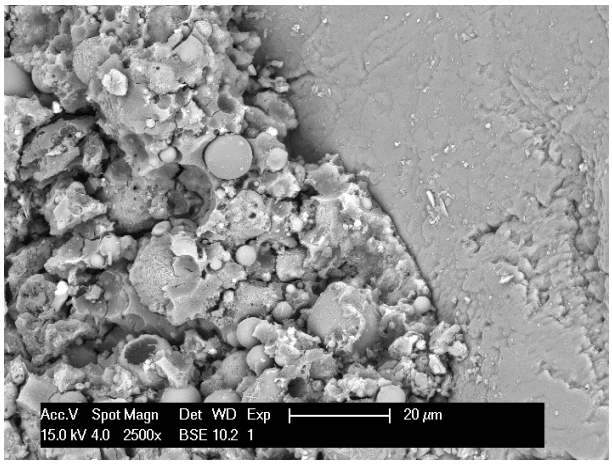

(b) after 142 days immersion

Figure 15. Interfacial transition zone change of AA concrete sample in non-accelerated test

4.2.2 Brushing

Within the core, of the AA concrete samples subjected to brushing, no significant differences in SEM and EDX analysis with those in non-accelerated test were observed. Whilst SEM analysis was not possible close to the edge of specimens, the severely roughened surface shown in figure 5(a) also indicates that the brushing damages the bond between the aggregate and non-degraded matrix when removing the degraded layer of AA concrete specimens.

4.2.3 Wetting and drying cycling

The AA concrete samples subjected to wetting and drying cycling also showed no significant difference in SEM and EDX analysis with those in non-accelerated test. Despite the specimens being immersed for only half of the time of the comparison tests, the acid consumption, corrosion rate and mass change was very close to the non-accelerated test and those subjected to brushing, shown in figure 7(b), (c) and (d).

4.2.4 Increased acid concentration

Figure 16 presents the SEM images of AA concrete samples subjected to increased acid concentration after 114 days sulfuric acid immersion, and table 7 presents the surface element analysis by EDX of the marked area in figure 16. It can be seen from figure 16(a) that the AA fly ash matrix near coarse aggregate shows the presence of many monoclinic crystals, and the surface element analysis in area A shows that the atomic ratio of calcium and sulfur is close to 1, indicating that these monoclinic crystals are gypsum. It can be inferred that the calcium compounds were dissolved and the calcium ions escaped from the coarse aggregate in the extremely low pH environment, generating gypsum with the sulphate ion diffused in the matrix. The formation of expansive gypsum increases the porosity of the structure. The area without coarse aggregate around point B in figure 16(b) shows a porous structure without any presence of crystals, and at this location the atomic ratio of silicon and aluminium increased to around 4. It can be inferred that the equilibrium in the chemical reaction was altered by the higher concentration sulfuric acid, leading to more severe aluminium ejection. This dissolving of N-A-S-H resulted in the significant reduction in compressive strength, shown in figure 7(e). The formation of gypsum and porous matrix structure further increase the diffusion of sulfuric acid, leading to a more rapid corrosion.

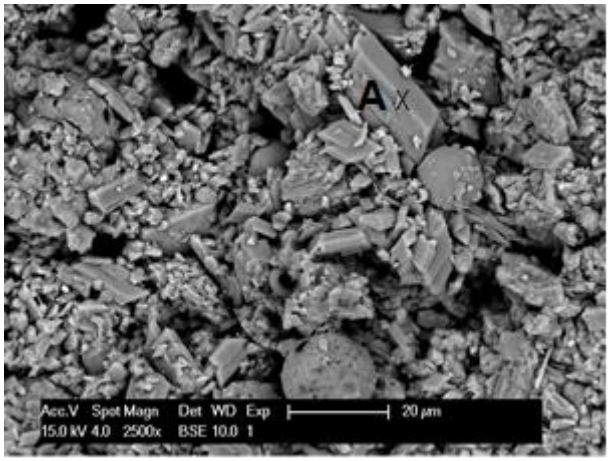

(a) area near coarse aggregate

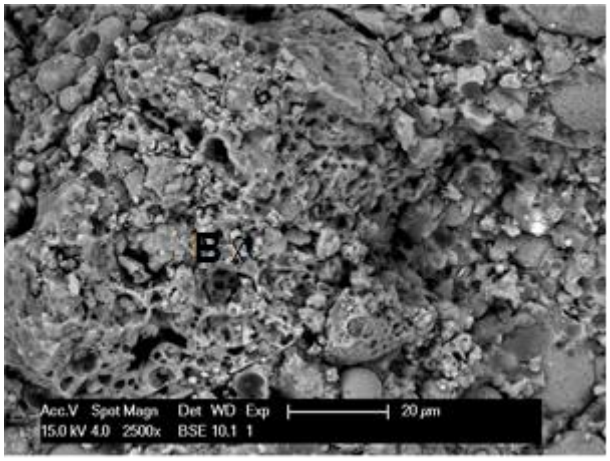

(b) area without coarse aggregate around

Figure 16. SEM images of AA concrete sample subjected to increased acid concentration

Table 7. Surface element analysis of AA concrete sample subjected to increased acid concentration

	Element	Carbon	Oxygen	Sodium	Aluminium	Silicon	Sulfur	Potassium	Calcium
Area A	Wt.%	4.9	45.8	-	-	-	20.8	0.5	28.0
	At.%	8.8	61.8	-	-	-	14.0	0.3	15.1
Area B	Wt.%	8.6	45.9	0.7	8.6	35.1	-	1.1	-
	At.%	13.7	55.1	0.6	6.2	24.0	-	0.5	-

Wt. %: Weight percentage; At. %: Atom percentage

Figure 17 presents the SEM images of the ITZ change of AA concrete samples subjected to increased concentration. It can be seen from figure 17(a) that the ITZ with coarse aggregate shows a weak bond due to the presence of many gypsum crystals. The ITZ with fine aggregate in figure 17(b) also shows a weak bond due to the porous structures and micro-cracks in the structure. The weak ITZ in the AA concrete also results in the significant reduction in compressive strength shown in figure 7(e) and the spalling in figure 5(c). Therefore, the specimens subjected to increased acid concentration have the most rapid degradation, simulating the field condition of the sewage pipe made of AA concrete with very high concentration of H_2S in the atmosphere.

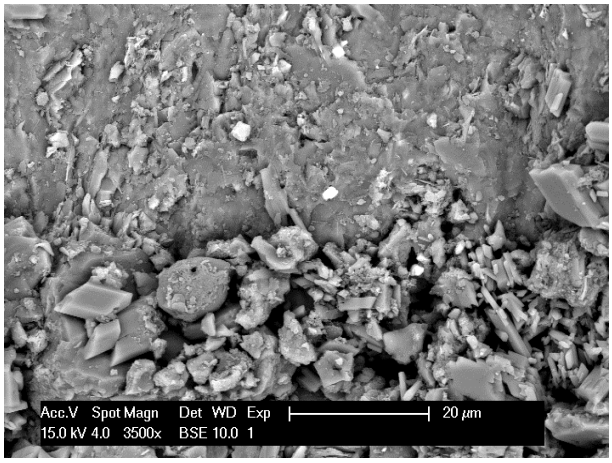

(a) ITZ with coarse aggregate

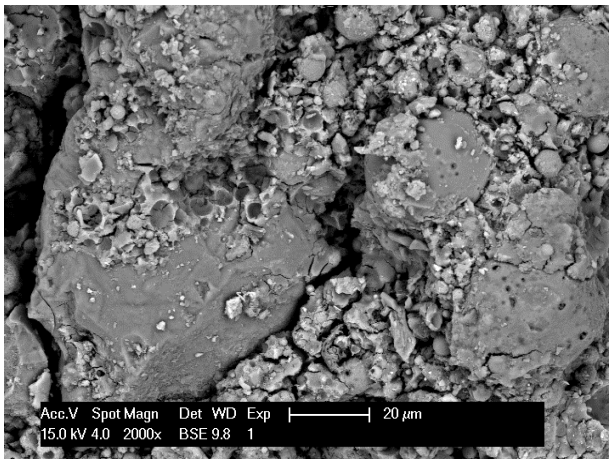

(b) ITZ with fine aggregate

Figure 17. Interfacial transition zone change of AA concrete sample subjected to increased acid concentration

5. Comparison of acceleration approaches and measurement techniques

With the aim of developing a unified test methodology for indicating the susceptibility of a given cementitious material to biogenic or sulfuric acid attack, methods of acceleration and measurement of degradation are assessed here.

Taking compressive strength as the baseline for comparing approaches, the time series graphs for the change in strength of OPC shown in Figure 4(e) and AAC in Figure 7(e) demonstrate that only the specimens subjected to increased acid concentration underwent significantly accelerated degradation compared to the standard test approach. Further it is shown that neither wetting and drying cycling nor brushing had a significant influence on the rate of strength change. These results are difficult to compare with previous studies such as of De Belie et al.

[12], as these tests underwent combined wetting and drying and brushing. Therefore the influence of each approach cannot be distinguished, nor did these studies compare with standard accelerated test methodologies. Further studies are required to identify the frequency of wetting and drying cycles and brushing as well as the force applied during brushing.

Continued strength development throughout the testing period may also lead to difficulties in comparing different types of cementitious materials particularly for materials such as AAC which are known to develop strength over a longer period of time than OPC. Thus a minimum test period must be specified such that gains in compressive strength do not mask the degradation. The observations of this work indicate that exposure periods of at least 60 days are required, however this requires further verification on different strength materials.

Having established that increase acid concentration is most effective acceleration method, let us now compare the different indicators of the extent of degradation. A heat map which shows the degradation in the high acid concentration (pH 0.5) with respect to the standard acid concentration (pH 1) is shown in Figure 18. As compressive strength reduces with degradation the results have been inverted in Figure 18 to align with the other indicators.

Figure 18: Heat map showing the degradation in the high acid concentration (pH 0.5) normalised with respect to the standard acid concentration (pH 1) (a) 2 weeks exposure; (b) 6 weeks exposure; (c) 14 weeks exposure

Figure 18(a) indicates that a 2 week exposure time is generally insufficient to measure a change in compressive strength as the variation shown (5%-9%) is within the natural variation associated with this test. Moreover the continued hydration of both the OPC and ACC may mask the true level of degradation. Indicators of degradation (acid consumption, corrosion depth, mass loss, length change), are inconsistent both within a given material and between materials indicating that in general they do not provide a generic methodology for identifying acid resistance at this time period.

Now considering the results at 6 weeks exposure in Figure 18(b), it can be seen that a sufficient reduction in compressive strength has occurred such that it will not be masked by the natural variation in strength or continued hydration. This indicates that a measurement period of 6 weeks is sufficient if considering compressive strength as the measure of degradation.

Considering the individual indicators, it can be seen that length change alone yields mixed results in terms of indicating the amount of degradation, this is in contrast to the suggestion of ASTM C 267 [8] which is applied to sulphate attack of OPC. Hence the results of the current study demonstrate that the use of length change may not be applied as a generic test for different cementitious materials.

The remaining indicators (acid consumption, corrosion depth and mass loss) all provide a reasonable indicator of the occurrence of degradation but cannot be used as a measure. That is, the indicators are not in the same ratio as the compressive strength change.

An assessment of the measurement techniques employed in this study has highlighted the potential advantages and limitations including:

1. Measuring the diameter of residual alkalinity (parallel to the direction of degradation) can provide a simple quantitative measure, however the technique can be clouded by the distribution of aggregates and is not necessarily a direct measure of the corrosion depth.

2. The change in length of a specimen (perpendicular to the direction degradation) again provides a simple indication of degradation, but is very difficult to isolate degradation dependant effect from shrinkage effects. The use of oven drying to attempt to regulate to pore water content can itself lead to mechanical damage.
3. The mass change of a specimen also suffers from the difficulties associated with regulation of the pore water content and the transport of reaction products out of the specimen.
4. Recording the consumption of acid can provide an indirect measure of degradation and has the advantage that it is easy to obtain. Caution is however required as gradients of concentration in the immersion tank can affect the consumption rates if a regular mixing regime is not followed.

6. Conclusions

This paper has further assessed test methodologies commonly applied to OPC, including a standard non-accelerated test, brushing, wetting and drying cycling, and increased acid concentration, for sulfuric acid corrosion for both OPC and AA concrete. The results show that:

1. Sulfuric acid corrosion of OPC concrete in non-accelerated test is mainly due to the dissolving of C-H and C-S-H and formation of expansive gypsum in the matrix. The chemical change results in porous OPC matrix and weak ITZ, leading to reduction in mass and compressive strength and expansion in length.
2. Sulfuric acid corrosion of AA concrete in non-accelerated test is mainly due to the dissolving of N-A-S-H. Such chemical change results in slightly porous AA fly ash matrix and no significant change in ITZ. Although the matrix lost alkalinity, AA concrete in non-accelerated tests retain most of the physical and mechanical properties after 142 days immersion.
3. OPC and AA concrete subjected to brushing show no significant difference in microstructure in comparison to non-accelerated test conditions. However, brushing results in a roughening of the surface of specimens which may influence indicators of degradation such as measurements of mass loss.
4. OPC concrete subjected to wetting and drying cycling shows the formation of ettringite crystals in the matrix. The AA concrete subjected to wetting and drying cycling shows no significant difference in microstructure in comparison with that in non-accelerated test.

5. The OPC and AA concrete subjected to increased acid concentration displayed the most rapid degradation.

Whilst the measurement methods employed (acid consumption, corrosion depth, mass loss, length change) are simple to conduct they only give an indication of the change in mechanical or transport properties within a specimen. In this study, to qualitatively correlate mechanical properties with the simple measurements, regular strength testing has been conducted. The rate of change of the simple measures was found to be highly mix dependent and therefore unsuitable for the comparison of the degradation performance of different materials.

The continued hydration of the materials can make the use of compressive strength tests difficult and hinder the design of a relatively simple and rapid test methodology. Techniques, such as heat curing, may be required to ensure that the strength of the material has plateaued within a reasonably short timeframe. This also requires prior knowledge of the rate of acceleration of the hydration for a given material and requires care to ensure that the material is not damaged in the accelerated curing process.

References

1. M. Alexander, A. Bertron, N. De Belie, Performance of cement-based materials in aggressive aqueous environments (Vol. 10), Springer, Dordrecht, 2013

2. Ma. G. D. Gutiérrez-Padilla, A. Bielefeldt, S. Ovtchinnikov, M. Hernandez, J. Silverstein, Biogenic sulfuric acid attack on different types of commercially produced concrete sewer pipes, Cem. Concr. Res. 40(2) (2010) 293-301.

3. J. Monteny, E. Vincke, A. Beeldens, N. De Belie, L. Taerwe, D. Van Gemert, W. Verstraete, Chemical, microbiological, and in situ test methods for biogenic sulfuric acid corrosion of concrete, Cem. Concr. Res. 30(4) (2000) 623-634.

4. J. Herisson, Biodétérioration des matériaux cimentaires dans les ouvrages d'assainissement–Etude comparative du ciment d'aluminate de calcium et du ciment Portland, 2012 (Doctoral dissertation, Université Paris-Est).

5. R. L. Islander, J. S. Devinny, F. Mansfeld, A. Postyn, H. Shih, Microbial ecology of crown corrosion in sewers, J. Environ. Eng. 117(6) (1991) 751-770.

6. K. Hormann, F. Hofmann, M. Schmidt, Stability of concrete against biogenic sulfuric acid corrosion, a new method for determination. In Proceedings of the 10th international congress on the chemistry of cement, Gothenburg, 1997.
7. T. Mori, T. Nonaka, K. Tazaki, M. Koga, Y. Hikosaka, S. Noda, Interactions of nutrients, moisture and pH on microbial corrosion of concrete sewer pipes, Water Res. 26(1) (1992) 29-37.
8. ASTM, C. 267-01: Standard Test Methods for chemical resistance of mortars, grouts and monolithic surfacing and polymer concretes, ASTM International, West Conshohocken, USA, 2012.
9. C. W. Fourie, Acid resistance of sewer pipe concrete, 2007 (Doctoral dissertation, University of Cape Town).
10. J. P. Frost, D. J. Armstrong, Concrete and silage effluent-a cyclical exposure method for accelerated corrosion testing, Farm Building Progress 116 (1994) 27-30.
11. N. De Belie, J. Monteny, L. Taerwe, Apparatus for accelerated degradation testing of concrete specimens, Mater. Struct. 35(7) (2002) 427-433.
12. N. De Belie, J. Monteny, A. Beeldens, E. Vincke, D. Van Gemert, W. Verstraete, Experimental research and prediction of the effect of chemical and biogenic sulfuric acid on different types of commercially produced concrete sewer pipes, Cem. Concr. Res. 34(12) (2004) 2223-2236.
13. J. Herisson, E. D. van Hullebusch, M. Moletta-Denat, P. Taquet, T. Chaussadent, Toward an accelerated biodeterioration test to understand the behavior of Portland and calcium aluminate cementitious materials in sewer networks, Int. Biodeterior. Biodegrad. 84 (2013) 236-243.
14. N. I. Fattuhi, B. P. Hughes, The performance of cement paste and concrete subjected to sulphuric acid attack, Cem. Concr. Res. 18(4) (1988) 545-553.
15. K. Torii, M. Kawamura, Effects of fly ash and silica fume on the resistance of mortar to sulfuric acid and sulfate attack, Cem. Concr. Res. 24(2) (1994) 361-370.
16. F. Jahani, J. Devinny, F. Mansfeld, I. G. Rosen, Z. Sun, C. Wang, Investigations of sulfuric acid corrosion of concrete. I: modelling and chemical observations, J. Environ. Eng. 127(7) (2001) 572-579.
17. J. Monteny, N. De Belie, L. Taerwe, Resistance of different types of concrete mixtures to sulfuric acid, Mater. Struct. 36(4) (2003) 242-249.
18. F. Girardi, W. Vaona, R. Maggio, Resistance of different types of concretes to cyclic sulfuric acid and sodium sulfate attack, Cem. Concr. Compos. 32(8) (2010) 595-602.

19. E. K. Attiogbe, S. H. Rizkalla, Response of concrete to sulfuric acid attack, Mater. J. 85(6) (1988) 481-488.
20. N. I. Fattuhi, B. P. Hughes, Ordinary Portland cement mixes with selected admixtures subjected to sulfuric acid attack, Mater. J. 85(6) (1988) 512-518.
21. S. Xie, L. Qi, D. Zhou, Investigation of the effects of acid rain on the deterioration of cement concrete using accelerated tests established in laboratory, Atmos. Environ. 38(27) (2004) 4457-4466.
22. E. Hewayde, M. Nehdi, E. Allouche, G. Nakhla, Effect of mixture design parameters and wetting-drying cycles on resistance of concrete to sulfuric acid attack, J. Mater. Civ. Eng. 19(2) (2007) 155-163.
23. J. Gao, Z. Yu, L. Song, T. Wang, S. Wei, Durability of concrete exposed to sulfate attack under flexural loading and drying–wetting cycles, Constr. Build. Mater. 39 (2013) 33-38.
24. N. I. Fattuhi, B. P. Hughes, Effect of acid attack on concrete with different admixtures or protective coatings, Cem. Concr. Res. 13(5) (1983) 655-665.
25. G. Jiang, J. Keller, P. L. Bond, Determining the long-term effects of H 2 S concentration, relative humidity and air temperature on concrete sewer corrosion, Water Res. 65 (2014) 157-169.
26. E. Vincke, S. Verstichel, J. Monteny, W. Verstraete, A new test procedure for biogenic sulfuric acid corrosion of concrete, Biodegradation,10(6) (2000) 421-428.
27. S. Thokchom, P. Ghosh, S. Ghosh, Resistance of fly ash based geopolymer mortars in sulfuric acid, ARPN J. Eng. Appl. Sci. 4(1) (2009) 65-70.
28. P. Chindaprasirt, U. Rattanasak, Improvement of durability of cement pipe with high calcium fly ash geopolymer covering, Constr. Build. Mater. 112 (2016) 956-961.
29. T. Bakharev, Resistance of geopolymer materials to acid attack, Cem. Concr. Res. 35(4) (2005) 658-670.
30. A. M. Izzat, A. M. M. Al Bakri, H. Kamarudin, L. M. Moga, G. C. M. Ruzaidi, M. T. M. Faheem, A. V. Sandu, Microstructural analysis of geopolymer and ordinary Portland cement mortar exposed to sulfuric acid, Mater. Plast. 50(3) (2013) 171-174.
31. M. A. M. Ariffin, M. A. R. Bhutta, M. W. Hussin, M. M. Tahir, N. Aziah, Sulfuric acid resistance of blended ash geopolymer concrete, Constr. Build. Mater. 43 (2013) 80-86.
32. M. Albitar, M. M. Ali, P. Visintin, M. Drechsler, Effect of granulated lead smelter slag on strength of fly ash-based geopolymer concrete, Constr. Build. Mater. 83 (2015) 128-135.
33. M. Albitar, P. Visintin, M. M. Ali, M. Drechsler, Assessing behaviour of fresh and hardened geopolymer concrete mixed with class-F fly ash, KSCE J. Civil Eng. 19(5) (2015) 1445-1455.

34. H. F. W. Taylor, Cement chemistry, second ed., Thomas Telford, London, 1997.
35. A. Gabrisova, J. Havlica, S. Sahu, Stability of calcium sulphoaluminate hydrates in water solutions with various pH values, Cem. Concr. Res. 21(6) (1991) 1023-1027.
36. J. L. Provis, J. S. J. Van Deventer, Geopolymers: structures, processing, properties and industrial applications, Woodhead, Cambridge, 2009.
37. V. Sata, A. Sathonsaowaphak, P. Chindaprasirt, Resistance of lignite bottom ash geopolymer mortar to sulfate and sulfuric acid attack, Cem. Concr. Compos. 34(5) (2012) 700-708.
38. M. D. Cohen, B. Mather, Sulfate attack on concrete: research needs, Mater. J. 88(1) (1991) 62-69.

Chapter 3. Journal Paper 2 – Long-term Behaviour of Concretes and Evaluation of Measurement Technique

Introduction

This chapter contains the paper "sulphuric acid exposure of conventional concrete and alkali-activated concrete: assessment of test methodologies". Having established that increase acid concentration is the most effective degradation test method in Chapter 2, this chapter focuses on the assessment of the indicators of susceptibility to corrosion, including acid consumption, change of mass, length, compressive strength, and cross-section via the investigation on long-term behaviour of OPC and AA concrete under 1% sulphuric acid attack in comparison with the test under 3% sulphuric acid attack. This chapter also investigates the long-term behaviour of concrete with coarse aggregate chosen to be susceptible to attack under sulphuric attack. The results show that a test procedure to indicate the susceptibility of concretes can be performed within a reasonable time frame for standard testing. The influence of limestone coarse aggregate on the sulphuric acid resistance of OPC and AA concrete is investigated to further understand the degradation mechanism of concretes under sulphuric acid attack.

List of manuscripts

Gu, L., Bennett, T. and Visintin, P., 2018. Sulphuric acid exposure of conventional concrete and alkali-activated concrete: assessment of test methodologies. Submitted to *Construction and Building Materials.*

Statement of Authorship

Title of Paper	Sulphuric acid exposure of conventional concrete and alkali-activated concrete: assessment of test methodologies
Publication Status	☐ Published ☐ Accepted for Publication ☑ Submitted for Publication ☐ Unpublished and Unsubmitted work written in manuscript style
Publication Details	Gu, L., Bennett, T. and Visintin, P., 2018. Sulphuric acid exposure of conventional concrete and alkali-activated concrete: assessment of test methodologies. Submitted to *Construction and Building Materials.*

Principal Author

Name of Principal Author (Candidate)	Lei Gu		
Contribution to the Paper	Developed the test methodologies, performed analysis on all samples, interpreted data, and wrote manuscript.		
Overall percentage (%)	70		
Certification:	This paper reports on original research I conducted during the period of my Higher Degree by Research candidature and is not subject to any obligations or contractual agreements with a third party that would constrain its inclusion in this thesis. I am the primary author of this paper.		
Signature		Date	5/9/2018

Co-Author Contributions

By signing the Statement of Authorship, each author certifies that:

i. the candidate's stated contribution to the publication is accurate (as detailed above);

ii. permission is granted for the candidate in include the publication in the thesis; and

iii. the sum of all co-author contributions is equal to 100% less the candidate's stated contribution.

Name of Co-Author	Terry Bennett		
Contribution to the Paper	Supervised development of work, helped in data interpretation and manuscript evaluation.		
Signature		Date	5/9/2018

Name of Co-Author	Phillip Visintin		
Contribution to the Paper	Supervised development of work, helped in data interpretation and manuscript evaluation.		
Signature		Date	05/09/2018

Sulphuric acid exposure of conventional concrete and alkali-activated concrete: assessment of test methodologies

Lei Gu[1], Terry Bennett[1] and Phillip Visintin[1]
[1]School of Civil, Environmental and Mining Engineering, The University of Adelaide, SA 5005, Australia

Abstract: Biogenic sulphuric acid corrosion can lead to significant degradation of Ordinary Portland Cement Concrete (OPCC) and cause significant damage to wastewater infrastructure. Recent studies have suggested that alkali-activated concrete (AAC) has improved durability compared to OPCC in a range of aggressive environments. In this study, the resistance of both OPCC and AAC to sulphuric acid is investigated in order to develop a simple laboratory test method, capable of indicating and the susceptibility of both materials to biogenic acid corrosion. Tests that provide an indication of the susceptibility of cementitious materials to corrosion (change of mass, length, compressive strength, and cross-section) are undertaken under exposure to 1% and 3% sulphuric acid concentration for 495 and 112 days respectively, in order to establish the ability to accelerate testing. Further, characterization tests are conducted to investigate the change of specimens at the microstructural level. The indicators of susceptibility to corrosion are discussed based on their potential advantages and limitations as well as application to both OPCC and AAC. The results show that although the alkali-activated matrix partially retains strength after sulphuric acid attack, the coarse aggregates in the alkali-activated concrete are more prone to attack than those in an Ordinary Portland Cement matrix. It is also shown that using a higher concentration sulphuric acid accelerates the degradation of specimens sufficiently to perform an indicator test within 90 days.

Keywords: concrete degradation; sulphuric acid corrosion; microstructure; alkali-activated concrete; assessment of test methodologies

1. Introduction

One of the most rapid cases of concrete degradation is that which occurs in sewage collection systems. In these systems the combination of bacteria, moisture, and oxygen in the atmosphere results in the production of biogenic sulphuric acid [1, 2]. It has been estimated that the annual maintenance costs associated with biogenic corrosion are over €450 million in Germany and £85 million in the UK; while United States it is expected that US$390 billion dollars will be spent on the repair of wastewater infrastructure over the period from 2002 to 2022 [3, 4].

The mechanism of biogenic sulphuric acid corrosion is complex, and its replication in a laboratory environment requires sophisticated experimental apparatus and bacterial growth. Although possible in a multidisciplinary university research environment [5], the equipment and skills required are not readily available in a typical civil engineering materials testing laboratory. As an alternative to the direct simulation of the wastewater environment, previous studies have instead focused on the exposure of cementitious materials to chemical sulphuric acid, in this way it is possible to expose materials to pH typical of wastewater environments but without the need for generating it through bacterial action [5-8].

In addition to simplification of the exposure regime, a simple, repeatable methodology is desirable. Candidate approaches, such as length change, mass loss, corrosion depth, acid consumption and reduction in alkalinity provide a means of indicating the durability performance of Ordinary Portland Cement Concrete (OPCC), but may not translate well to other cementitious materials. For example, the standard test methodology for acid resistance (ASTM C 267 [9]) only covers silicate concrete and other hydraulic materials, and is not specifically applicable to other concretes.

Recently, alkali-activated concrete (AAC) has been suggested as an alternative to OPCC, with potential for enhanced durability characteristics in civil engineering applications [10, 11]. This improved durability has been mainly attributed to the different chemical composition of the matrix material. For example, Izzat et al. [12] found that class C fly ash based geopolymer mortar had lower mass loss and compressive strength reduction when samples were immersed in 3% sulphuric acid solution for 120 days when compared to the Ordinary Portland Cement (OPC) mortar. Thokchom et al. [10] also concluded that class F fly ash based geopolymer mortar had good resistance against 10% sulphuric acid for 18 weeks.

The aim of this programme of work is to assess the applicability of a simplified exposure regime and commonly applied durability indicators to vastly different binders. Further, it is intended that a test methodology be developed that can capture degradation in a short period of time. While both OPCC and AAC are considered, direct comparison of the performance of OPCC and AAC is not the intended focus as this would be highly dependent on the material design.

This paper initially provides the details of the experimental program, including material

information, test procedures and instrumentation. The results of the experimental program are then presented, and the different measurement techniques are discussed in reference to their potential advantages and limitations. A detailed discussion on the results is then presented, where the different measurement techniques are assessed based on their ability to represent changes in compressive strength.

2. Materials and methodologies

Specimens are manufactured to provide an indication of sulphuric acid degradation in terms of acid consumption, mass loss, length change, pH change, corrosion depth and microstructural change. As a direct measure of the impact of degradation the change in compressive strength is also quantified.

In this section, information on the materials used to manufacture the concrete, details of test specimens and the test methodology employed are presented.

2.1 Sample preparation

As the primary focus of this study is to evaluate test methodologies, the materials to be investigated have been chosen to be to be susceptible to attack, that is conventional concretes are manufactured using OPC rather than Sulphate Resisting Cement, and with crushed limestone and river sand as coarse and fine aggregate respectively.

The complete chemical composition of the General Purpose cement is provided in Table 1, along with that of the fly ash used to manufacture the AAC. Crushed limestone having specific gravity of 2.65 and fineness modulus of 5.4 was used as coarse aggregate. River sand having specific gravity of 2.61 and fineness modulus of 2.3 was used as fine aggregate. The activator used in the manufacture of the AAC consisted of laboratory grade sodium silicate (Na_2SiO_3) and 14 molar sodium hydroxide (NaOH) which was pre-mixed in a ratio of Na_2SiO_3: NaOH of 1.5:1.

Table 1. Chemical composition of binders

Oxide (wt%)	SiO_2	Al_2O_3	Fe_2O_3	CaO	MgO	Na_2O	K_2O	SO_3	TiO_2	P_2O_5	Mn_2O_3	LOI*
Cement	19.89	4.69	3.16	63.35	1.94	0.22	0.40	2.77	0.27	0.03	0.07	3.55
Fly ash	54.24	28.94	4.01	3.58	1.80	0.60	1.46	0.25	1.21	0.27	0.06	3.12

LOI: Loss on ignition

The mix proportions of the (OPCC and the AAC are given in Table 2, in which the AA concrete mix was designed according to Albitar et al. [13]. The water to cement ratios of OPCC_30 and OPCC_50 were 0.64 and 0.47, respectively and were designed according to [14]. All the aggregates were used in saturated surface dry condition.

After casting, the OPCC specimens were cured in their moulds at 20±2°C for 24 hours before demoulding, after which they were cured in a fog room at a constant temperature of 22 °C for 28 days. The AAC specimens were cured in moulds at 20±2°C for 48 hours before demoulding, specimens were then covered using double layer vacuum bags and cured in the fog room at 22°C for 28 days. As a control the 28 day compressive strength of all mixes was determined from compressive tests conducted on standard 100 mm x 200 mm cylinders according to ASTM C39 [15] and was found to be 36.4 MPa, 57.8 MPa and 22.2 MPa for mixes OPCC_30, OPCC_50 and AAC respectively.

Table 2. Mix proportion of OPC and AA concrete

Mix ID	Cement (kg/m^3)	Fly ash (kg/m^3)	Limestone (kg/m^3)	Sand (kg/m^3)	Water (kg/m^3)	Superplasticizer (kg/m^3)	NaOH (kg/m^3)	Na_2SiO_3 (kg/m^3)
CC_30	280	0	1110	740	180	0	0	0
CC_50	360	0	1110	740	171	1	0	0
AAC	0	424.8	1176	576	16.8	48	63.4	95.0

2.3 Test methodology

For testing, the specimens were laid on a plastic grid and submerged in a bath of 1% (w/w %) sulphuric acid solution. In order to manage the pH change, the sulphuric acid solution to specimen ratio was chosen as 4.5 (suggested by ASTM C1012 [16] in sulphate attack test). The pH level was maintained at 1.0±0.05, monitored by a portable digital pH meter, and adjusted twice a week by the addition of 35% (w/w %) sulphuric acid. Throughout the test period the solution was continuously circulated using pumps to avoid the development of strong ion gradients, to assist with this a minimum spacing of 5 cm between specimens was maintained. To eliminate the influence of evaporation, lids was used to cover the test tubs.

The choice of 1% sulphuric acid was based on simulating a pH that can exist in wastewater environments where severe degradation is observed [4, 6]. The immediate exposure to 1% sulphuric acid is however accelerated in comparison to field like conditions where the process of bacterial growth can take several years to reach this pH level [17].

To provide an indication of sulphuric acid degradation, acid consumption, mass loss, length change, pH change, corrosion depth and microstructural change were all observed for a period of 495 days. As a direct measure of the impact of degradation the change in compressive strength is also quantified. The methodology for each test is summarised as follows:

- Coarse aggregate samples were immersed in 1% sulphuric acid solution and EDX analysis performed at 14 and 495 days to determine the chemical composition of the reaction product.
- The microstructural change of OPCC and AAC specimens before and after sulphuric acid attack (at days 42, 142 and 495) was examined by scanning electron microscopy (SEM) and energy dispersive x-ray (EDX) using a Phillips XL 30 instrument. For the analysis, samples were taken from the surface (4~5 mm depth) at the mid-height of a standard (100 × 200 mm) cylindrical specimen. Samples were coated with platinum prior to SEM analysis, and EDX was performed at an accelerating voltage of 15 kV.
- The consumption of acid solution was recorded twice weekly, when the pH of the sulphuric acid solution was measured and adjusted accordingly.
- Change in surface alkalinity was determined using a 1% Phenolphthalein solution to identify the proportion of the cross section with a pH greater than 8.2. This solution was applied to a cylindrical disk of diameter 100mm and thickness 10 mm that was cut from the mid-height of a standard 100 mm x 200 mm cylinder. The change in alkalinity was measured at 42, 140, 260, 375, 495 days. The depth of area with a pH of greater than 8.2 was determined by measuring the radius of unaffected area at nine locations via a digital microscope.
- The change in mass after periods of exposure was measured using prism specimens 75 mm by 75 mm in cross section and 285 mm in length according to ASTM C 267 [9]. The mass of a single specimen was periodically measured (at days 9, 23, 51, 142, 260, 375, and 495). In order to remove the influence of surface moisture, according to De Belie et al. [2], prior to weighing, the specimen was dried at 20±2°C for 48 hours.

- The length change of a prismatic specimen (75 × 75 × 285 mm) was determined by measuring the length of a single specimen, per concrete, between the DEMEC gauges according to ASTM C1012 [16]. Tests were conducted after 4 hours of drying at 20±2°C, according to De Belie et al. [18].
- The compressive strength of cylindrical specimens (100 mm in diameter and 200 mm in height) was determined according to ASTM C39 [15]. To ensure the loading faces were parallel to the loading platens the ends of the specimens that had been damaged by exposure to sulphuric acid were capped with a gypsum paste.

3. Test Results of Concretes under 1% Sulphuric Acid Attack

In this section, the change in physical, mechanical and microstructural properties of the OPCC and ACC samples exposed to 1% sulphuric acid are presented.

3.1 Visual appearance

Figure 1 shows the visual appearance of OPCC and AAC specimens after 495 days immersion in 1% sulphuric acid. In Figure 1(a) it can be seen that the OPCC_30 specimen showed a mild degree of corrosion, characterised by a small degree of expansion and spalling of cement paste and aggregates. The OPCC_50 specimen in Figure 1(b) showed severe corrosion, characterised by significant expansion and large areas in which the cement matrix and aggregates in the surface spalled, leading to a very porous surface structure. The AAC specimen Figure 1(c) showed the most significant corrosion with a large amount of spalling of the mortar and coarse aggregates, leading to an irregular shape and smaller size of the specimen when compared to that before immersion.

(a) (b) (c)

Figure 1. Specimens after immersion in 1% sulphuric acid for 18 months: (a) OPCC_30; (b) OPCC_50; (c) AAC

3.2 Influence of sulphuric acid on coarse aggregate

Figure 2 presents the visual appearance of limestone aggregate before and after 1% sulphuric acid exposure. It can be seen that apart from the formation of a white leachate, the limestone aggregate after 14 days immersion in sulphuric acid in Figure 2(b) showed no significant difference to that before immersion (Figure 2(a)). Figure 3 shows the results of an XRD analysis of the white leachate which can be concluded to be predominantly gypsum.

Although it is hard to distinguish the source of gypsum in OPCC because of the presence of C-H and C-S-H in the matrix, the additional gypsum formed on the surface of limestone aggregate would grow together with the gypsum formed from cement paste.

Figure 2(c) shows the severe degradation of limestone after 495 days immersion in 1% sulphuric acid. This severe degradation can be attributed to the continued leaching of calcium causes and resulted in a very weak internal structure due to the high CaO contents of aggregate (43-46%).

(a) Before immersion

(b) 14 days immersion

(c) 495 days immersion

Figure 2. Limestone aggregate before and after 1% sulphuric acid exposure

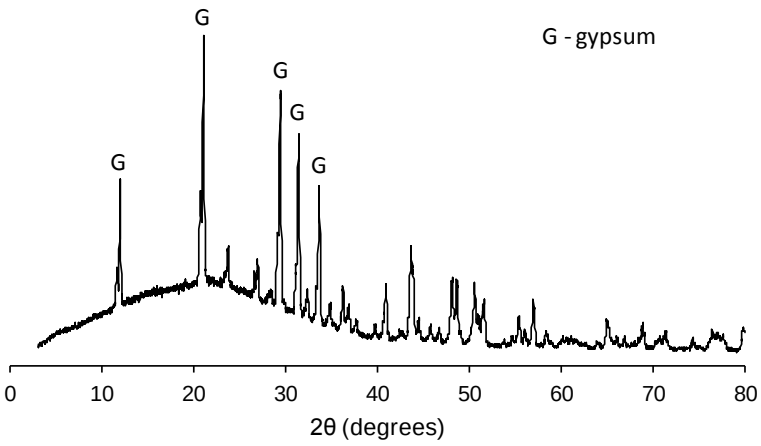

Figure 3. XRD pattern of the white leachate from limestone aggregate after 1% sulphuric acid exposure

3.2 Microstructural performance

3.2.1 Surface morphology and element change of OPC and AAC matrix

Figure 4 shows the SEM images of the OPCC and AAC concrete samples before and after 495 days sulphuric acid immersion, while Table 3 shows the results of surface element analysis by EDX at the areas marked A to E in Figure 4. The cement matrix in area A in Figure 4(a) showed a dense amorphous structure before immersion with the typical calcium silica hydrate (C-S-H) chemical composition expected from OPC [19] (Table 3). The rod like structure in area B of Figure 4(a) was identified as ettringite which formed as a result of the high aluminium and sulphur concentrations identified in Table 3. The sulphur content observed in the sample before immersion is present due to the addition of gypsum during cement manufacture [19].

After 495 days of immersion in sulphuric acid, the OPC paste in Figure 4(b) exhibited monoclinic crystals which were reasoned to be gypsum ($CaSO_4 \cdot 2H_2O$), based on the atomic ratio of Ca:S:O obtained from the EDX analysis (see Table 3). Also of note in Figure 4(b) is that some amorphous structures are attached to the gypsum crystals, these can be inferred to be silica gels leached from the C-S-H during the sulphuric acid attack, as identified by high silicon and oxygen concentrations detected by EDX. The leaching of silica gels from C-S-H under sulfuric acid attach is also observed by previous study [20]. The presence of a large amount of expansive gypsum crystals in the matrix resulted in the porous structure shown in Figure 4(b). No ettringite was observed in degraded area shown in Figure 4(b), as ettringite is only stable above pH over 10.7, and when pH below 10.0 only gypsum and soluble aluminium sulphate are the stable phases [4].

The AA paste in area D in Figure 4(c) also showed a dense amorphous structure before immersion with a typical sodium aluminosilicate hydrate (N-A-S-H) chemical composition [21] shown in in Table 3. The AA paste after 495 days immersion in area E in Figure 4(d) showed a similar structure in morphology from that in Figure 4(c) before immersion. However, from the Table 3, the surface element analysis showed the atomic ratio of Si-to-Al increased from 2.0 in area D to 3.1 in area E. According to Bakharev [22] this is because the Si-O-Al bond in N-A-S-H is broken by the hydrogen ions during the sulphuric acid attack, dissolving of tetrahedral aluminium from the N-A-S-H framework.

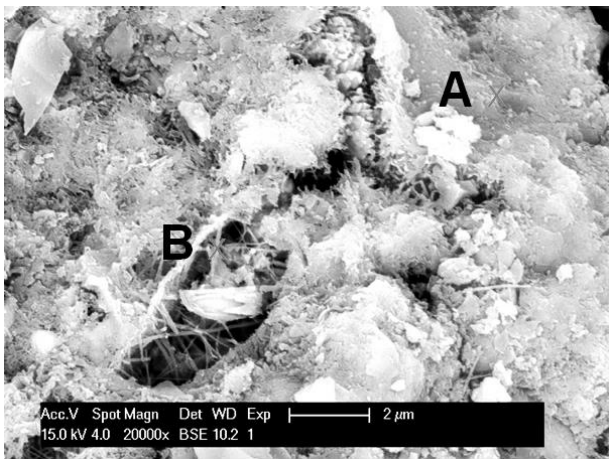

(a) OPC matrix before immersion

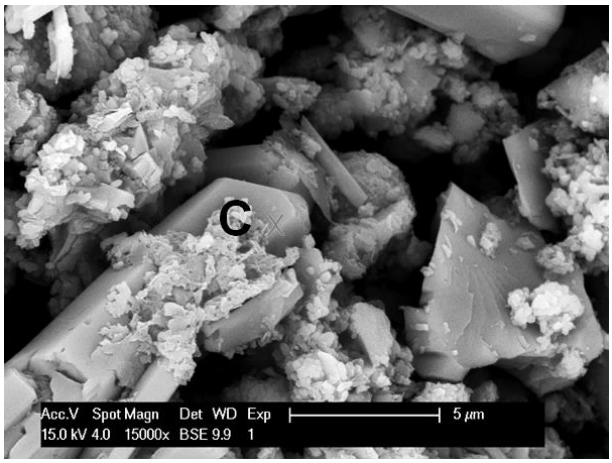

(b) OPC matrix after immersion

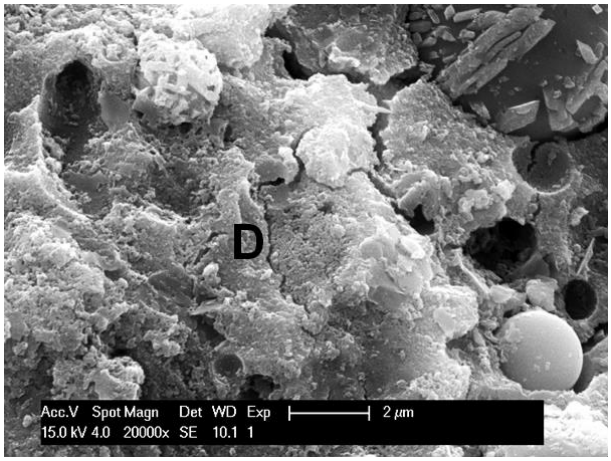

(c) AAC matrix before immersion

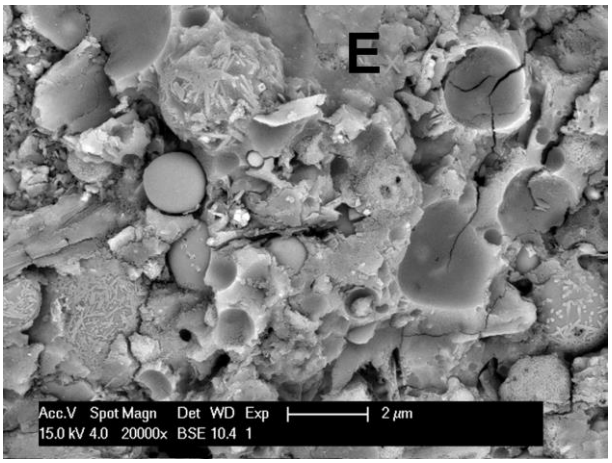

(d) AAC matrix after immersion

Figure 4. SEM images and surface element analysis of OPC and AAC matrix before and after 495 days immersion

Table 3. Surface element analysis in the marked area in Figure 4 by EDX

	Area A		Area B		Area C		Area D		Area E	
Element	Wt.%	At.%	Wt.%	At.%	Wt.%	At.%	Wt.%	At.%	Wt.%	At.%
Oxygen	40.7	60.8	39.0	59.5	56.4	74.4	41.6	55.7	40.2	54.4
Sodium	-	-	-	-	-	-	3.6	3.3	2.2	2.0
Aluminium	3.0	2.7	4.8	4.3	-	-	16.4	13.0	12.0	9.6
Silicon	14.0	11.9	1.3	1.2	-	-	34.0	26.0	39.4	30.4
Sulphur	-	-	9.9	7.6	19.6	12.9	-	-	3.2	2.1
Potassium	2.7	1.6	-	-	-	-	-	-	1.4	0.8
Calcium	35.6	21.2	45.0	27.5	24.0	12.7	2.1	1.1	-	-
Iron	4.0	1.7	-	-	-	-	2.3	0.9	1.74	0.7

Wt. %: Weight percentage; At. %: Atom percentage

3.2.2 Change of fine aggregate interfacial transition zone

Figure 5 shows the change in interfacial transition zone (ITZ) between the paste and fine aggregates of OPCC and AAC samples. It can be seen from Figures 5(a) and (c) that the ITZ of both unexposed OPCC and AAC samples indicate a firm bond between the matrix and aggregate. After 495 days of exposure to sulphuric acid solution, the OPCC samples show the formation of gypsum crystals (Figure 5(b)). The development of gypsum crystals in the ITZ causes the debonding of aggregates from the specimens shown in Figures 1(a) and (b) and leads to significant decrease in the strength of the specimen.

The ITZ with fine aggregates of an AAC sample after immersion (Figure 5(d)) showed a similar structure in morphology from that before immersion in Figure 5(c) suggesting AA paste remained in good form under sulphuric acid attack. A similar observation has also been made in previous studies [21].

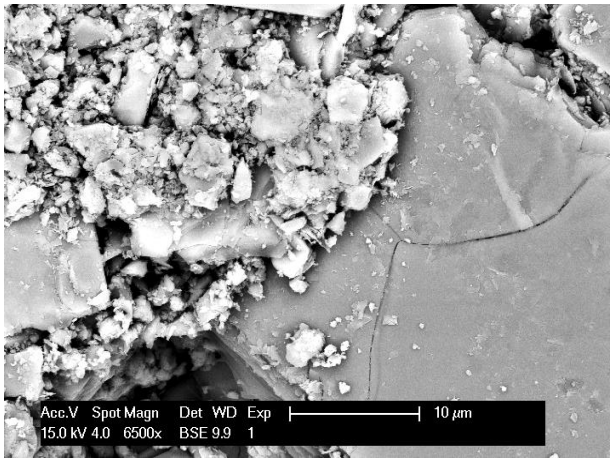

(a) OPCC samples before immersion

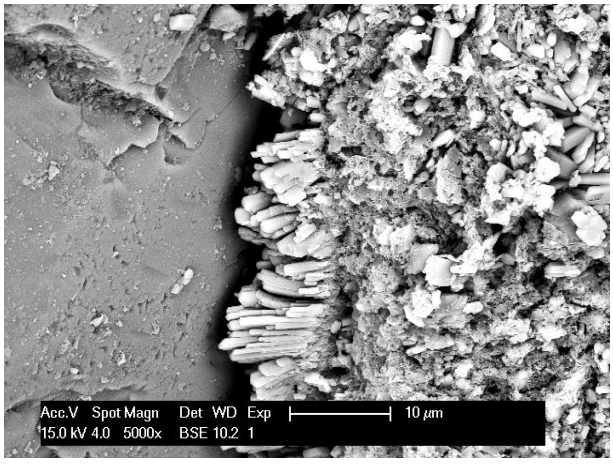

(b) OPCC samples after 495 days immersion

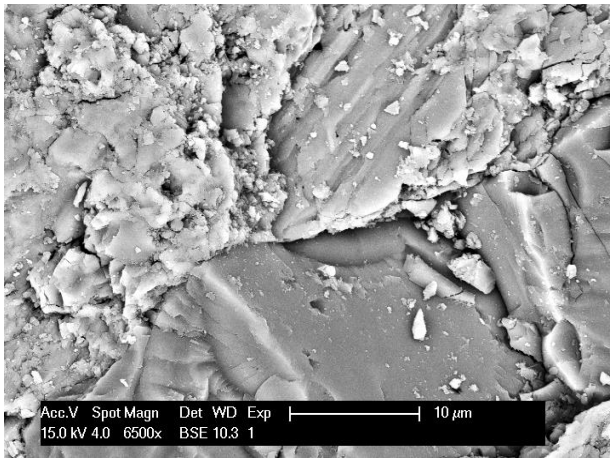

(c) AAC samples before immersion

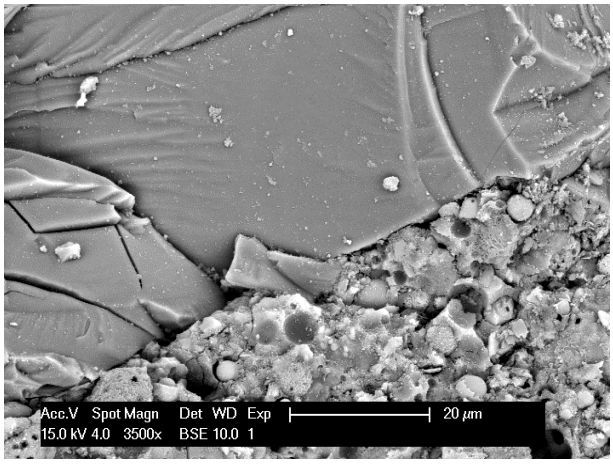

(d) AAC samples after 495 days immersion

Figure 5. Change of fine aggregate interfacial transition zones

3.2.3 Change of coarse aggregate interfacial transition zone in AAC

The SEM image in Figure 6 show the presence of gypsum in the vicinity of the ITZ surrounding the coarse aggregate in an AAC sample, as identified by the chemical composition obtained from EDX analysis (Table 4). This expansive mechanism caused the significant spalling of aggregates as seen in Figure 1(c).

Unlike the OPCC degradation under sulphuric acid attack, the degradation process in AAC does not generate any product that can act as a short-term protective barrier [4]. Therefore, when sulphuric acid penetrates through the AA fly ash matrix, the aggregates are directly expose to the acidic environment. This allows for a more rapid dissolution of the calcium compounds from the coarse aggregate (limestone). These calcium ions subsequently formed gypsum when the sulphate ions diffused in the matrix, resulting in a porous and soft structure

near the ITZ, leading to the debonding of aggregates from the specimens shown in Figure 1(c) and significant decrease in the strength of the specimen. As discussed in the previous section, the degraded AA fly ash matrix and the ITZ near the fine aggregate showed a similar structure in morphology from that before immersion, thus the formation of expansive gypsum at the ITZ with the coarse aggregate is the primary deterioration mechanism in AAC. Hence it can be suggested from this experiment that investigations of durability must focus not only on the performance of the paste but must also consider the influence of the aggregate.

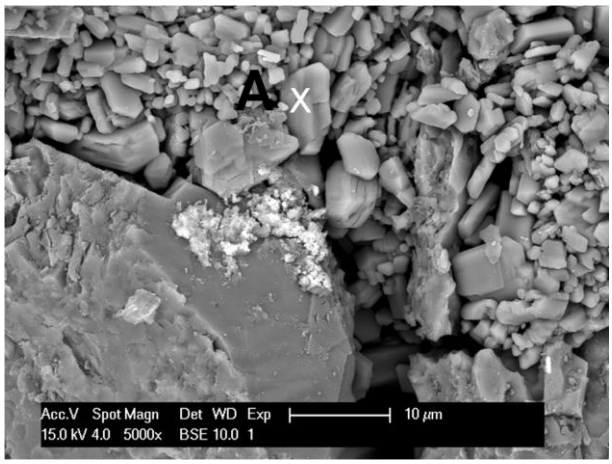

Figure 6. Coarse aggregate interfacial transition zone in AAC after 495 days immersion

Table 4. Surface element analysis in the marked area in Figure 3 by EDX

	Element	Oxygen	Aluminium	Silicon	Sulphur	Calcium
Area A	Wt.%	53.2	1.3	4.3	16.7	24.4
	At.%	71.4	1.0	3.3	11.2	13.1

Wt. %: Weight percentage; At. %: Atom percentage

3.3 Consumption of sulphuric acid

Acid consumption per specimen provides the quantity of sulphuric acid consumed, indicating the quantity of the chemical reactions including hydrogen ions, sulphate ions and concrete specimens (including both cementitious matrix and aggregates) during the corrosion process [4]. Therefore, acid consumption might be viewed as a direct chemical indicator of the performance of the cementitious material when exposed to an acidic environment.

Figure 7(a) presents the consumption of sulphuric acid per specimen for all material types. The acid consumption of OPCC_30 specimens increased slowly to 0.35 kg during the initial 260 days and subsequently stabilised. The acid consumption of OPCC_50 specimens increased

rapidly to 0.43 kg during the initial 142 days, and also subsequently increased at a reduced rate to 0.78 kg after 142 days. From these results, it is shown that OPCC specimens with higher cement content (i.e. 380 kg/m^3 in OPCC_50) have higher acid consumption than those with lower cement content (i.e. 280 kg/m^3 in OPCC_30).

The acid consumption of AAC specimens remained at 0 during the first 14 days of exposure before increasing significantly. This phenomenon was attributed to the formation of barrier of carbon dioxide on the surface of AAC specimens discussed in Gu et al. [25]. After this initial period acid consumption increased at a relatively constant rate. Among all the tests, the AAC specimens consumed much more sulphuric acid than the OPCC specimens.

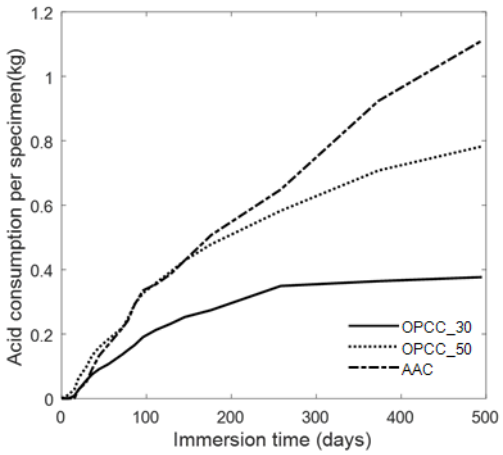

Figure 7. Acid consumption of OPC and AA concrete specimens under 1% sulphuric acid attack

3.4 Depth of the area lost alkalinity

Using Phenolphthalein, the depth into the specimens at which the pH of the concrete has reduced to less than 8.2 was measured from the average of nine measurements on a sample. The results from four unique samples, per concrete type, are shown in Figure 8 at each exposure time.

Examining the results in Figures 7 and 8 together, it can be seen that the more sulphuric acid consumed by specimens, the larger depth of the area lost alkalinity developed. Furthermore, the OPCC_30 and OPCC_50 specimens showed a much smaller depth of reduced alkalinity (less than 9 mm) than that of AAC (greater than 40 mm) in figure 8.

The AAC fly ash matrix has lower initial pH environment in its pore fluid (i.e. 10.5-12.6 [26]) than that in hydrated OPCC matrix (i.e. 13-14 [27]). The depth of the area lost alkalinity can only be an indicator to represent the degradation when comparing the same material (i.e. OPCC_30 and OPCC_50) and is unlikely to be a reasonable indicator for comparing the performance of OPCC and AAC.

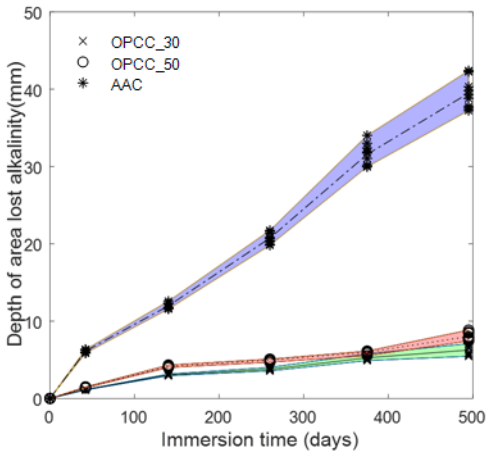

Figure 8. Depth of lost alkalinity of OPC and AA concrete specimens under 1% sulphuric acid attack

3.5 Mass change

Figure 9 presents the mass loss of concrete specimens relative to the initial weight of the specimen prior to immersion, with three measurements taken at each time. It can be observed that the mass loss of OPCC_30 specimens increased to around 2% during the initial 142 days and subsequently stabilised. The mass loss of OPCC_50 specimens increased almost linearly to around 5.5% during the entire test period. The mass loss of AAC specimens increased slowly during the initial 51 days and subsequently rapidly increased to over 40% after 495 days.

The difference in mass loss between the OPCC and AAC specimens is an indicator of the degradation level of the specimens. That is, as shown in Figure 1, OPCC_30 and OPCC_50 specimens only suffered from minor spalling compared to AAC which suffered a significant loss of aggregate due to damage to the ITZ. Thus, mass loss may be a reliable indicator only when minor degradation occurs, and would be significantly affected by de-bonding and spalling off of coarse aggregates and large pieces of mortar when severe degradation occurs.

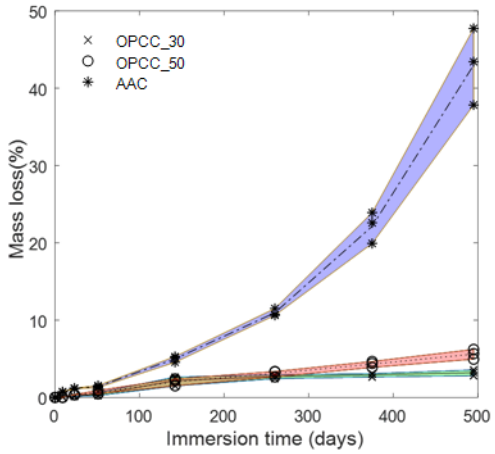

Figure 9. Mass loss of OPC and AA concrete specimens under 1% sulphuric acid attack

3.6 Length change

Figure 10 presents the change in length of the concrete specimens relative to their initial length. As shown in Figure 8, the sulphuric acid only penetrates 5-9 mm from the surface in OPC concrete specimens whereas the acid penetrates around 40 mm in AA concrete specimens. Thus, the expansion products in OPCC specimens are only generated near to the surface whereas, a large proportion of the AAC specimens are affected by sulphuric acid. It can be seen in Figure 10 that a significant increase in length was observed in AAC after 260 days immersion. This phenomenon can be explained by that the limestone coarse aggregate in AAC was attacked by sulphuric acid, generation expansive gypsum in the ITZ, causing significant expansion of the entire specimen after large proportion of the AAC specimens affected by sulphuric acid. The differences in length change is useful for interpreting how the different materials degrade, but can only be used as an indicator to represent the degradation when comparing similar materials.

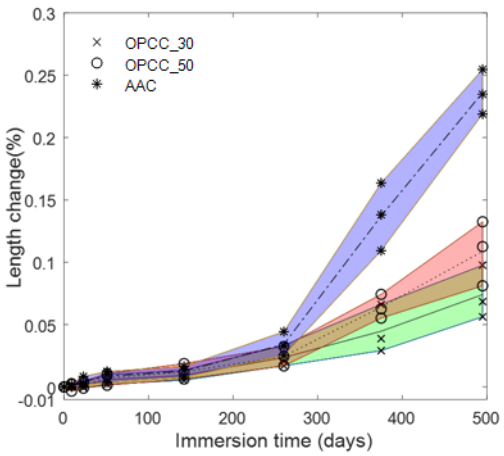

Figure 10. Length change of OPC and AA concrete specimens under 1% sulphuric acid attack

3.7 Compressive strength

Figure 11 presents the compressive strength of the concrete specimens, in which three specimens were tested at each time period. It can be noted that at early ages for both OPCC_30 and ACC a strength gain occurs due to the continued hydration of the OPCC and AAC fly ash matrix as discussed in Gu et al. [25].

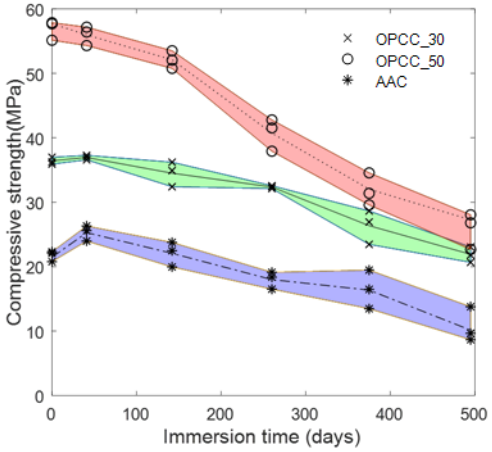

Figure 11. Compressive strength change of OPC and AA concrete specimens under 1% sulphuric acid attack

4. Discussion

In order to identify a test methodology for rapidly assessing the performance of cementitious materials subjected to sulphuric acid attack, the results of the long term exposure tests presented in section 3 (exposure to 1% sulphuric acid solution for 495 days) are compared to those obtained from identical concrete specimens subjected to 3% (w/w %) sulphuric acid exposure for a period of 112 days.

The tests performed at 1% sulphuric acid concentration, or pH 1, are representative of the lowest pH expected to be encountered in field conditions where sulphur oxidising bacteria are present and have developed over time [17]. These tests required a period of at least one year to observe a noticeable reduction in compressive strength. To further accelerate the test methodology, to perform a test within a reasonable amount of time, specimens prepared at the

same time were immersed in 3%, pH 0.52, sulphuric acid concentration. The results of these tests are documented in [25] and are here compared with the current results.

The cement content of OPCC has significant influence on the sulphuric acid resistance of concrete based on the test results presented in section 3. It is shown that specimens with higher cement content (i.e. 380 kg/m^3 in OPCC_50) have more severe degradation in visual appearance, higher acid consumption, larger depth of lost alkalinity, larger mass loss, larger expansion in length, and larger compressive strength loss than those with lower cement content (i.e. 280 kg/m^3 in OPCC_30). A similar observation has also been made by Aiken et al. [29]. The morphology and surface element change of OPCC_30 and OPCC_50 before and after immersion detected by SEM and EDX was similar for both materials, indicating no difference in the reaction process for each material. Further, higher strength concrete usually has lower porosity than that of lower strength concrete [14, 19], indicating that the difference in strength reduction can be explained in terms of initial porosity. It is likely that during the sulphuric acid degradation process, the C-H and C-S-H in the OPC paste is dissolved, generating expansive gypsum and amorphous silica as discussed in section 3. In this process, the higher cement content in concretes with a higher initial strength, would lead to the production of more expansive gypsum, leading to higher porosity in the degraded zone of specimens. This in turn would allow easier penetration of the acid in concretes with a higher cement content. Further study on the performance (porosity, permeability, diffusivity) in the front of acid attack of concrete should be conducted to support the hypothesis.

The visual appearance of typical specimens at the end of their immersion periods are shown in Figure 12. It can be observed by comparing Figure 12(a) with (b) that the OPCC specimens immersed in the 3% concentration displayed greater degradation on its surface than the specimen exposed to the lower concentration (1%), albeit for a greater period of time. Thus indicating that there is pH dependence on the degradation mechanism.

Figure 12(c) and (d) show representative samples of AAC at the end of their respective immersion periods. On initial inspection the 1% acid concentration appears to give rise to greater degradation, however both specimens had a large amount of loose material on their surface, which was removed in Figure 12(c) to show the intact core.

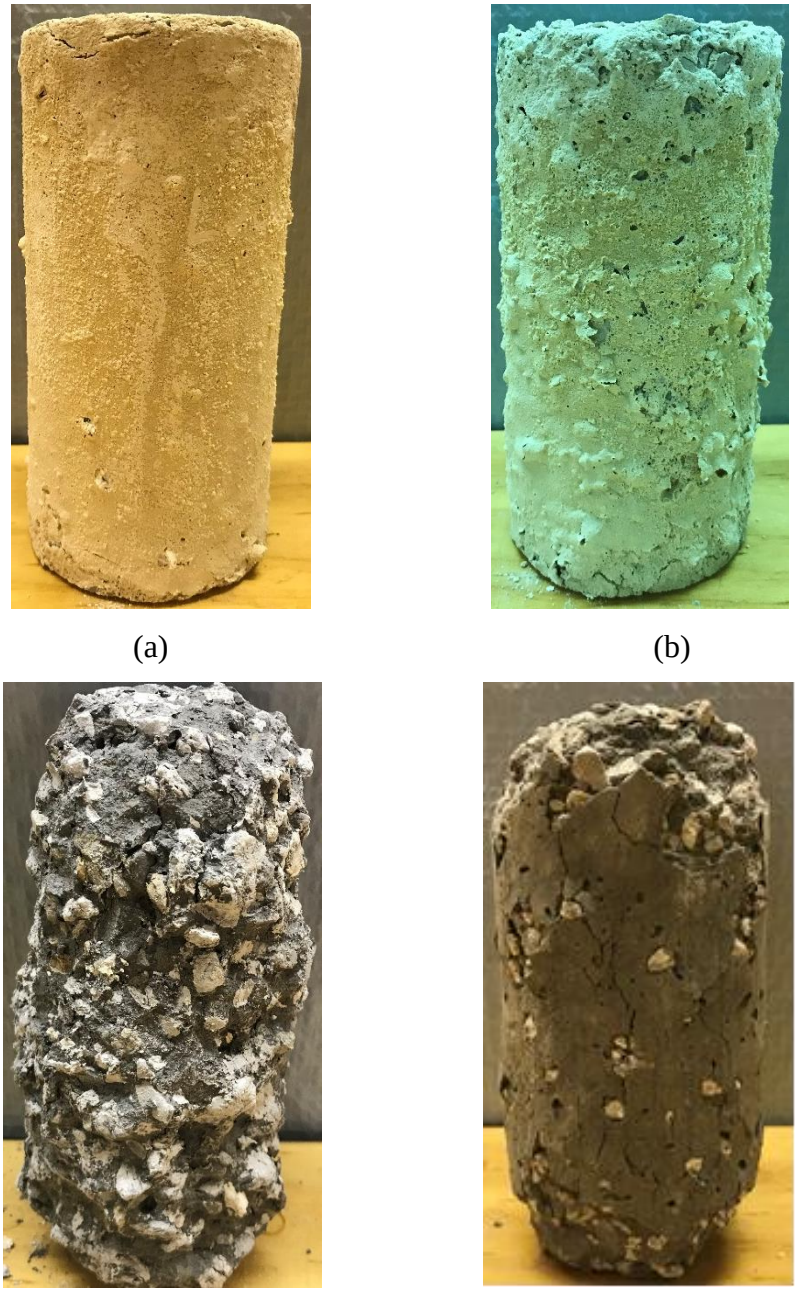

(a) (b)

(c) (d)

Figure 12. The comparison of the visual appearance of OPCC and AAC under 1% sulphuric acid attack for 495 days and 3% sulphuric acid attack for 112 days: (a) OPCC_30 1%; (b) OPCC_30 3%; (c) AAC 1%; (d) AAC 3%

In Figure 13 the mean indicator measurements and compressive strength development with immersion time are plotted for both concrete types and immersion regimes. In Figure 13(a) the marked difference seen between acid consumption levels for the different concretes at lower acid concentration is not repeated when subjected to higher concentration.

The depth of lost alkalinity shown in Figure 13(b) indicates very similar acid penetration depths for OPCC under the differing exposure regimes. The higher acid consumption in 3% concentration (shown in Figure 13(a)), however suggests that the degradation mechanism is altered with pH as the higher ion gradient would be expected to give rise to greater penetration depth. It is possible that the different concentration of sulphuric acid affects the development of gypsum crystals and the development of a protective barrier. This protective barrier could be either chemical via a local reduction of pH [2] or physical in the form of a blocking of the pore space.

In contrast, the depth of penetration in AAC continues to increase with time suggesting that the reaction products in AAC have a much smaller effect in creating an impediment to diffusion. The larger depth of penetration in AAC under 1% acid leads to larger area of paste and coarse aggregate exposed to the sulphuric acid than that under 3% acid, resulting in larger acid consumption. This was also observed in numerous studies of acid resistance of AA pastes and mortars [10, 28, 29], an in depth description of the differences observed in AA and OPC pastes and mortars, particularly with respect to the role of the Ca/Si ratio of the virgin material in creating expansive reaction products, is elucidated by Aiken et al. [29].

The mass loss of OPCC in 1% concentration decelerates after 142 days exposure, whereas in 3% concentration is appears to accelerate after 42 days. This difference in mass loss can be attributed to the different levels of degradation observed on the surface of the 3% exposure specimens as shown in Figure 12(b) compared to that seen in the 1% specimens (Figure 12(a)). The mass loss, in both exposure regimes, for the AAC specimens is accelerating with time, and is reflective of the large amount of spalling of materials seen in Figures 12(c) and (d).

A noticeable difference in length change is observed between the two concrete types in Figure 13(d). This is not unexpected, as measurements were performed with a DEMEC gauge at the centre of the specimens and therefore this reflects the depth of penetration of the acid.

The substantial mass loss recorded in these particular AAC specimens and increased length change further demonstrates that whilst the resistance of a paste or mortar might be indicative of the potential for a material to be resistant to acid attack, the composite material as a whole must be considered. The limestone used in this study might have contributed to the formation

of a beneficial diffusion barrier (chemical or physical) in OPCC, but deleterious expansion in AAC.

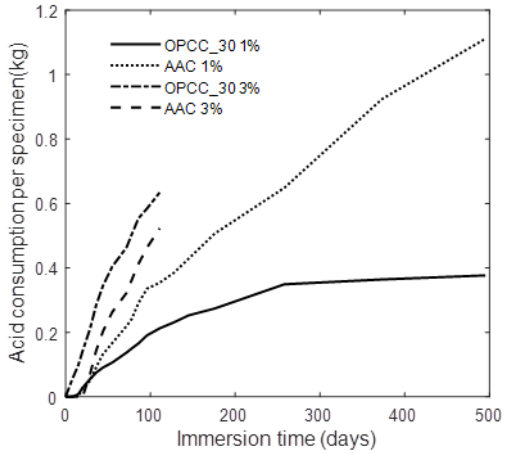

(a)

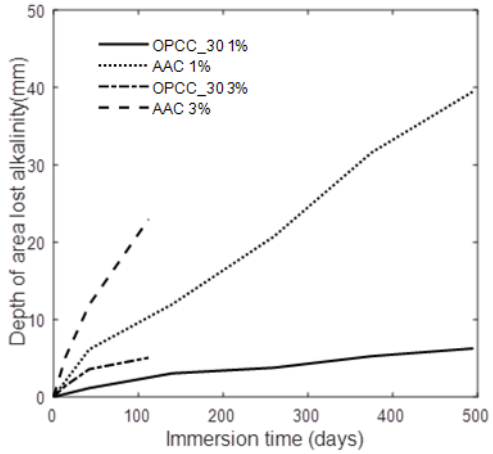

(b)

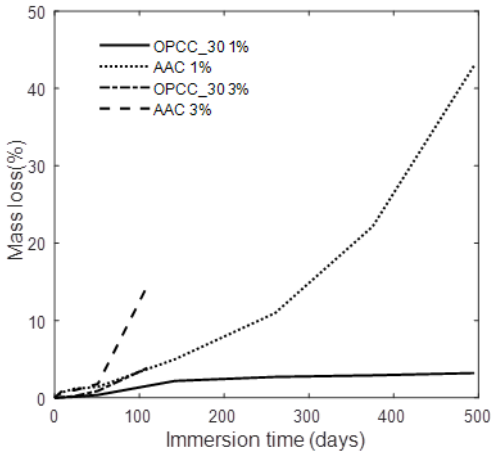

(c)

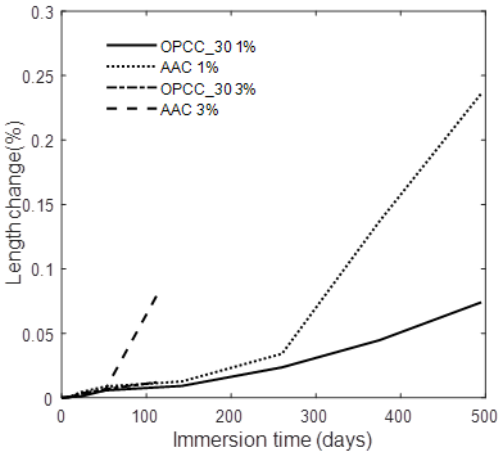

(d)

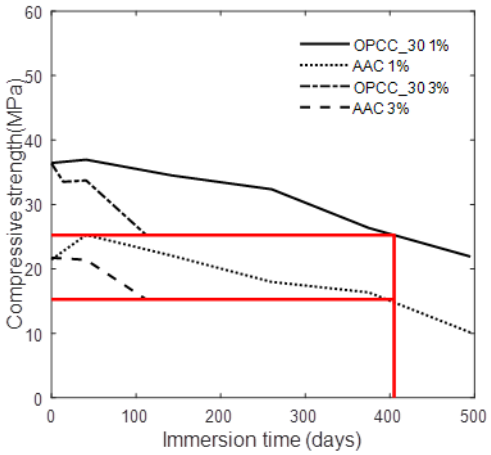

(e)

Figure 13. The comparison of properties under 3% sulphuric acid attack and normalised properties under 1% sulphuric acid attack: (a) acid consumption (b) depth of area lost alkalinity; (c) mass loss; (d) length change; (e) compressive strength change

In Figure 13(e) the change in compressive strength over time of both the OPCC and AAC concretes under both exposure regimes are shown. These results indicate that the total exposure period required to observe the same reduction in strength, for both materials, is substantially reduced (from 400 days to 110 days). This result implies that when using the direct measure of compressive strength, that the exposure to a higher concentration acid is a potential means for accelerating testing.

The similar reductions in compressive strengths are used to assess the reliability of the other measurements to be utilised as indicators. To facilitate this we choose to normalise mass loss and loss of alkalinity. The normalised depth of alkalinity $|d_{Alk}|$ is calculated as

$$|d_{Alk}| = \frac{d_{pH}}{D}$$

where d_{pH} is the depth of lost alkalinity and D is the original diameter of the specimen. The normalized mass loss $|M|$ is calculated as

$$|M| = \frac{M_t}{M_0}$$

where M_t is the mass at an immersion time t and are shown in Figure 14.

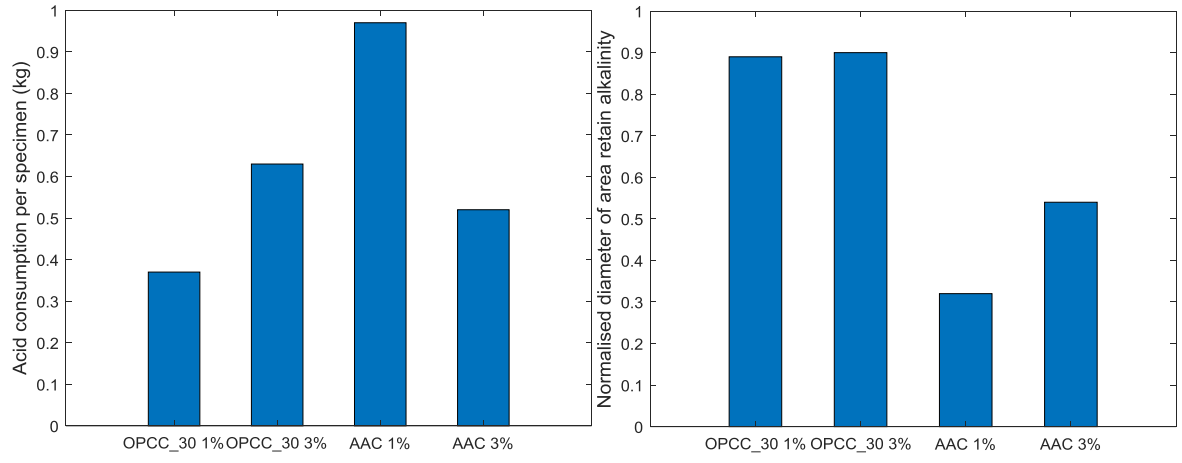

(a) (b)

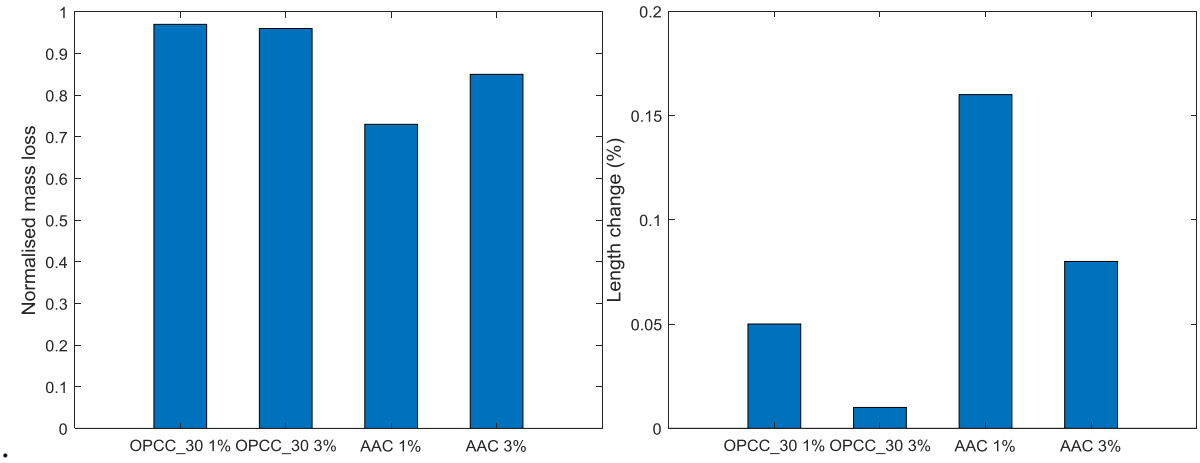

(c) (d)

Figure 14. The properties of 405-day OPCC and AAC under 1% sulphuric acid attack: (a) Acid consumption per sample; (b) Normalised depth of area lost alkalinity; (c) Normalised mass loss; (d) Length change

From the inspection of the sensitivity of the measurements to changes in compressive strength it can be concluded that:

- the retained alkalinity and mass loss could be employed as indicators for OPC based materials;
- none of the measurements appear to give a reliable indicator of the loss of compressive strength for AAC and therefore none can be used as means for comparing the performance of different cementitious materials.

The reduction of compressive strengths shown in Figure 13(e), does however suggest that a rapid test of sulphuric acid resistance could be performed using compressive strength measurements, with complimentary testing of other performance measures, such as depth of penetration, within a reasonable time frame of circa 100 days.

5. Conclusions

An OPC based concrete and Alkali activated concrete were immersed in 1% sulphuric acid solutions for 18 months (495 days). The results of microstructural analysis, strength and a range of candidate indicator measurements are presented. This was performed in order to identify a simple and rapid test procedure to identify the susceptibility of a variety of cementitious materials.

The results presented here are compared with tests on identical concretes (prepared in the same batches) but subjected to 3% sulphuric acid concentrations. From a combination of the microstructural analyses, recorded acid consumption per specimen and the depth of acid penetration (as indicated through measuring the depth of lost alkalinity) it was found that:

- The mechanism of acid degradation was different between the two material types.
- The response of OPCC specimens was dominated by the development of a barrier of expansive products which impeded the diffusion process. The observed strength reduction resulted from changes in the microstructure of the material.
- Continued penetration of sulphuric acid was observed in AAC specimens. The meso-structural mechanism of spalling due to expansion of the coarse aggregates dominated the reduction in strength.

The evaluation of the measurements taken reveal that there was no single universal indicator of resistance to sulphuric acid that could be applied as a simple test technique for both materials.

Equivalent reductions in compressive strength were observed at approximately 100 days in 3% solution to that of 400 days of 1% solution. Measureable changes in the mass loss, acid consumption, length change and loss of alkalinity at 100 days in 3% solution, therefore demonstrates that a test procedure to indicate the susceptibility of concretes can be performed within a reasonable time frame for standard testing.

References

1. H. Yuan, P. Dangla, P. Chatellier, T. Chaussadent, Degradation modeling ofconcrete submitted to biogenic acid attack, Cem. Concrete Res. 70 (2015) 29–38

2. N. De Belie, J. Monteny, A. Beeldens, E. Vincke, D. Van Gemert, W. Verstraete, Experimental research and prediction of the effect of chemical and biogenic sulfuric acid on different types of commercially produced concrete sewer pipes, Cem. Concr. Res. 34(12) (2004) 2223-2236.

3. Ma. G. D. Gutiérrez-Padilla, A. Bielefeldt, S. Ovtchinnikov, M. Hernandez, J. Silverstein, Biogenic sulfuric acid attack on different types of commercially produced concrete sewer pipes, Cem. Concr. Res. 40(2) (2010) 293-301.

4. C. Grengg, F. Mittermayr, N. Ukrainczyk, G. Koraimann, S. Kienesberger, M. Dietzel, Advances in concrete materials for sewer systems affected by microbial induced concrete corrosion: A review, Water res. 134 (2018) 341-352.
5. J. Monteny, E. Vincke, A. Beeldens, N. De Belie, L. Taerwe, D. Van Gemert, W. Verstraete, Chemical, microbiological, and in situ test methods for biogenic sulfuric acid corrosion of concrete, Cem. Concr. Res. 30(4) (2000) 623-634.
6. M. Alexander, A. Bertron, N. De Belie, Performance of cement-based materials in aggressive aqueous environments (Vol. 10), Springer, Dordrecht, 2013
7. C. W. Fourie, Acid resistance of sewer pipe concrete, 2007 (Doctoral dissertation, University of Cape Town).
8. J. P. Frost, D. J. Armstrong, Concrete and silage effluent-a cyclical exposure method for accelerated corrosion testing, Farm Building Progress 116 (1994) 27-30.
9. ASTM, C. 267-01: Standard Test Methods for chemical resistance of mortars, grouts and monolithic surfacing and polymer concretes, ASTM International, West Conshohocken, USA, 2012.
10. S. Thokchom, P. Ghosh, S. Ghosh, Resistance of fly ash based geopolymer mortars in sulfuric acid, ARPN J. Eng. Appl. Sci. 4(1) (2009) 65-70.
11. P. Chindaprasirt, U. Rattanasak, Improvement of durability of cement pipe with high calcium fly ash geopolymer covering, Constr. Build. Mater. 112 (2016) 956-961.
12. A.M. Izzat, A.M.M. Al Bakri, H. Kamarudin, L.M. Moga, G.C.M. Ruzaidi, M.T.M. Faheem, A.V. Sandu, Microstructural analysis of geopolymer and ordinary Portland cement mortar exposed to sulfuric acid, Mater. Plast. 50 (3) (2013) 171-174.
13. M. Albitar, M. M. Ali, P. Visintin, M. Drechsler, Effect of granulated lead smelter slag on strength of fly ash-based geopolymer concrete, Constr. Build. Mater. 83 (2015) 128-135.
14. Neville AM. Properties of concrete. Burnt Mill, Harlow, England: Longman House; 1995.
15. ASTM, C. 39: Standard A. Standard Test Methods for Compressive Strength of Cylindrical Concrete Specimens, ASTM International, West Conshohocken, USA, 2018.
16. ASTM, C. 1012: Standard Test Method for Length Change of Hydraulic-Cement Mortars Exposed to a Sulfate Solution, ASTM International, West Conshohocken, USA, 2018.
17. R. L. Islander, J. S. Devinny, F. Mansfeld, A. Postyn, H. Shih, Microbial ecology of crown corrosion in sewers, J. Environ. Eng. 117(6) (1991) 751-770.
18. N. De Belie, J. Monteny, L. Taerwe, Apparatus for accelerated degradation testing of concrete specimens, Mater. Struct. 35(7) (2002) 427-433.
19. H. F. W. Taylor, Cement chemistry, second ed., Thomas Telford, London, 1997.

20. C. Shi, P.V. Krivenko, D.M. Roy, Alkali-Activated Cements and Concretes, Taylor & Francis, Abingdon, UK, 2006.
21. J. L. Provis, J. S. J. Van Deventer, Geopolymers: structures, processing, properties and industrial applications, Woodhead, Cambridge, 2009.
22. T. Bakharev, Resistance of geopolymer materials to acid attack, Cem.Concr. Res. 35 (4) (2005) 658–670.
23. V. Sata, A. Sathonsaowaphak, P. Chindaprasirt, Resistance of lignite bottom ash geopolymer mortar to sulfate and sulfuric acid attack, Cem. Concr. Compos. 34(5) (2012) 700-708.
24. M. A. M. Ariffin, M. A. R. Bhutta, M. W. Hussin, M. M. Tahir, N. Aziah, Sulfuric acid resistance of blended ash geopolymer concrete, Constr. Build. Mater. 43 (2013) 80-86.
25. L. Gu, P. Visintin, T. Bennett, Evaluation of accelerated degradation test methods for cementitious composites subject to sulfuric acid attack; application to conventional and alkali-activated concretes, Cem. Concr. Compos. 87 (2018) 187-204.
26. M. Izquierdo, X. Querol, J. Davidovits, D. Antenucci, H. Nugteren, C. FernándezPereira, Coal fly ash-slag-based geopolymers: microstructure and metal leaching, J. Hazard. Mater. 166 (1) (2009) 561–566.
27. C.L. Page, K.W.J. Treadaway, Aspects of the electrochemistry of steel in concrete, Nature 297 (1982) 109–115.
28. R.R. Lloyd, J.L. Provis, J.S.J. van Deventer, Acid resistance of inorganic polymer binders. 1. Corrosion rate, Mater. Struct. 45 (2012) 1–14.
29. T. A. Aiken, J. Kwasny, W. Sha, M. N. Soutsos, Effect of slag content and activator dosage on the resistance of fly ash geopolymer binders to sulfuric acid attack, Cem. Concr. Res. 2018.

Chapter 4. Journal Paper 3 – Degradation Mechanism of Chemical Reaction under Sulphuric Acid Attack and Scale of Manufacture

Introduction

This chapter contains the paper "A multiscale approach to investigating the resistance of cementitious materials to the sulphuric acid exposure: the degradation mechanism of chemical reaction and scale of manufacture" which provides a comprehensive investigation on the degradation mechanism of vastly different binders under sulphuric acid attack in terms of chemical reaction and scale of manufacture.

Repeatable and rapid test conditions are developed in this study. The well-designed experimental apparatus and procedures create 'reservoir' boundary conditions with almost constant pH levels maintained throughout the immersion period. Well-designed specimen manufacture procedure is applied in this study. The specimens are coated with wax prior to immersion to provide a physical barrier to the acid attack at the ends of the specimens to provide a firm platform for performing compression tests and induce one dimensional radial acid penetration in the majority of a specimen's length.

A series of comprehensive characterization tests, including inductively coupled plasma mass spectrometer (ICP-MS), scanning electron microscopy (SEM), energy dispersive x-ray (EDX), X-ray diffraction (XRD), Fourier transform infrared spectroscopy (FTIR) and micro-computed tomography (CT) are undertaken to understand the physical and chemical change in the OPC and AA paste over time. The physical and mechanical properties of OPC and AA in mortar level are discussed in comparison with that in paste level to investigate the different degradation mechanism influenced by scale of manufacture.

List of manuscripts

Gu, L., Visintin, P. and Bennett, T., 2018. A multiscale approach to investigating the resistance of cementitious materials to the sulphuric acid exposure: the degradation mechanism of chemical reaction and scale of manufacture. To be submitted to *Cement and Concrete Research.*

Statement of Authorship

Title of Paper	A multiscale approach to investigating the resistance of cementitious materials to the sulphuric acid exposure: the degradation mechanism of chemical reaction and scale of manufacture
Publication Status	☐ Published ☐ Accepted for Publication ☐ Submitted for Publication ☑ Unpublished and Unsubmitted work written in manuscript style
Publication Details	Gu, L., Visintin, P. and Bennett, T., 2018. A multiscale approach to investigating the resistance of cementitious materials to the sulphuric acid exposure: the degradation mechanism of chemical reaction and scale of manufacture.

Principal Author

Name of Principal Author (Candidate)	Lei Gu		
Contribution to the Paper	Developed the test methodologies, performed analysis on all samples, interpreted data, and wrote manuscript.		
Overall percentage (%)	70		
Certification:	This paper reports on original research I conducted during the period of my Higher Degree by Research candidature and is not subject to any obligations or contractual agreements with a third party that would constrain its inclusion in this thesis. I am the primary author of this paper.		
Signature		Date	5/9/2018

Co-Author Contributions

By signing the Statement of Authorship, each author certifies that:

i. the candidate's stated contribution to the publication is accurate (as detailed above);

ii. permission is granted for the candidate in include the publication in the thesis; and

iii. the sum of all co-author contributions is equal to 100% less the candidate's stated contribution.

Name of Co-Author	Phillip Visintin		
Contribution to the Paper	Supervised development of work, helped in data interpretation and manuscript evaluation.		
Signature		Date	05/09/2018

Name of Co-Author	Terry Bennett		
Contribution to the Paper	Supervised development of work, helped in data interpretation and manuscript evaluation.		
Signature		Date	5/9/2018.

A multiscale approach to investigating the resistance of cementitious materials to the sulphuric acid exposure: the degradation mechanism of chemical reaction and scale of manufacture

Lei Gu[1], Phillip Visintin[1] and Terry Bennett[1]
[1]School of Civil, Environmental and Mining Engineering, The University of Adelaide, SA 5005, Australia

Abstract: The degradation mechanism of conventional cement (CC) is relatively well-understood, whereas the alkali-activated (AA) paste in the literature was not expected to be similar, and in some cases was even in direct contrast. The degradation mechanism of CC and AA mortar and concrete is further influenced by the scale of manufacture (paste to mortar to concrete). This study presents an investigation into the durability of CC and AA class F fly ash paste and mortar when exposed to 5% sulphuric acid for up to 84 days. Both CC and AA mortar were prepared with two sand-to-binder ratios. The ion change in reservoir solution was examined using inductively coupled plasma mass spectrometer (ICP-MS). The degradation was examined using scanning electron microscopy (SEM), energy dispersive x-ray (EDX), X-ray diffraction (XRD), Fourier transform infrared spectroscopy (FTIR) and micro computed tomography (CT). Macroscopic measurements were undertaken to establish the cross-section change, mass loss, compressive strength, products of degradation and microstructure changes. The results also showed that the durability of a cementitious material was heavily influenced by the scale of manufacture (paste, mortar, and concrete) and further complicated by mix design.

Keywords: paste and mortar degradation; sulphuric acid corrosion; microstructure; alkali-activated paste and mortar; durability

1. Introduction

Sulphuric acid corrosion of conventional cement (CC) based materials has attracted attention in recent decades due to the deteriorating effect of sulphuric acid media on CC based constructions [1-5] which can occur in solution in the mining industry, agriculture and wastewater systems [6-10]. This increased interest has been accompanied by the development of alkali-activated (AA) cementitious materials, which have potentially enhanced durability-related properties [11-13]. AA cementitious materials are expected to have higher sulphuric acid resistance than that of CC based materials due to the different chemical composition of the matrix materials [14-18].

The behaviour of cementitious materials, subject to sulphuric acid exposure, involves the complex interactions of chemical reactions, transport processes and response under applied stress, which is further complicated with scale issues as which can affect a materials efficacy against degradation. As the material is up scaled from paste to mortar to concrete, the addition of fine aggregates, and subsequently, coarse aggregates creates interfacial transition zones which can alter the paste's material properties and/or the overall properties of the composite, for example if coarse aggregates are themselves susceptible to corrosion and volumetric changes [1].

Therefore a multiscale approach to understanding how cementitious materials respond to the external acidic environment is required, both in terms of scale of manufacture (paste to mortar to concrete) and in levels of observation from microscopic to macroscopic measurements.

Repeatable and rapid test conditions are required in order that comparisons between different materials may be performed in a reasonable timeframe for laboratory studies. To this end, the design of experimental apparatus and procedures are developed to create 'reservoir' boundary conditions with almost constant pH levels maintained throughout the immersion period.

The chemical response of CC pastes exposed to sulphuric acid is relatively well understood. However, whether gypsum or ettringite is mainly responsible for this damage is still not clear. Monteny et al. [3] suggested under the sulphuric acid attack, the C-H transfers to gypsum as equation (1)

$$Ca(OH)_2 + H_2SO_4 \rightarrow CaSO_4 \cdot 2H_2O \quad (1)$$

the tricalcium aluminate reacts with gypsum, generating ettringite as equation (2)

$$3CaO \cdot Al_2O_3 \cdot 12H_2O + 3(CaSO_4 \cdot 2H_2O) + 14H_2O \rightarrow 3CaO \cdot Al_2O_3 \cdot 3CaSO_4 \cdot 32H_2O \quad (2)$$

and the C-S-H transfers to gypsum and silica gels as equation (3)

$$CaO \cdot SiO_2 \cdot 2H_2O + H_2SO_4 \rightarrow CaSO_4 + Si(OH)_4 + H_2O. \quad (3)$$

Monteny et al. [3] also suggested the formation of ettringite is mainly responsible for the large volume expansion, leading to the increase of internal pressure and deterioration of the CC matrix. However, Gabrisova et al. [19] suggested ettringite is only stable above pH over 10.7, and when pH below 10.0 only gypsum and aluminium sulphate are the stable phases. Grengg et al. [2] also suggested ettringite formation is limited to high pH areas (>10.7) such as the transition zone between non-corroded and strongly affected concrete layers where alkaline

conditions still dominate but sulphate rich pore fluids are already present. Yuan et al. [20] suggested the expansion of gypsum in the pore structure leads to pressure increase until the inner pressure exceeds the ultimate bearing capacity of the pore, and then the pore structure is damaged. Pavlik [21, 22] suggested under the sulphuric acid attack, the decalcification of C-S-H leaves a layer of silica and aluminosilicate gels that prevents un-corroded cement pastes from further corrosion.

To further elucidate the mechanism XRD and FTIR analysis, including deconvolution spectra, is performed to detect the phase change in the CC paste, complimented with EDX analysis to detect the chemical composition in the degraded zone of material and ICP-MS analysis of the concentration change of elements in the reservoir.

Tests are performed at the macroscale to understand how the microstructural changes affect the mass, strength and physical dimensions and how the scales of observation may be linked through the consumption of acid from the reservoir.

Alkali-activated cementitious materials are usually precipitated by reacting an active aluminosilicate (metakaolin, fly ash, slag) with an appropriate proportion of an alkali metal (Na, K, Ca) under very high alkalinity conditions in which the water content is strictly controlled [23, 24]. Generally, the main component of AA cementitious materials with low calcium content is amorphous sodium aluminosilicate hydrate (N-A-S-H) [25]. During the degradation process under sulphuric acid attack, the alkali metal ions, which charge compensation cations of the aluminosilicate framework, are leached out and exchanged by hydrogen or hydronium ions from the solution. At the same time, tetrahedral Al from the aluminosilicate framework is dissolved by breaking the Si-O-Al bonds [2, 6, 26, 27]. Some authors [2, 6, 26] have suggested the framework vacancies formed by tetrahedral aluminium dissolution are mostly re-occupied by silicon atoms resulting in the formation of an imperfect highly siliceous framework. Allahverdi and Skvara [26] suggested the ejected aluminium, converted to octahedrally coordinated aluminium, mostly accumulates in the intra-framework space. However, Bakharev [27] suggested the sulphuric acid attack causes breakage of the Si–O–Al bonds, increased number of Si–OH and Al–OH groups in the matrix and an increased amount of silicic acid ions and dimers in solution.

FTIR analysis is employed to determine if the condensation of polymeric ions enriched with silicon occurs, with EDX used to detect aluminium content in the degraded material, with XRD and FTIR performed to detect any phase changes that may occur in the aluminium based phases. The external sulphuric acid solution is examined using ICP-MS to determine the presence of dissolved aluminium.

The morphological change within a sample before and after sulphuric acid attack is presented by Bakharev [27] and Ariffin et al. [14] using SEM and Allahverdi and Skvara [28] provide the X-ray line analysis of AA fly ash and slag blended paste under nitric acid attack. Bakharev [27] suggested the AA fly ash paste exposed to sulphuric acid became very porous and fragile. Ariffin et al. [14] observed that AA concrete exhibited better performance than the OPC concrete when exposed to sulphuric acid. Aiken et al. [5] provide the element distribution analysis of CC and AA fly ash and slag blended paste under sulphuric acid attack. To understand how the degradation proceeds with depth into a specimen, EDX analysis is performed at regular intervals from the surface and into the unaffected pastes, with the Ca to Si ratio in CC and Al to Si ratio in AA samples.

The degradation mechanism of both OPC based and AA cementitious materials is mainly investigated at paste level [5, 25, 27]. However, the difference between the paste, mortar and concrete was investigated rarely in the past. The role of fine aggregate on the response to sulphuric acid exposure is explored. Mortar specimens with different sand-to-binder ratios were manufactured with both CC and AA binders.

The paper is organised as follows. Sample preparation, immersion regime design and instrumentation are detailed in section 2. The microscopic and macroscopic observations on both CC and AA pastes are recorded in section 3, followed by the macroscopic measurements recorded for mortars in section 4. In section 5, our observations on the effect of binder types and upscaling from pastes to mortars are discussed before the paper is concluded.

2. Materials and methodologies

2.1 Materials

General purpose cement and class F fly ash were used as binders in the CC and AA paste and mortar. The chemical compositions of these binders are supplied in Table 1. For all AA mixes, the alkaline solution phase consisted of a combination of sodium silicate (Na_2SiO_3) and 14

molar sodium hydroxide (NaOH), pre-mixed with a ratio of Na_2SiO_3:NaOH of 1.5:1. The XRD patterns of class F fly ash are shown in Figure 1. It is mainly glassy with some crystalline phases of quartz and mullite.

Table 1. Chemical composition of binders

Oxide (Wt. %)	SiO_2	Al_2O_3	Fe_2O_3	CaO	MgO	Na_2O	K_2O	SO_3	TiO_2	P_2O_5	Mn_2O_3	LOI*
Cement	19.89	4.69	3.16	63.35	1.94	0.22	0.40	2.77	0.27	0.03	0.07	3.55
Fly ash	54.24	28.94	4.01	3.58	1.80	0.60	1.46	0.25	1.21	0.27	0.06	3.12

LOI: Loss on ignition

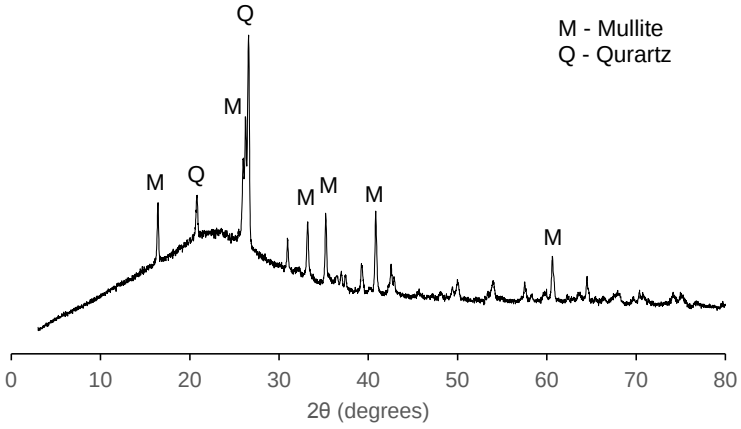

Figure 1. XRD patterns of fly ash

2.2 Specimen preparation

Six batches of specimens, including two batches of paste (conventional cement paste (CCP) and alkali-activated fly ash paste (AAP)) and four batches of mortar (two conventional cement mortars (CCM) and two alkali-activated mortars (AAM)), were manufactured. The mix proportions of paste and mortar mixes are given in Table 2. River sand having specific gravity of 2.61 and fineness modulus of 2.3 was used as fine aggregate. The sand-to-cement ratios of mortar mixes for each type of binder were 2.25 and 3.0 and the sand was used in saturated surface dry condition. All the paste and mortar mixes were mixed for 10 minutes in a concrete mixer.

Table 2. Mix proportion of conventional and alkali-activated paste and mortar

Mix ID	Cement (kg/m^3)	Fly ash (kg/m^3)	Sand (kg/m^3)	Water (kg/m^3)	Superplasticizer (kg/m^3)	NaOH (kg/m^3)	Na_2SiO_3 (kg/m^3)
CCP	1470	0	0	632	0	0	0
AAP	0	1218	0	146	0	243	365
CCM_1	570	0	1283	242	4	0	0
CCM_2	470	0	1413	203	10	0	0
AAM_1	0	500	1128	32	40	80	120

AAM_2	0	415	1248	0	71	66	99

After casting, the CCP and mortar specimens were cured in a hot water bath inside the moulds at 80°C bath according to AS1012 [29] for 16 hours before demoulding. The AA paste and mortar specimens were maintained at ambient temperature (~20°C) for 24 hours, after which the specimens were oven cured at 80 °C for 48 hours to accelerate the hydration or polymerization process of the materials in order to eliminate the influence of continued strength gain.

As a control the compressive strength before immersion of all mixes was determined from compressive strength test conducted on 75 × 150 mm cylinders and was found to be 68.2 MPa, 59.6 MPa for CCP and AAP, and 44.5 MPa, 32.1 MPa, 43.1 MPa, 39.1 MPa for CCM_1, CCM_2, AAM_1, AAM_2, respectively. Considering the continued hydration of materials, the compressive strength of all mixes was also determined from compressive strength test of control specimens immersed in distilled water at the same immersion periods.

All the specimens were coated with wax prior to immersion to provide a physical barrier to the acid attack at the ends of the specimens as shown in Figure 2(a) to provide a firm platform for performing compression tests and induce one dimensional radial acid penetration in the majority of a specimen's length. The efficacy of this is demonstrated in Figure 2(b) where the colour change of a coated AAM specimen after 12 weeks immersion in 5% sulphuric acid shows that the penetration is predominantly radial 2 cm from each end. To achieve this the wax was placed in a beaker and melted in an oven at 110 °C. The 75 × 150 mm cylindrical specimens were then immersed in the liquid wax to a depth of 15 mm at both ends. In order to generate a sufficiently thick coating, each specimen was subjected to a number of cycles of dipping and cooling. It can be seen that the wax coating provided sufficient protection to both ends, maintaining the same colour as the centre part of the specimen.

(a) (b)

Figure 2. Wax coating of specimens: (a) Wax coating remain good sealing after 12 week immersion in the sulphuric acid; (b) Colour change of the cross-section of specimens with wax coating

2.3 Test methodology

The specimens were placed in a bath of 5% (w/w %) sulphuric acid solution. In order to manage the pH change, the sulphuric acid solution to specimen volume ratio was chosen as 4.5 which is employed in sulphate attack tests according to ASTM C1012 [30]. The pH level was maintained at 0.28±0.05, monitored by a portable digital pH meter, and adjusted twice a week by the addition of 35% (w/w %) sulphuric acid. Throughout the test period the solution was continuously circulated using pumps to avoid the development of strong ion gradients, to assist with this a minimum spacing of 5 cm between specimens was maintained. To eliminate the influence of evaporation, plastic lids were used to cover the test tubs.

To provide an indication of sulphuric acid degradation, acid consumption, mass loss, macroscopic degradation depth, compressive strength, ion concentration change in the solution and microstructural change were all observed for a period of 84 days. The methodology for each test is summarised as follows:

- The macroscopic degradation depth was determined via a cylindrical disk of diameter 75 mm and thickness 10 mm that was cut from the mid-height of a 75 × 150 mm cylinder. The macroscopic degradation depth of a cross-section was measured at 1, 3,

6, and 12 weeks. The macroscopic degradation depth was determined by measuring the diameter of no colour change area at nine locations via a combination use of Vernier caliper and digital microscope.

- The change in mass after periods of exposure was measured via 75 × 150 mm cylindrical specimens. The mass of a single specimen was periodically measured (at weeks 1, 3, 6, and 12). In order to remove the influence of surface moisture, prior to weighing, the specimen was oven dried at 80°C for 6 hours.
- The compressive strength was determined by cylindrical specimens (75 mm in diameter and 150 mm in height), with the wax coating removed prior to testing.
- The consumption of acid solution was recorded twice weekly when the pH of the sulphuric acid solution was measured and adjusted accordingly.
- The ion concentration change in the sulphuric acid solution was examined at 1, 3, 6, and 12 weeks by inductively coupled plasma mass spectrometer (ICP-MS) using an Agilent 8900 Triple Quadrupole instrument. The sulphuric acid solution was examined at 1, 3, 6, and 12 weeks.
- The phase change of paste was examined by X-ray diffraction (XRD). For the XRD analysis, the paste was carefully removed from the surface in the middle height of the specimens. Each paste sample was finely ground prior to the XRD analysis. The samples used in XRD analysis were taken before sulphuric acid exposure and after 12 weeks of immersion. XRD analysis was made using a Rigaku-Miniflex diffractometer with the following conditions: 40 kV, 15 mA, Cu–Kα radiation. The XRD patterns were obtained by scanning from 3° to 80° (2θ) at 10° (2θ) per min and in steps of 0.02° (2θ).
- The phase change of paste was also examined by Fourier transform infrared spectroscopy (FTIR) using the same grounded powder sample in XRD via a Nicolet 6700 FTIR Spectrometer. The spectra were gathered between 400 and 4000 cm^{-1} wavenumber at 2 cm^{-1} resolution.
- The morphology change and surface element change of CCP and AAP samples before and after 12 weeks of immersion were examined by scanning electron microscopy (SEM) and energy dispersive x-ray (EDX) using a Phillips XL 30 instrument, respectively. For the analysis, samples were cut perpendicularly to the exposed surface at the mid-height of a cylindrical specimen (75 × 150 mm). Samples were dried by a vacuum oven at 50 °C for 24 hours, impregnated with epoxy resin, cut, polished and coated with platinum prior to SEM analysis, and EDX was performed at an accelerating

voltage of 15 kV.

- The microstructure and porosity of CCP and AAP sample before and after sulphuric acid attack (at 6 and 12 weeks) was examined by X-ray micro computed tomography (CT) using a SkyScan 1076 instrument. For the analysis, samples were cut into approximately 10 mm × 10 mm ×15 mm cuboids perpendicularly to the exposed surface at the mid-height of a cylindrical specimen (75 × 150 mm). Measurements were carried out with a parallel beam configuration using a hard X-ray synchrotron radiation of 100 keV with 0.5° rotation of exposure per step. X-ray detection was attained with a scintillator and charge coupled device camera with a resolution of 1024 × 1024 pixels and a voxel resolution of 9.5 μm.

3. Microscopic and macroscopic observations

3.1 Element concentration change in solution

Figure 3 presents the concentration change of Na, Al, Si, and Ca in the sulphuric acid solution. It is clear that a tiny amount of Na^+ is dissolved in CCP due to the tiny Na_2O content in the cement shown in Table 1. Whereas a large amount of Na^+ in AAP is dissolved in sulphuric acid solution due to Na^+ in N-A-S-H is exchanged by H^+ or H_3O^+ ions from the sulphuric acid solution [26, 27]. The concentration of Na^+ in AAP increased at a reduced rate to 7449 ppm after 12 weeks immersion.

The concentration of Al^{3+} in CCP increased at a reduced rate to 1624 ppm after 12 weeks immersion. Ettringite dissolved and generated soluble aluminium sulphate under the 5% sulphuric acid attack as ettringite is only stable above pH 10.7 [19]. The concentration of Al^{3+} in AAP also increased at a reduced rate to 4884 ppm after 12 weeks immersion as tetrahedral aluminium is ejected out from the Si-O-Al bond in N-A-S-H [26, 27].

The concentration of Si in both CCP and AAP stabilized in the range from 69.0 to 74.3 ppm. The solubility of amorphous silica in water is shown to involve an equilibrium between the solid phase and a monomeric form of silica in solution, presumably silicic acid, and the solubility of amorphous silica is affected by the pH value of solution [31]. Iller [32] suggested that silicic acid may be liberated from silicates in the acidic condition. In the environment of pH 0.28, the solubility of silicic acid is very small so that the amorphous silica leached out from the silicate in both CCP and AAP reached the saturation point within 1 week.

The concentration of Ca^{2+} in CCP stabilized in the range from 635 to 670 ppm as Ca^{2+} reached the saturation point within 1 week in CCP as Ca^{2+} reached the saturation point (0.24 g/100 ml at 20 °C [33]) within 1 week. The concentration of Ca^{2+} in AAP increased at a reduced rate to 502 ppm after 12 weeks immersion due to the presence of CaO (3.58%) in the fly ash shown in Table 1.

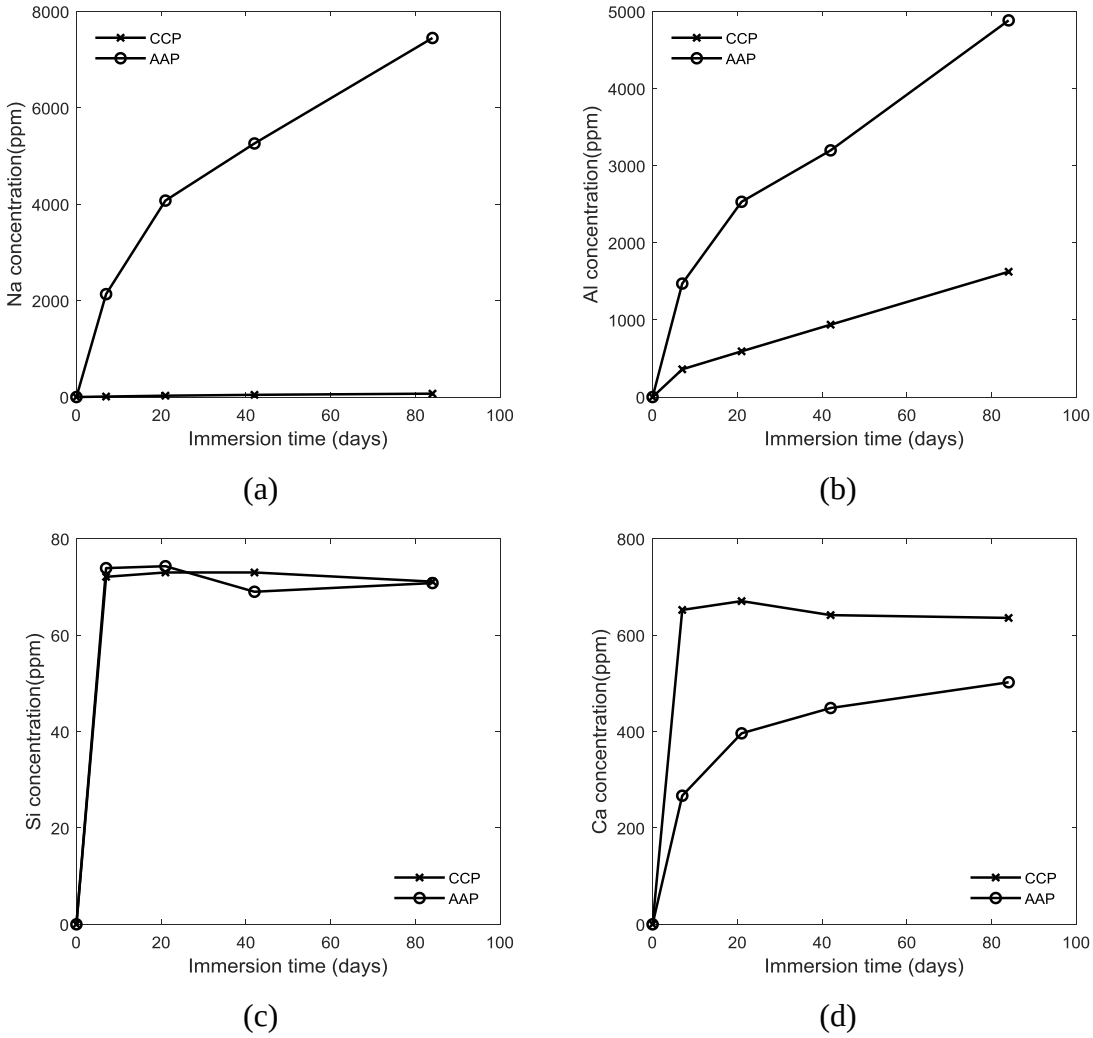

Figure 3. Na, Al, Si, and Ca concentration change in the sulphuric acid solution

3.4 X-ray diffraction

Figure 4 presents the XRD patterns of a CCP sample before and after 12 weeks of immersion in sulphuric acid solution. Calcite, ettringite and portlandite were detected in the sample prior to immersion. The calcite was probably formed due to the reaction of carbon dioxide in the

atmosphere with Portlandite in the CCP. The ettringite was formed due to the hydrated C_3A reacting with gypsum added during cement manufacture [34]. After 12 weeks of immersion, the composition of the CCP sample was changed significantly as shown with the traces dominated by gypsum and the peaks for calcite and Portlandite phases significantly reduced.

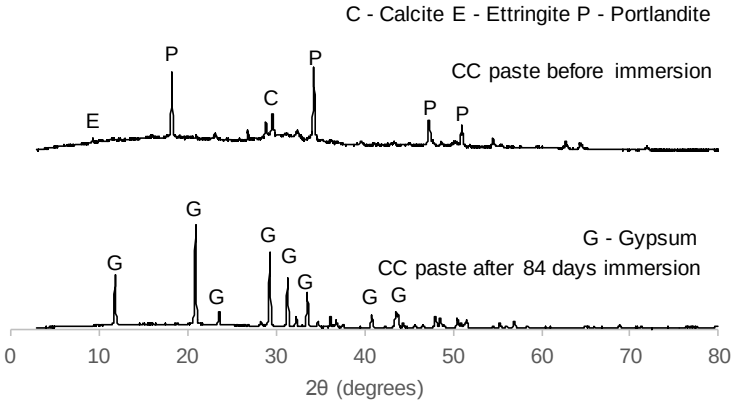

Figure 4. XRD patterns of CCP samples before and after immersion

Figure 5 presents the XRD patterns of AAP before and after 12 weeks of immersion in sulphuric acid. Examining the results in Figures 1 and 5 together, the main products of AAP before immersion are amorphous phase with the same crystalline minerals in unreacted fly ash particles, which is also observed by previous studies [5, 35]. Allahverdi and Skvara [28] suggested that the alkali-activation of fly ash results in the formation of amorphous zeolite-like aluminosilicate hydrates. After 12 weeks immersion, peaks due to mullite and quartz in unreacted fly ash particles still can be seen, in addition to the gypsum peaks observed in the traces. A similar change in XRD patterns of AAP before and after immersion in 5% sulphuric acid was observed by Aiken et al. [5].

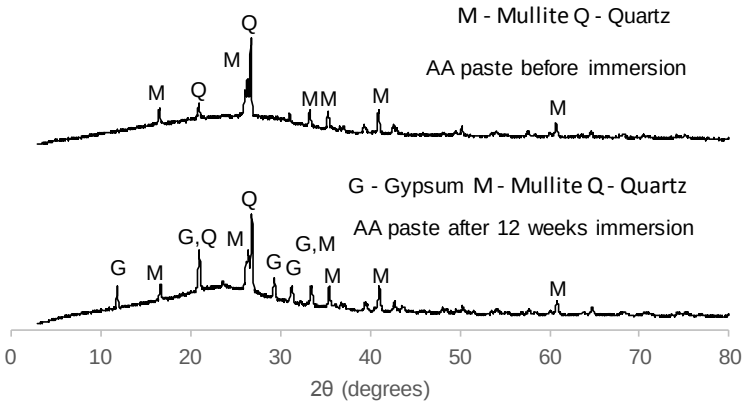

Figure 5. XRD patterns of AAP samples before and after immersion

3.5 Scanning electron microscopy and energy dispersive X-ray analysis

Figure 6 shows the SEM images of the CCP specimens before and after 12 weeks immersion in sulphuric acid, while Table 3 shows the results of surface element analysis by EDX at the areas marked A to F in Figure 6. The cement paste before immersion in area A in Figure 6(a) showed C-S-H gels as a result of the typical C-S-H chemical composition shown in Table 3 [34], and the details of the amorphous structure of C-S-H gels are shown in Figure 6(b) with a high magnification (×10000). Figure 6(c) shows the CCP sample after immersion with a low magnification (×80). It can be seen that at least four layers of the sample with different in Figure 6(c), marked as layers 1-4, where layer 1 was closest to the surface.

Figure 6(d) shows the details of a porous amorphous structure in layer 1, where area B showed a highly siliceous composition. The chemical composition in Area B also showed a small amount of calcium and sulphur with an atomic ratio close to 1, which was identified as the presence of gypsum reported by XRD analysis. The low content of gypsum in layer 1 was possibly due to the gypsum being dissolved in the water during the polishing process. The cement paste after immersion in area C of layer 2 in Figure 6(e) also showed a highly siliceous composition similar as that in layer 1, whereas the structure in Figure 6(e) was less porous than that observed in Figure 6(d).

Figure 6(f) shows the details of layers 3 and 4, where an amorphous layer was observed between the layers 3 and 4. The layer 4 showed a relative denser structure than that of layer 3, the area marked D in layer 4 had a Ca:Si atomic ratio of 1.18 whereas this was reduced to 0.33 in area F of layer 3. This indicates that the leaching out of calcium in C-S-H gels of layer 3 was more severe than that of layer 4. The chemical composition of area E showed a concentration of silicon elements, indicating the amorphous layer between the layers 3 and 4 was mainly silica gels. The silica gels potentially act as a protective barrier. A similar observation has also been made in previous studies [21, 22].

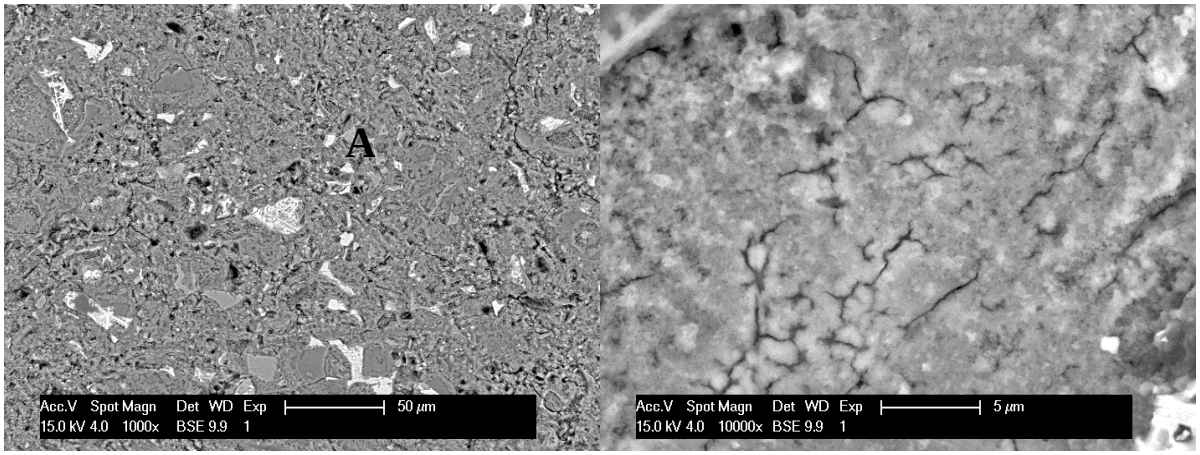

(a) CC paste before immersion (X1000) (b) amorphous C-S-H (x10000)

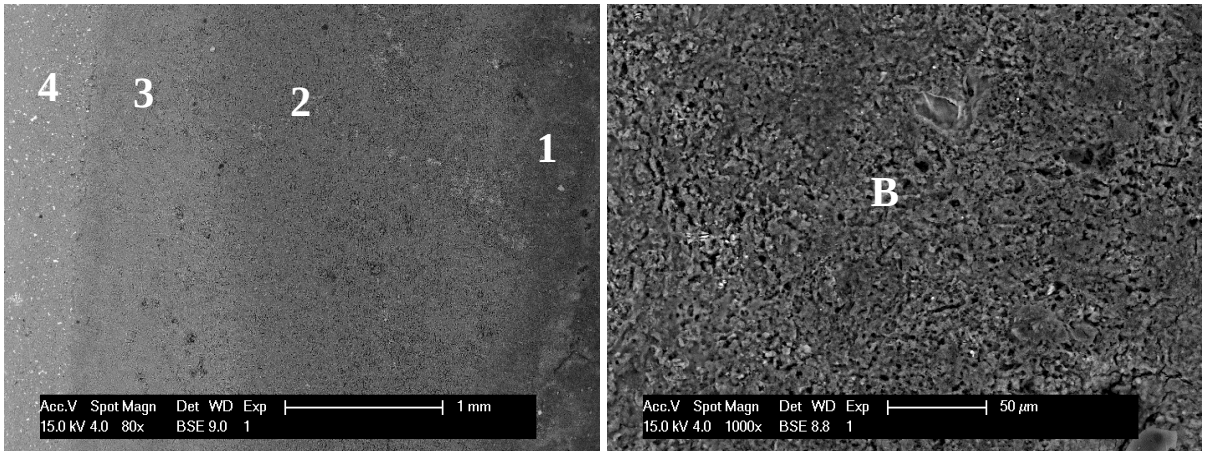

(c) CC paste after immersion (X80) (d) layer 1 (x1000)

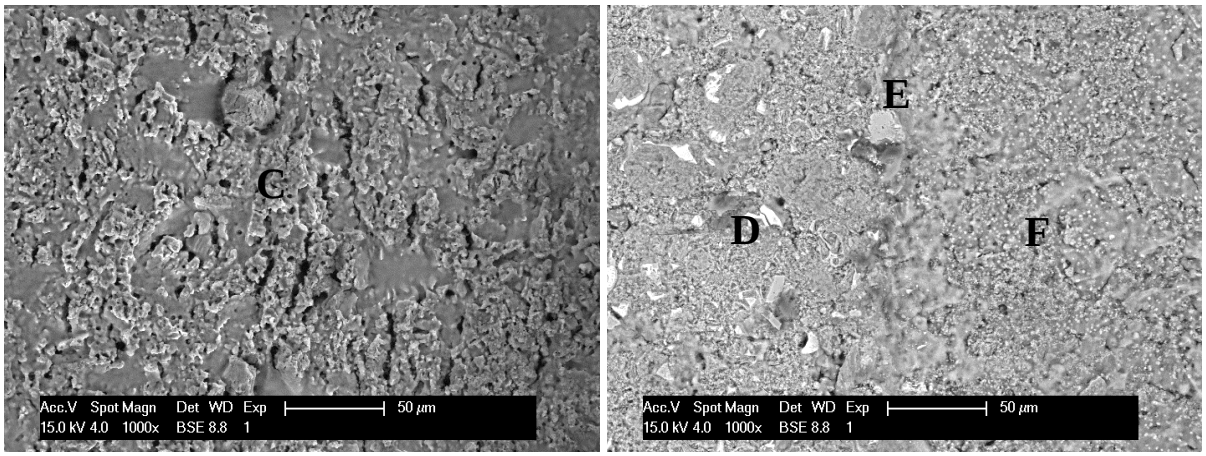

(e) layer 2 (x1000) (f) layers 3 and 4 (X1000)

Figure 6. Comparison of CCP samples before and after immersion

Table 3. Surface element analysis of CCP samples in selected areas

	Area A		**Area B**		**Area C**		**Area D**		**Area E**		**Area F**	
Element	Wt.%	At.%	Wt.%	At.%	Wt.%	At.%	Wt.%	At.%	Wt.%	At.%	Wt.%	At.%
Oxygen	53.3	70.1	45.6	60.6	51.7	65.6	54.1	71.3	55.1	69.1	53.4	68.7
Sodium	-	-	-	-	-	-	0.4	0.4	-	-	-	-

Magnesium	2.5	2.2	-	-	-	-	0.9	0.8	-	-	2.2	1.9
Aluminium	2.3	1.8	1.1	2.7	-	-	1.8	1.4	1.0	0.7	-	-
Silicon	12.7	9.6	42.6	32.3	45.0	32.5	15.4	11.5	38.5	27.5	29.1	21.4
Sulfur	-	-	4.7	3.1	1.2	0.8	1.5	1.0	-	-	1.6	1.0
Calcium	29.2	15.5	6.0	3.2	2.1	1.1	26.0	13.6	5.4	2.7	13.7	7.0

In order to show the degradation process of CCP under sulphuric acid attack, the Ca to Si atomic ratio was measured in 1 mm increments from the surface to a radial depth of 10 mm after 12 weeks immersion. It can be seen in Figure 7 that the Ca to Si ratio stabilized in a very low range in the first 7 mm from the surface, and subsequently increased significantly to 1.49 after 7 mm from the surface.

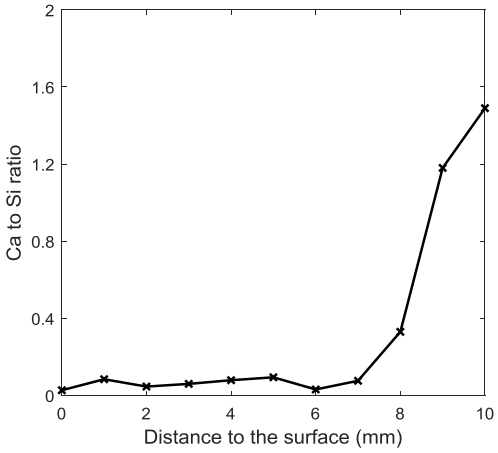

Figure 7. The Ca to Si atomic ratio of CCP sample after 12 weeks immersion in sulphuric acid

Figure 8 shows the SEM images of the AAP specimens before and after 12 weeks immersion in sulphuric acid, while Table 4 shows the results of surface element analysis by EDX at the areas marked A to D in Figure 8. The AA paste before immersion in area A in Figure 8(a) showed N-A-S-H gels as a result of the typical N-A-S-H chemical composition shown in Table 4 [34], which the details of the amorphous structure of N-A-S-H gels are shown in Figure 8(b) with a high magnification (×10000). Figure 8(c) shows the AAP sample after immersion with a low magnification (×80). It can be seen that at least three layers of the sample in Figure 8(c), marked as layer 1-3 from the surface inwards. A few cracks can be observed along the radial direction in layers 1 and 2, whereas cracks occurred vertically to the radial direction were observed as the boundary between the layer 2 and layer 3.

Figure 8(d) shows the detailed structure in layer 1, where the unreacted fly ash particles seem to have lost bond with N-A-S-H matrix and the polished surface was less smooth, compared to those in Figure 8(a). It is possible that the N-A-S-H matrix after sulphuric acid attack lost some stiffness when compared to that before immersion [11]. The sodium content decreased significantly in area B of layer 1, compared to that in AAP before immersion. The hydronium ion (H_3O^+) or hydrogen ion (H^+) in the solution substitutes the Na^+ ion in the N-A-S-H framework under the sulphuric acid attack. The Al to Si atomic ratio in area B of layer 1 was 0.29, compared to that of 0.47 in AAP before immersion. Therefore, the aluminium leached out from N-A-S-H matrix after the sulphuric acid attack. In general, AA paste appears to remain in good form after sulphuric acid attack, similar to observations made in previous studies [5, 27].

Figure 8(e) shows the details of layer 2, where many micro-cracks were observed in this layer. The Al to Si atomic ratio in area C of layer 2 was 0.439, which is higher than that in layer 1. Figure 8(f) shows a quite similar morphology to that before immersion, and the chemical composition in area D of layer 3 was also similar to that in unexposed N-A-S-H. Therefore, the layer 3 is the almost unaffected area in the AAP sample after 12 weeks immersion in sulphuric acid.

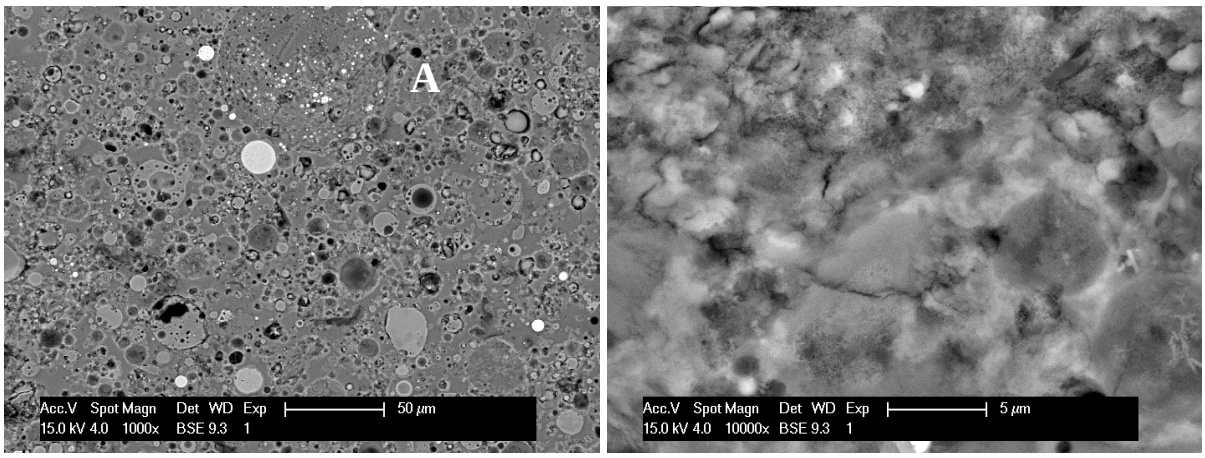

(a) AA paste before immersion (X1000) (b) amorphous N-A-S-H (x10000)

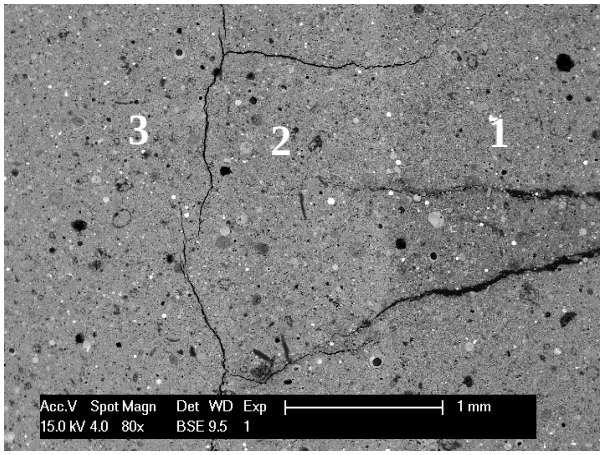

(c) CC paste after immersion (X80)

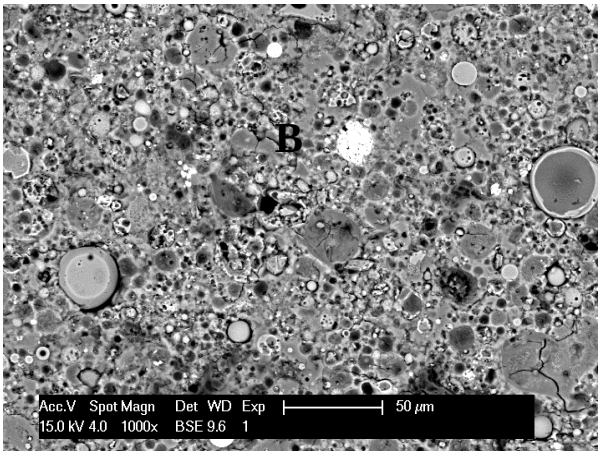

(d) layer 1 (x1000)

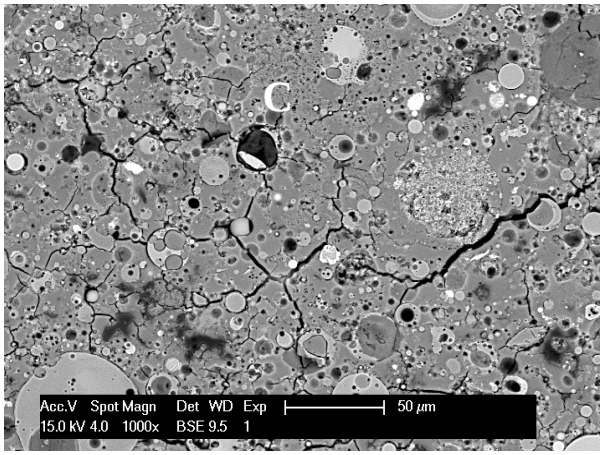

(e) layer 2 (X1000)

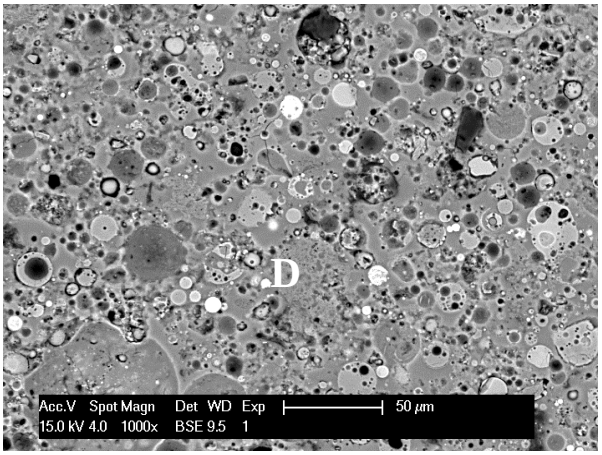

(f) layer 3 (x1000)

Figure 8. Comparison of AAP samples before and after immersion

Table 4. Surface element analysis of AAP samples in selected areas

	Area A		Area B		Area C		Area D	
Element	Wt.%	At.%	Wt.%	At.%	Wt.%	At.%	Wt.%	At.%
Oxygen	49.3	63.1	47.1	60.7	47.2	61.6	44.0	58.0
Sodium	5.4	4.8	2.1	1.9	1.3	1.2	5.3	4.8
Magnesium	1.0	0.8	-	-	-	-	2.2	1.9
Aluminium	11.7	8.9	10.4	8.0	13.6	10.5	14.1	11.0
Silicon	26.7	19.5	37.7	27.7	32.1	23.9	28.6	21.4
Sulfur	-	-	2.7	1.7	1.5	1.0	-	-
Potassium	1.0	0.5	-	-	-	-	1.3	0.7
Calcium	4.8	2.45	-	-	1.6	0.8	2.9	1.5
Iron	-	-	-	-	2.7	1.0	0.6	0.6

The Al to Si atomic ratio is measured every 3 millimetres to a depth of 30 mm in the radial direction. It can be seen in Figure 9 that the Al to Si ratio increases gradually to a depth of 21 mm, before a sharp rise and subsequently stabilising.

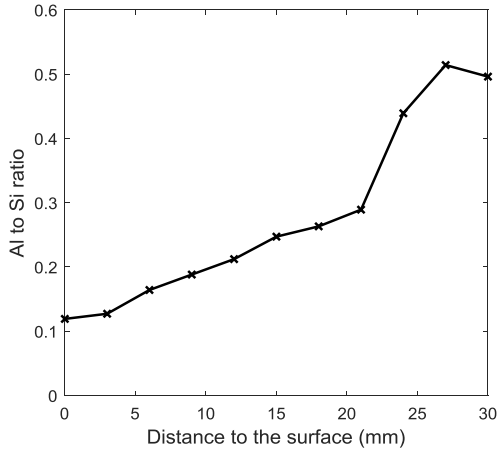

Figure 9. The Al to Si atomic ratio of AAP sample after 12 weeks immersion in sulphuric acid

3.6 Fourier transform infrared spectroscopy

Figure 10(a) presents the FTIR spectra of CCP before and after 12 weeks of immersion in sulphuric acid. Table 5 summarises the FTIR data for the CCP before and after immersion and lists the band assignments derived in this study. The O-H asymmetric stretching vibration (band 1) in Table 5 was due to the presence of Portlandite as reported by XRD analysis, which disappears after sulphuric acid attack. Bands 2-3 in Table 5 indicates the presence of water molecules, and the double peaks at band 2 (3402 and 3528 cm^{-1}) and 3 (1620 and 1683 cm^{-1}) shown in the spectrum of CCP after immersion are associated with the formation of gypsum [5, 12, 36]. The C-O vibration (band 4 and 8) in Table 5 was due to the presence of calcite reported by XRD analysis, which also vanishes after sulphuric acid attack. A few bands (bands 5, 6, 10 and 11) due to the presence of SO_4^{2-} group was observed in CCP after immersion are associated with the formation of gypsum as reported by XRD analysis.

The main band in the region between 800 and 1300 cm^{-1} are broadened and asymmetric, implying the overlap of more bands. The deconvolution of the spectra was performed with Gaussian peak shapes and the regression coefficient (r^2) over 0.99. The deconvolution procedure was in accordance with procedures described in the previous studies [25, 37, 38]. Figure 10(b) presents the deconvolution of the "main band" in CCP before immersion. The

three broad bands at 861, 967, and 1098 cm^{-1} are associated with Si-O symmetric stretching vibrations in Q^1 (silicon bonded through oxygen to one other silicon [39]) unit, Si-O asymmetric stretching vibrations in Q^2 (middle group of chains [39]) units, and Si-O asymmetric stretching vibrations in Q^3 (branching group that consists of sheets [39]) units, respectively[25, 40]. The sharp band at 872 cm^{-1} are associated with C-O bending vibration due to the presence of calcite.

Figure 10(c) presents the deconvolution of the "main band" in CCP after immersion. The bands at 1003, 1115, and 1144 cm^{-1} are associated with the S-O stretching vibrations due to the formation of gypsum [36, 41]. The bands at 963, 1080, and 1164 cm^{-1} are associated with Si-O asymmetric stretching vibrations in Q^2 units, Si-O asymmetric stretching vibrations in Q^3 units, and Si-O asymmetric stretching vibrations in Q^4 (silicon bonded through oxygen to four other silicon, which are three-dimensionally cross-linked groups [39]) units, respectively. Examining the results in EDX analysis and FTIR spectra deconvolution, it indicates that these C–S–H gels were partially dissolved after sulphuric acid attack, where the calcium in the C-S-H gels leached out and formed gypsum with the sulphate ion in the acid, leading to a high silica to calcium ratio in C-S-H gels or amorphous silica gels in the structure.

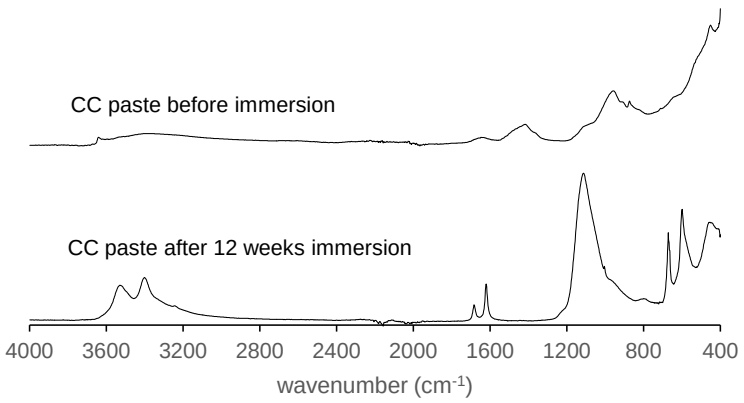

(a)

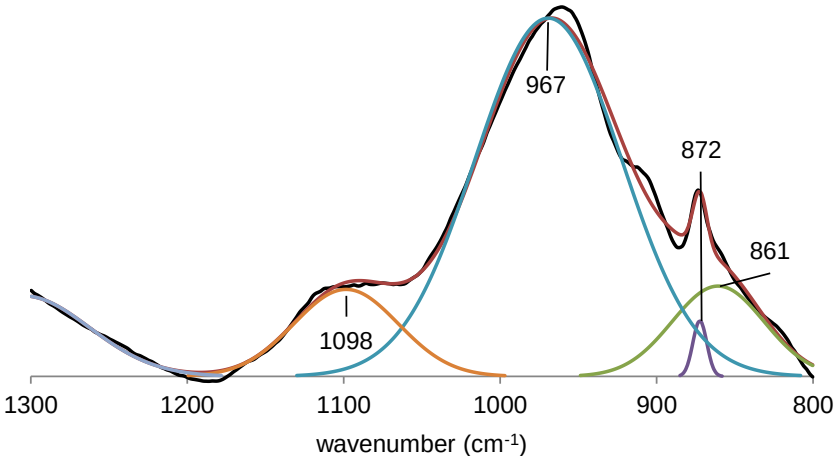

(b)

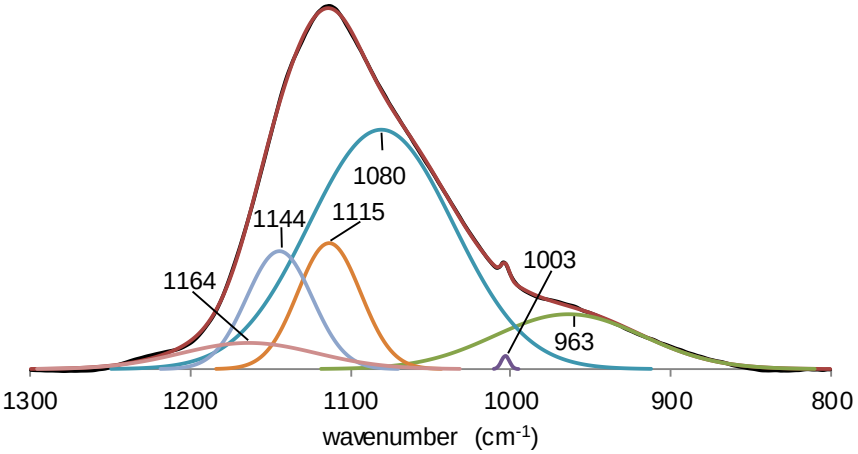

(c)

Figure 10. FTIR spectra of CCP samples before and after immersion: (a) FTIR spectra from 400 to 4000 cm^{-1}; (b) Deconvolution of the "main band" of CCP before immersion (r^2=0.995); (c) Deconvolution of the "main band" of CCP after immersion (r^2=0.999)

Table 5. Assignment of FTIR bands of AAP samples before and after immersion

Band	CCP Before immersion (cm^{-1})[a]	CCP After immersion (cm^{-1})	Assignment[b]	References
1	3641s	-	ν_3 O-H ($Ca(OH)_2$)	[5, 36, 41]
2	3390s	3402s and 3528s	ν_3 O-H (H_2O)	[5, 14, 36, 41]
3	1647s	1620s and 1683s	ν_2 O-H (H_2O)	[5, 14, 36, 41]
4	1417s	-	ν_3 C-O (CO_3^{2-})	[5, 14, 36, 41]
5	-	1113s	ν_3 S-O (SO_4^{2-})	[36, 41]
6	-	1003w	ν_1 S-O (SO_4^{2-})	[36, 41]
7	958s	-	ν_3 Si-O (C-S-H)	[25]
8	873s	-	ν_2 C-O (CO_3^{2-})	[25, 41]
9	-	800m	ν_1 Si-O	[25]

10	-	671s	ν_4 S-O (SO_4^{2-})	[36, 41]
11	-	599s	ν_4 S-O (SO_4^{2-})	[36, 41]
12	451s	459s	ν_2 Si-O (Internal SiO_4 tetrahedral)	[25]

a: s: strong; m: medium; w: weak.

b: ν_1: symmetric stretching; ν_2: in plane bending; ν_3: asymmetric stretching; ν_4: out of plane bending

Figure 11(a) presents the FTIR spectra of AAP before and after 12 weeks of immersion in sulphuric acid. Table 6 summarised the FTIR data for the AAP before and after immersion and listed the band assignments derived in this study. Bands 1-2 in Table 6 indicates the weakly bonded water molecules adsorbed on the surface or trapped in the pore space [27]. The C-O asymmetric stretching vibration (band 3) in Table 6 was due to the presence of carbonate which is formed in the reactions involving atmospheric CO_2, disappearing after sulphuric acid attack. The main band appearing at 991 cm^{-1} shifted to 1074 cm^{-1}, which can be attributed to the fact that the T-O (T is a Si or Al atom) stretching modes are sensitive to Si to Al ratio in N-A-S-H framework composition and shift to a higher frequency with decreasing Al content identified in EDX analysis [26]. The intensity of the T-O band decreased slightly, indicating that the length of aluminosilicate chains decreased. In addition to the main band, the T-O symmetric stretching vibration appearing at 668 cm^{-1} shifted to 736 cm^{-1}, and the double ring vibration appearing at 546 cm^{-1} shifted to 574 cm^{-1} under the sulphuric acid attack. However, the Si-O symmetric stretching vibration (band 6) due to the presence of quartz in unreacted fly ash and the Si-O bending vibration appearing at 432 cm^{-1} had no change under the sulphuric acid attack. García-Lodeiro et al. [25] suggested the intensity of Si-O bending mode does not depend on the degree of crystallization. The Si-O bending mode is therefore not sensitive to aluminium substitution. This observation is also in agreement with the previous studies [12, 15, 25, 27].

The main band assigned to T-O asymmetric stretching vibration in the region between 800 and 1300 cm^{-1} are broadened and asymmetric, implying the overlap of more bands. Figure 11(b) and (c) presents the deconvolution of the "main band" assigned to T-O asymmetric stretching mode in AAP before and after immersion, respectively. It can be seen that, under the sulphuric acid attack, the band at 877 cm^{-1} due to the T-OH asymmetric stretching vibration shifted to 939 cm^{-1} and became stronger, the band at 995 cm^{-1} due to the T-O asymmetric stretching vibration of internal TO_4 tetrahedral shifted to 1064 cm^{-1}, and the band at 1119 cm^{-1} due to the T-O asymmetric stretching vibration of external linkage related to framework topology shifted to 1144 cm^{-1} [42]. A similar observation has also been made in previous studies [25-27]. As

discussed above, all these T-O stretching modes are sensitive to Si to Al ratio and shift to a higher frequency with decreasing Al content.

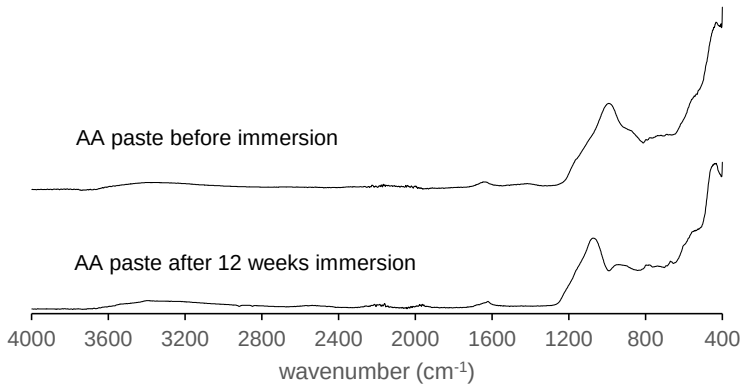

(a)

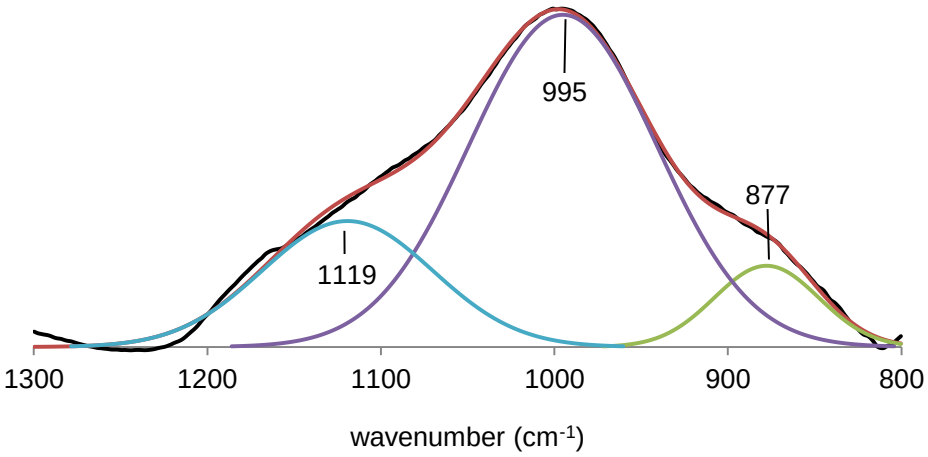

(b)

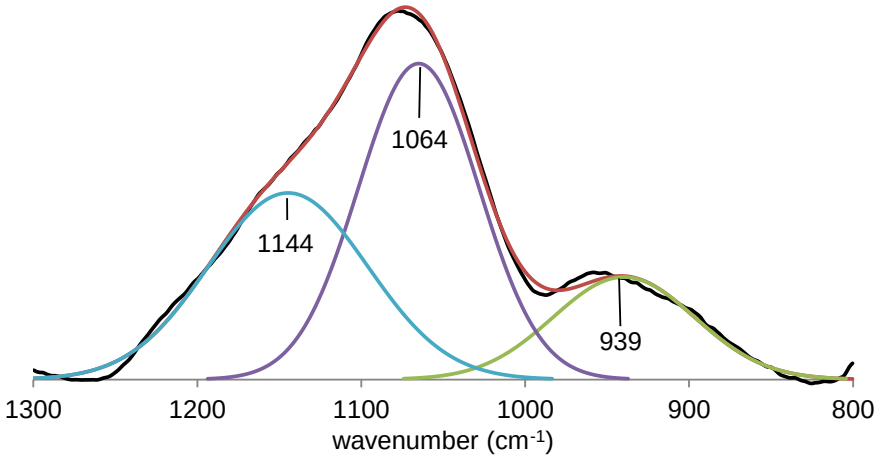

(c)

Figure 11. FTIR spectra of AAP samples before and after immersion: (a) FTIR spectra from 400 to 4000 cm^{-1}; (b) Deconvolution of the "main band" of AAP before immersion (r^2=0.997); (c) Deconvolution of the "main band" of AAP after immersion (r^2=0.998)

Table 6. Assignment of FTIR bands of AAP samples before and after immersion

Band	AAP Before immersion (cm^{-1})[a]	AAP After immersion (cm^{-1})	Assignment[b]	References
1	3359s	3397s	ν_3 O-H (H_2O)	[5, 12, 14, 27, 38]
2	1647s	1622s	ν_2 O-H (H_2O)	[5, 12, 14, 25, 27, 38]
3	1415s	-	ν_3 C-O (CO_3^{2-})	[14, 25, 43]
4	991s	1074s	ν_3 T-O (Internal TO_4 tetrahedral)	[5, 12, 14, 25-27, 37, 38]
5	876sh	939s	ν_3 T-O (Si-OH and Al-OH)	[27, 37]
6	796w	796m	ν_1 Si-O (unreacted quartz)	[5, 36, 37]
7	688w	736m	ν_1 T-O (Internal TO_4 tetrahedral)	[26, 27, 37]
8	546w	574sh	Double rings	[25-27]
9	432s	432s	ν_2 Si-O (Internal SiO_4 tetrahedral)	[25-27]

a: s: strong; m: medium; w: weak; sh: shoulder

b: ν_1: symmetric stretching; ν_2: in plane bending; ν_3: asymmetric stretching

3.7 Porosity change measured by micro-CT

Figure 12 shows the typical re-constructed cross-section image in the middle height of CCP and AAP samples after immersion analysed by micro-CT. As the cross-section image was around 5 mm away from the cutting surface, it can be seen from Figure 12 that the cracks in both CCP and AAP sample was due to the degradation rather than the surface damage caused by cutting process. It should be noted that only pores with the diameter greater than 9.5 μm were measurable leading to lower porosity results compared to those measured by mercury intrusion porosimetry (MIP) tests [5].

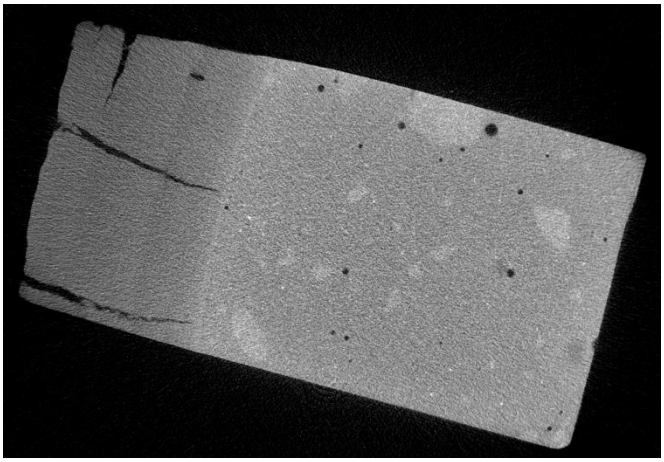

(a) CC paste sample

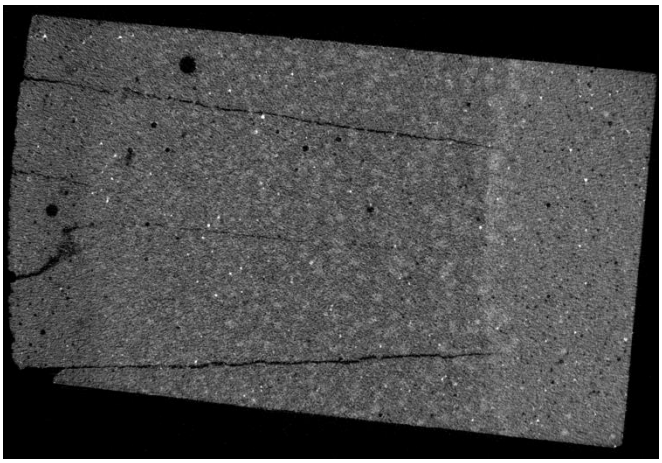

(b) AA paste sample

Figure 12. Typical micro-CT re-constructed image of CCP and AAP samples before and after immersion

Table 7 presents the porosity change of CCP and AAP samples before and after 6 and 12 weeks immersion. The porosity shown in Table 7 was analysed by taking the average porosity values of nine 0.2 mm cubes in both non-degraded and degraded area. It can be seen that the porosity in the non-degraded area of samples before and after 6 and 12 weeks immersion stabilized in a range of 1.82% - 2.03 % for CCP sample and 2.52% - 2.94% for AAP sample and therefore porosity changes only occurred in the colour changed area.

The porosity in degraded area of CCP samples after 6 and 12 weeks immersion stabilized in a range of 11.5% - 12.27%, whereas that of AAP samples continued to increase with immersion time.

Table 7. Porosity of CC and AA paste measured by micro-CT

Immersion time	CC paste		AA paste	
	Non-degraded area	Degraded area	Non-degraded area	Degraded area
Before immersion	1.92%	-	2.52%	-
Six weeks	1.82%	12.27%	2.53%	9.47%
Twelve weeks	2.03%	11.5%	2.94%	18.86%

4. Macroscopic measurements

4.1 CC and AA paste

Figure 13 shows the visual appearance of CCP and AAP specimens after 12 weeks of immersion in 5% sulphuric acid. In Figure 13(a) it can be seen that the CCP specimen showed severe corrosion in the surface, characterised by significant expansion and large areas in which the degraded cement paste in the surface spalled, leading to a very porous surface structure. However, the cross-section of CCP specimen in Figure 13 (c) showed that beyond the 7-9 mm from the surface of degraded material, the inner part of the CCP specimen was visually unaffected.

The AAP specimen Figure 13(b) showed very little obvious signs of corrosion with small cracks and darker colour in the exposed surface area. However, the cross-section of AAP specimen in Figure 13 (d) showed that the colour change area had a greater depth of ~24 mm and although the colour changed area remained intact, many radial cracks can be observed.

(a)

(b)

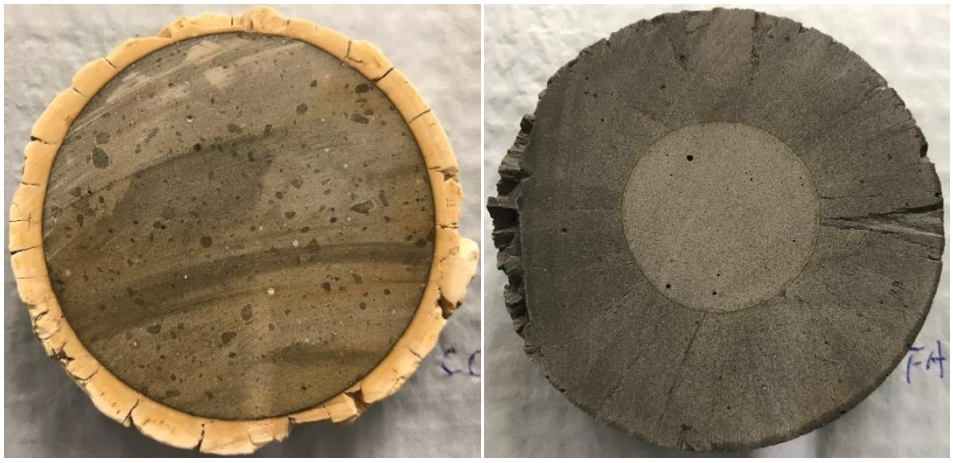

(c) (d)

Figure 13. Specimens after immersion in sulphuric acid: (a) CCP; (b) AAP; (a) Cross-section of CCP; (b) Cross-section of AAP

Figure 14(a) presents the consumption of sulphuric acid per specimen for both CCP and AAP. It can be seen that consumption of sulphuric acid for both CCP and AAP groups increased almost linear during the first 6 weeks immersion, and subsequently increased at a reduced rate.

Figure 14(b) presents the macroscopic degradation depth of specimens for both CCP and AAP. It can be seen that the macroscopic degradation depth for both CCP and AAP groups decelerated with immersion time. Examining the results in Figures 14(a) and (b) together, whilst it can be seen that the amount of sulphuric acid consumed is proportional to the macroscopic degradation depth, the CCP specimens consume more acid per mm of ingress.

Figure 14(c) presents the mass loss of both CCP and AAP specimens relative to the initial weight of the specimen prior to immersion. This large mass loss of CCP specimens was mainly due to the spalling of degraded cement paste from the surface shown in Figure 13(a), but also accompanied by a relatively large amount of precipitate found in the immersion containers. The mass loss of AAP specimens was in comparison relatively small with the specimens remaining intact and only a tiny amount of precipitate present in the immersion containers.

Examining the results in Figures 14(b) and (c) together, it can be seen that the mass loss of CCP specimens (38.5%) was close to the macroscopic degradation area fraction (39.0 %) compared to the total area of initial cross-section. However, the mass loss of AAP specimens

(12.1%) is much smaller than the macroscopic degradation area fraction (87.4 %) as the macroscopic degradation area remained stiffness shown in Figure 13(d).

Figure 14(d) presents the compressive strength of both CCP and AAP specimens after the 12 weeks of immersion with the compressive strength of control specimens, immersed in distilled water for the same immersion period. It can be seen that the residual compressive strength specimens exposed to sulphuric acid were 55.5% (CCP) and 37.4% (AAP) of the control samples.

Examining the results in Figures 14(b) and (d) together, it can be seen that the residual compressive strength fraction of CCP specimens (55.5%) was close to the macroscopic non-degradation area fraction (61%). However, the residual compressive strength fraction of AAP specimens (37.4 %) was much larger than the fraction of macroscopic non-degradation area (12.6 %), demonstrating that the macroscopic degradation depth is not directly related to loss of strength.

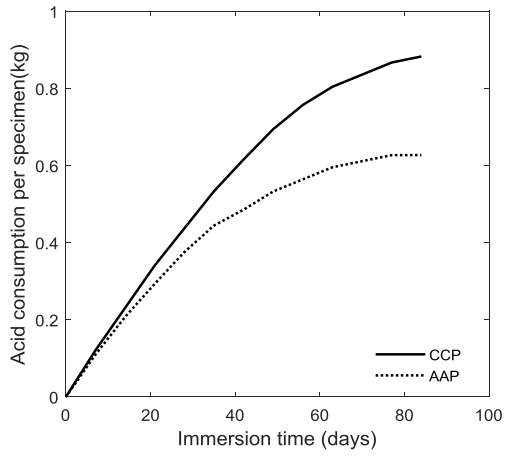

(a)

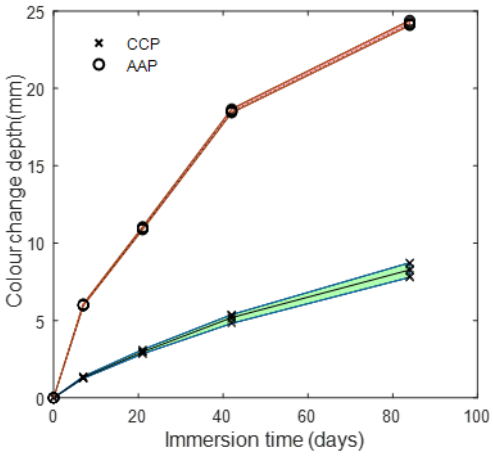

(b)

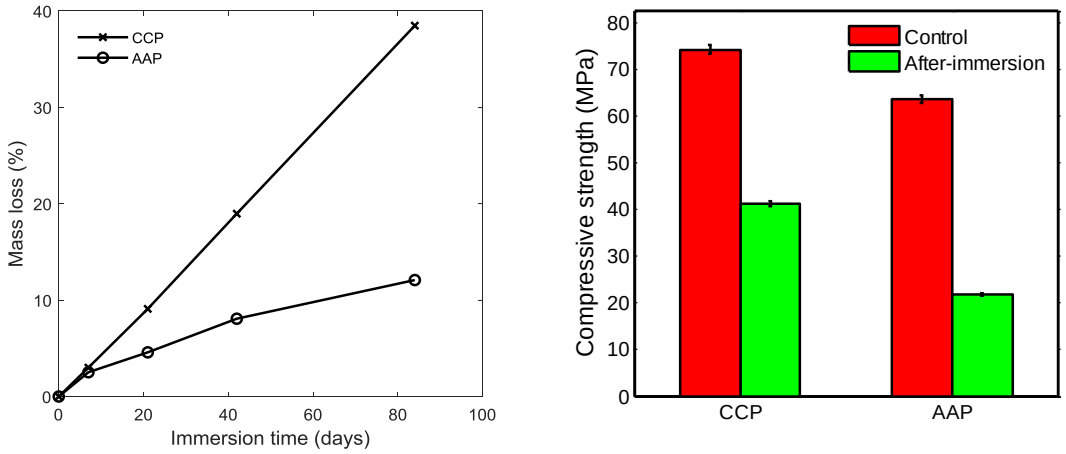

(c) (d)

Figure 14. Physical and mechanical properties change of CCP and AAP specimens under sulphuric acid attack: (a) sulphuric acid consumption; (b) macroscopic degradation depth; (c) mass loss; (d) compressive strength

4.2 CC and AA mortar

Figure 15 shows the visual appearance of CC and AA mortar specimens after 12 weeks immersion in 5% sulphuric acid. In Figures 15(a) and (b) it can be seen that the CC mortar specimens showed severe corrosion, characterised by a significant amount of mortar in the surface spalled, leading to a smaller diameter compared to those before immersion. The CCM_2 mortar sample with sand-to-cement ratio of 3.0 suffered a more severe corrosion and had a smaller diameter when compared to that of CCM_1 mortar with sand-to-cement ratio of 2.25. The cross-section of CC mortar specimen in Figures 15 (e) and (f) show that most of the degraded mortar spalled off, with only a tiny amount of colour changed paste attached on the surface. Larger pores are also evident in the higher sand content specimen.

The AA mortar specimens Figures 15(c) and (d) showed very little corrosion with rougher surface and deeper colour in the exposed surface area when compared those before immersion. However, the cross-section of AA mortar specimens in Figures 15(g) and (h) showed that the macroscopic degradation depth was over 15 mm. The macroscopic degradation depth in AAM_2 mortar sample with sand-to-cement ratio of 3.0 was smaller than that of AAM_1 with sand-to-cement ratio of 2.25.

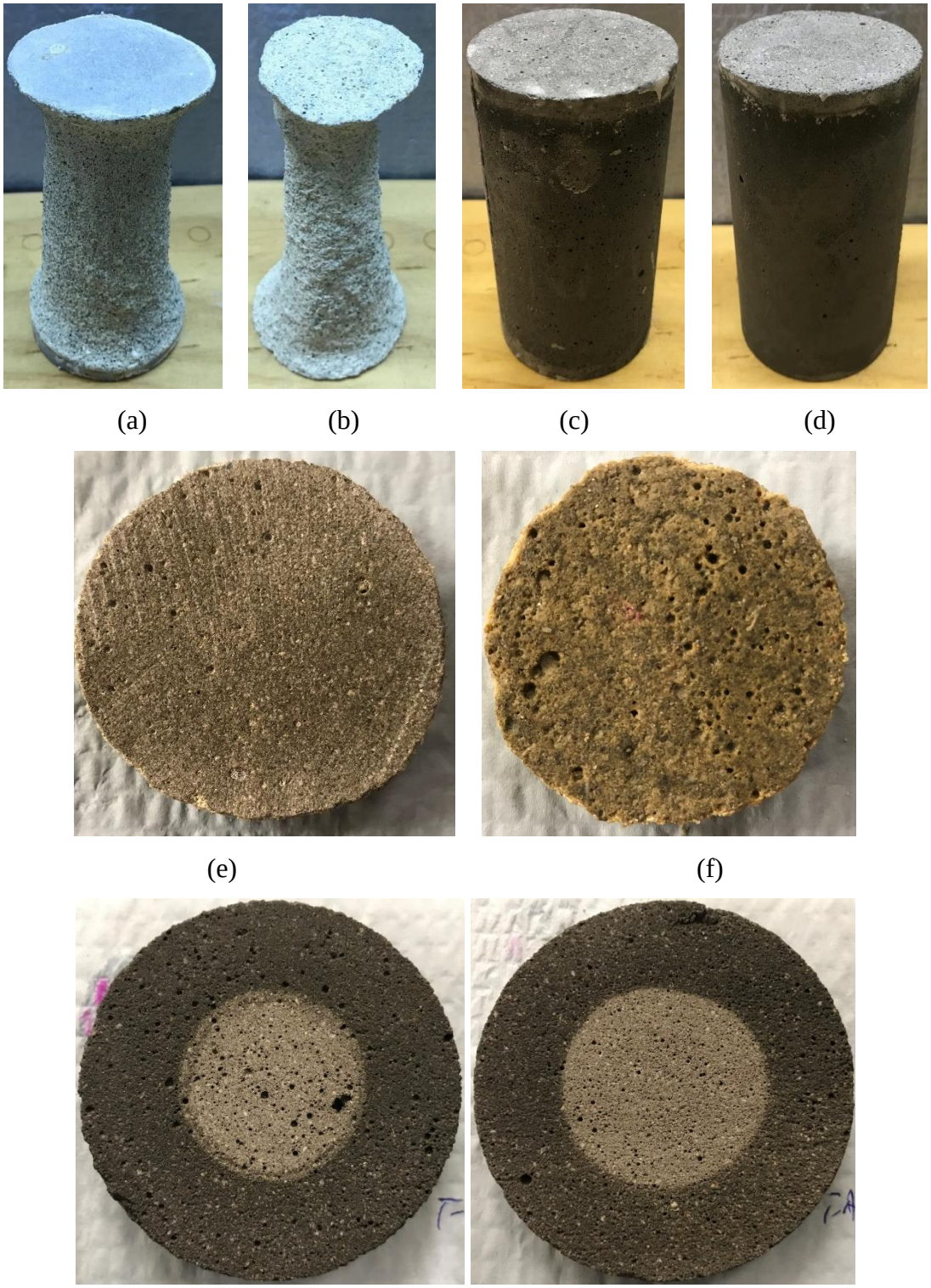

Figure 15. Specimens after immersion in sulphuric acid: (a)CCM_1; (b) CCM_2; (c) AAM_1; (d) AAM_2; (e) Cross-section of CCM_1; (f) Cross-section of CCM_2; (g) Cross-section of AAM_1; (h) Cross-section of AAM_2

Figure 16(a) presents the consumption of sulphuric acid per specimen for both CC and AA mortar groups. It can be seen that consumption of sulphuric acid of CCM_1 and CCM_2 mortars increased rapidly in the first 6 weeks immersion, and subsequently increased at a reduced rate. The consumption of sulphuric acid of AAM_1 and AAM_2 mortars increased rapidly in the first 2 weeks immersion, and subsequently increased at a reduced rate during the immersion period of 2 to 6 weeks, and subsequently stabilized after 6 weeks.

Figure 16(b) presents the macroscopic degradation depth, characterised by either colour change or reduced diameter due to spalling, of specimens for both CC and AA mortar groups. It can be seen that the degraded depth of CCM_1 and CCM_2 mortars increased rapidly in the first 6 weeks immersion, and subsequently increased at a reduced rate with the higher sand-to-cement ratio leading to larger macroscopic degradation depth.

The macroscopic degradation depth of AAM_1 and AAM_2 mortars decelerated with immersion time. The higher sand-to-cement ratio leads to smaller macroscopic degradation depth in AA mortar. Examining the results in Figures 16(a) and (b) together, it can be seen that the depth of degradation is related to the acid consumption but a direct comparison between materials is not possible.

Figure 16(c) presents the mass loss for both CC and AA mortar groups relative to the initial weight of the specimen prior to immersion. It can be seen that the mass loss of CCM_1 and CCM_2 mortars specimens decelerated with immersion time. The mass loss of CC mortar specimens was due to the spalling of the cement mortar as shown in Figures 15(a) and (b). The AA specimens exhibited relatively small mass loss in comparison to CC, with the specimens largely maintaining their original form and only a small amount of debris found in the bottom of the tanks at the end of the experiment. It can be seen on examination of Figures 16(b) and (c) that there is a direct correlation between the macroscopic degradation depth and the mass loss, however the coefficient of proportionality differs vastly between the two material types.

Figure 16(d) presents the compressive strength for both CC and AA mortar groups. The compressive strength of control specimens, immersed in distilled water at the same immersion periods, was 48.3 MPa, 36.2 MPa, 47.5 MPa, and 42.1 MPa for CCM_1, CCM_2, AAM_1, and AAM_2, respectively. It can be seen on examination of Figures 16(b) and (d) that there is

a direct correlation between the macroscopic degradation depth and the compressive strength, however the coefficient of proportionality differs vastly between the two material types.

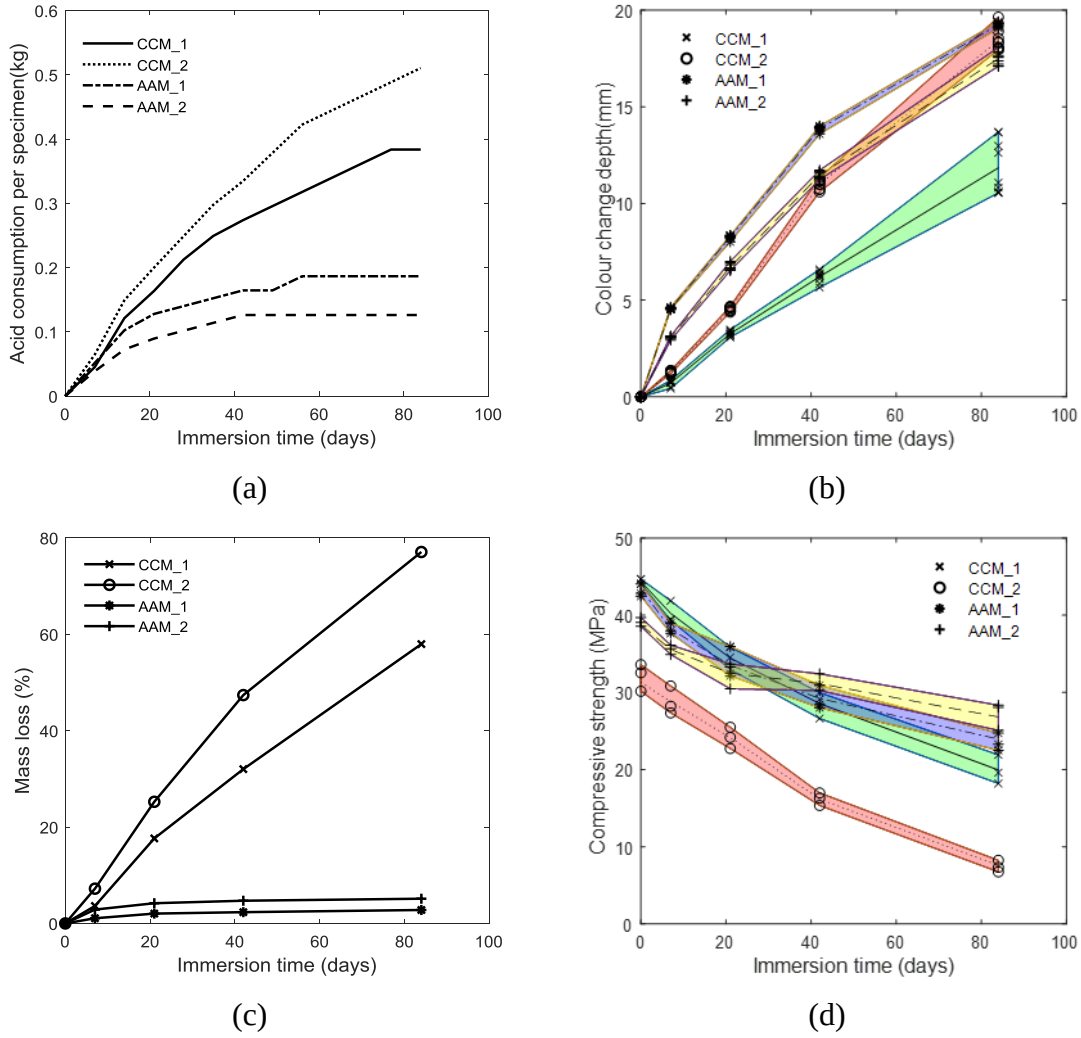

Figure 16. Physical and mechanical properties change of CC and AA mortar specimens under sulphuric acid attack: (a) sulphuric acid consumption; (b) macroscopic degradation depth; (c) mass loss; (d) compressive strength

5. Discussion

No discernible ettringite content was detected in the degraded CCP by XRD or FTIR analysis. The tiny amount of Al detected by EDX and the concentration of Al found in the reservoir (identified by ICP-MS) indicates that most of the ettringite and monosulphate is dissolved into the solution. The main phases identified in CCP, following sulphuric acid attack, were gypsum

and amorphous silica gels as identified via XRD and FTIR analysis. The silica gels were observed forming a barrier to ion transport.

The reduction of Na and Al identified by EDX suggests that the degradation of AAP is predominantly due to Na and Al leaching from the N-A-S-H, with micro-cracks observed from SEM images. It can be seen on examination of Figures 8 and 14 that the dark area of degraded AAP shown in Figure 13(d) retains compressive strength but is weaker than the non-degraded material due to the presence of micro-cracks. The intensity of the T-O band decreases slightly, indicating that the length of aluminosilicate chains is decreased and therefore, the condensation of silicic acid would likely be an infrequent occurrence in the N-A-S-H framework. The increasing Al concentration in the reservoir solution, identified by ICP-MS, would suggest that the Al ejected from the N-A-S-H framework is dissolved as opposed to accumulation on the framework space.

The degradation mechanisms in CCP and AAP are quite distinctive from one another. CCP degradation is characterised by a small penetration depth, but narrow transition zone from degraded to non-degraded material as seen in Figure 7. A similar observation has also been made in a previous study in concrete specimens [44]. In contrast, AAP degradation involves a large depth of ingress, but with a gradual changing of properties with depth as seen in Figure 9. The degraded material at the edge of CCP specimens is weak and easily dislodged, whereas the AAP material retains good form, as shown in Figure 17 and partial strength. The phenolphthalein also demonstrates that the reduction in pH in CCP correlates well with the phase change of the material, in AAP the phenolphthalein radius is smaller than the degradation depth indicating a more diffuse degradation front.

(a) CCP (b) AAP

Figure 17. Cross-sections of the samples sprayed with 1% phenolphthalein solution

The dark area of the samples shown in Figure 12 was due to higher porosity and matches the colour change shown in Figures 13(c) and (d). Therefore, the macroscopic degradation depth can be a good indicator to measure the porosity change area for both CCP and AAP samples.

Upon transitioning from paste to mortar manufacturing scales the change in degradation mechanism is evident on visual inspection, with the CCM specimens all subject to spalling of material from the surface as seen in Figure 15. At both scales of manufacture the AA materials retained good form and degradation was only ostensible from the colour change observed across sections.

Considering the pastes to be the limiting case of mortars, with a sand-to-binder ratio of zero, Figure 18 shows the macroscopic properties of the materials measured after 84 days of immersion. The residual mass is calculated as the ratio of the mass after immersion to the initial mass. The residual compressive strength is calculated as the ratio of the strength measured after immersion to the strength measured from a control specimen immersed in distilled water for the same length of time.

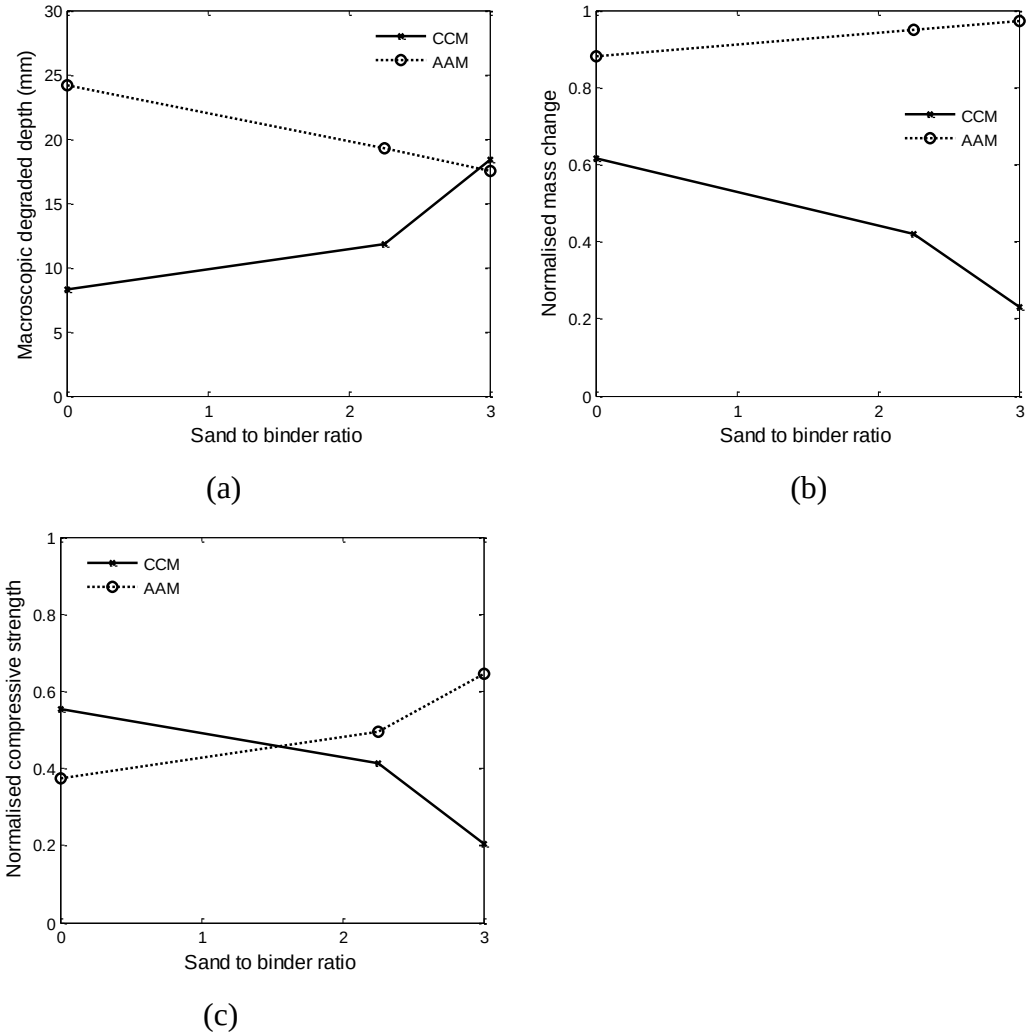

Figure 18. Macroscopic properties of the materials measured after 84 days of immersion: (a) macroscopic degraded depth; (b) residual mass percentage; (c) normalized residual compressive strength

Figure 18, shows the distinct differences in the degradation mechanism between AA and CC materials how increasing sand content influences the behaviour. The effects caused by the fine aggregate lead to the porosity change of mortar with the increase of sand-to-binder ratio [45, 46]. The porosity of CC mortar increases significantly when the sand-to-cement ratio increased [45], whereas the porosity of AA mortar decreases when the sand-to-binder ratio increased [46]. The effect of the reduction of porosity with sand-to-binder ratio in AA materials in manifest in the degradation depths seen in Figure 18(a), which is in contrast to the increasing depths seen in CC. It is clear that the porosity of the CC and AA mortar before immersion has significant effect on the development of degradation depth under sulphuric acid attack. However, Aiken et al. [5] observed CC mortar with lower initial porosity had more severe degradation than that

with higher initial porosity. Therefore, the performance (porosity, permeability, diffusivity) in the front of acid attack of cementitious materials could also be another significant parameter when investigating the macroscopic degradation of cementitious materials, which requires further studies. The loss of material via spalling from the samples observed with increasing sand-to-binder ratio with CC materials contrasts with AA where the degraded material remains in good form and mass loss is actually reduced seen in Figure 18(b). The loss of compressive strength of samples observed with increasing sand-to-binder ratio with CC materials contrasts with AA where the degraded material retains partial compressive strength seen in Figure 18(c).

A thorough appreciation of the interplay between chemical degradation effects observed at the paste scale of manufacture and ion transport which is heavily influenced by. The durability of a given material is therefore heavily influenced by the scale of manufacture (paste, mortar, concrete) and further complicated by mix design whereby a range of proportion of constituent materials may result in identical strengths but with vastly differing porosities.

The compressive strength of both CCP and AAP under 5% sulphuric acid attack was also done by Bakharev [27]. However, as the smaller diameter of specimens (25 mm in diameter and 50 mm in height) and no protection at both ends of the cylinder during the sample preparation, the results done by Bakharev [27] showed that the CCP specimens lost more compressive strength than that of AAP ones, contrasting with the results observed in Figure 14(d). The compressive strength of CC paste sample under sulphuric acid attack reduces more significantly when using smaller size specimens (i.e. 25mm) compared to that using larger size specimens (i.e. 75mm). Considering the direct correlation between the macroscopic degradation depth and the compressive strength, the macroscopic indicators of susceptibility to corrosion (change of mass, compressive strength, and cross-section) of a given material are therefore heavily influenced by the size of manufacture.

6. Conclusions

- The main phases identified in conventional cement paste, following sulphuric acid attack, are gypsum and amorphous silica gels rather than ettringite.
- Conventional cement paste degradation is characterised by a small penetration depth, but narrow transition zone from degraded to non-degraded material. The degraded

material at the edge of conventional cement paste specimens is weak and easily dislodged.

- The aluminium ejected from the N-A-S-H framework in alkali-activated paste is dissolved as opposed to accumulation on the framework space, and the condensation of silicic acid would likely be an infrequent occurrence in the N-A-S-H framework under 5% sulphuric acid attack.
- Alkali-activated paste degradation involves a large depth of ingress, but with a gradual changing of properties with depth. The alkali-activated material retains good form and partial strength.
- The durability of a cementitious material is heavily influenced by the scale of manufacture (paste, mortar, and concrete) and further complicated by mix design whereby a range of proportion of constituent materials may result in identical strengths but with vastly differing porosities.
- The macroscopic indicators of susceptibility to corrosion (change of mass, compressive strength, and cross-section) of a given material are heavily influenced by the size of manufacture.

References

1. L. Gu, P. Visintin, T. Bennett, Evaluation of accelerated degradation test methods for cementitious composites subject to sulfuric acid attack; application to conventional and alkali-activated concretes, Cem. Concr. Compos. 87 (2018) 187-204.

2. C. Grengg, F. Mittermayr, N. Ukrainczyk, G. Koraimann, S. Kienesberger, M. Dietzel, Advances in concrete materials for sewer systems affected by microbial induced concrete corrosion: A review, Water res. 134 (2018) 341-352.

3. J. Monteny, E. Vincke, A. Beeldens, N. De Belie, L. Taerwe, D. Van Gemert, W. Verstraete, Chemical, microbiological, and in situ test methods for biogenic sulfuric acid corrosion of concrete, Cem. Concr. Res. 30(4) (2000) 623-634.

4. J. Herisson, E. D. van Hullebusch, M. Moletta-Denat, P. Taquet, T. Chaussadent, Toward an accelerated biodeterioration test to understand the behavior of Portland and calcium aluminate cementitious materials in sewer networks, Int. Biodeterior. Biodegrad. 84 (2013) 236-243.

5. T. A. Aiken, J. Kwasny, W. Sha, M. N. Soutsos, Effect of slag content and activator dosage on the resistance of fly ash geopolymer binders to sulfuric acid attack, Cem. Concr. Res. 2018.

6. A. Allahverdi, F. Škvára, Sulfuric acid attack on hardened paste of geopolymer cements. Part 1. Mechanism of corrosion at relatively high concentrations, Ceram. Silik. 49 (4) (2005) 225–229.

7. J. Monteny, N. De Belie, L. Taerwe, Resistance of different types of concrete mixtures to sulfuric acid, Mater. Struct. 36 (258) (2003) 242–249.

8. N. De Belie, J. Monteny, A. Beeldens, E. Vincke, D. Van Gemert, W. Verstraete, Experimental research and prediction of the effect of chemical and biogenic sulfuric acid on different types of commercially produced concrete sewer pipes, Cem. Concr. Res. 34(12) (2004) 2223-2236.

9. N. De Belie, J. Monteny, L. Taerwe, Apparatus for accelerated degradation testing of concrete specimens, Mater. Struct. 35(7) (2002) 427-433.

10. M. Alexander, A. Bertron, N. De Belie, Performance of cement-based materials in aggressive aqueous environments (Vol. 10), Springer, Dordrecht, 2013

11. J. L. Provis, J. S. J. Van Deventer, Geopolymers: structures, processing, properties and industrial applications, Woodhead, Cambridge, 2009.

12. N.K. Lee, H.K. Lee, Influence of the slag content on the chloride and sulfuric acid resistances of alkali-activated fly ash/slag paste, Cem. Concr. Compos. 72 (2016) 168–179.

13. P. Chindaprasirt, U. Rattanasak, Improvement of durability of cement pipe with high calcium fly ash geopolymer covering, Constr. Build. Mater. 112 (2016) 956-961.

14. M. A. M. Ariffin, M. A. R. Bhutta, M. W. Hussin, M. M. Tahir, N. Aziah, Sulfuric acid resistance of blended ash geopolymer concrete, Constr. Build. Mater. 43 (2013) 80-86.

15. A.M. Izzat, A.M.M. Al Bakri, H. Kamarudin, L.M. Moga, G.C.M. Ruzaidi, M.T.M. Faheem, A.V. Sandu, Microstructural analysis of geopolymer and ordinary Portland cement mortar exposed to sulfuric acid, Mater. Plast. 50 (3) (2013) 171-174.

16. V. Sata, A. Sathonsaowaphak, P. Chindaprasirt, Resistance of lignite bottom ash geopolymer mortar to sulfate and sulfuric acid attack, Cem. Concr. Compos. 34(5) (2012) 700-708.

17. R.R. Lloyd, J.L. Provis, J.S.J. van Deventer, Acid resistance of inorganic polymer binders. 1. Corrosion rate, Mater. Struct. 45 (2012) 1–14.

18. S. Thokchom, P. Ghosh, S. Ghosh, Resistance of fly ash based geopolymer mortars in sulfuric acid, ARPN J. Eng. Appl. Sci. 4(1) (2009) 65-70.

19. A. Gabrisova, J. Havlica, S. Sahu, Stability of calcium sulphoaluminates in water solutions with various pH values, Cem. Concr. Res. 21 (6) (1991) 1023–1027.

20. H. Yuan, P. Dangla, P. Chatellier, T. Chaussadent, Degradation modeling of concrete submitted to sulfuric acid attack, Cem. Concr. Res. 53 (1) (2013) 267–277.
21. V. Pavlík, Corrosion of hardened cement paste by acetic and nitric acids: Part I. Calculation of corrosion depth, Cem. Concr. Res. 24 (1994) 551- 562.
22. V. Pavlík, Corrosion of hardened cement paste by acetic and nitric acids part II: formation and chemical composition of the corrosion products layer, Cem. Concr. Res. 24 (8) (1994) 1495–1508.
23. C. Li, H. Sun, L. Li, A review: The comparison between alkali-activated slag (Si+Ca) and metakaolin (Si+Al) cements, Cem. Concr. Res. 40 (2010) 1341–1349.
24. J.L. Provis, A. Palomo, C. Shi, Advances in understanding alkali-activated materials, Cem. Concr. Res. 78 (2015) 110–125.
25. I. García-Lodeiro, A. Fernández-Jiménez, M.T. Blanco, A. Palomo, FTIR study of the sol–gel synthesis of cementitious gels: C–S–H and N–A–S–H, J. Sol-Gel. Sci. Technol. 45 (1) (2008) 63–72.
26. A. Allahverdi, F. Škvára, Nitric acid attack on hardened paste of geopolymeric cements part 2, Ceram. Silik. 45 (4) (2001) 143–149.
27. T. Bakharev, Resistance of geopolymer materials to acid attack, Cem. Concr. Res. 35 (2005) 658–670.
28. A. Allahverdi, F. Škvára, Nitric acid attack on hardened paste of geopolymeric cements part 1, Ceram. Silik. 45 (3) (2001) 81–88.
29. Australian Standard AS 1012, Methods of Testing Concrete, Standards Australia, Sydney (2014)
30. ASTM, C. 1012: Standard Test Method for Length Change of Hydraulic-Cement Mortars Exposed to a Sulfate Solution, ASTM International, West Conshohocken, USA, 2018.
31. G.B. Alexander, W. Heston, R. Iler, The solubility of amorphous silica in water. J. Phys. Chem. 58 (1954) 453–455.
32. R.K. Iler, The Colloid Chemistry of Silica and Silicates, Cornell University Press, Ithaca, New York, 1955.
33. American Chemical Society, Reagent chemicals: specifications and procedures: American Chemical Society specifications, official from January 1, 2006, Oxford University Press, Washington, D.C, 2006.
34. H. F. W. Taylor, Cement chemistry, second ed., Thomas Telford, London, 1997.
35. R.R. Lloyd, J.L. Provis, J.S.J. van Deventer, Microscopy and microanalysis of inorganic polymer cements. 1: Remnant fly ash particles, J. Mater. Sci. 44(2) (2009) 608-619.

36. N.V. Chukanov, Infrared Spectra of Mineral Species: extended library, Springer, Chernogolovka, 2013.
37. W.K.W. Lee, J.S.J. van Deventer, The use of infrared spectroscopy to study geopolymerization of heterogeneous amorphous aluminosilicates, Langmuir 19 (21) (2003) 8726–8734.
38. P. Rovnanik, Effect of curing temperature on the development of hard structure of metakaolin-based geopolymer, Constr. Build. Mater. 24(7) (2010) 1176-1183.
39. K. Kupwade-Patil, S.D. Palkovic, A. Bumajdad, C. Soriano, O. Büyük€oztürk, Use of silica fume and natural volcanic ash as a replacement to Portland cement: micro and pore structural investigation using NMR, XRD, FTIR and X-ray microtomography. Constr. Build. Mater. 158 (2018) 574-590.
40. I. Garcia-Lodeiro, D.E. Macphee, A. Palomo, A. Fernández-Jiménez, Effect of alkalis on fresh C–S–H gels. FTIR analysis, Cem. Con. Res. 39 (2009) 147–153.
41. S.C.B. Myneni, S.J. Traina, G.A. Waychunas, T.J. Logan, Vibrational spectroscopy of functional group chemistry and arsenate coordination in ettringite, Geochimica et Cosmochimica Acta 62 (1998) 3499–3514.
42. E.M. Flanigan, H. Khatami, H.A. Szymanski, Molecular sieve zeolites, in: Advances in Chemistry Series, Vol. 101, American Chemical Society, Washington, DC, 1971.
43. S.A. Bernal, J.L. Provis, R. Mejía de Gutierrez, V. Rose, Evolution of binder structure in sodium silicate-activated slag-metakaolin blends, Cem. Concr. Compos. 33 (1) (2011) 46–54.
44. K. Kawai, S. Yamaji, T. Shinmi, Concrete deterioration caused by sulfuric acid attack, 10th DBMC International Conference On Durability of Building Materials and Component, 2005
45. H. Elaqra, N. Godin, G. Peix, M. R'Mili, G. Fantozzi, Damage evolution analysis in mortar, during compressive loading using acoustic emission and X-ray microtomography: Effects of the sand/cement ratio, Cem. Concr. Res. 37 (2007) 703–713.
46. J. Temuujin, A. van Riessen, K.J.D. MacKenzie, Preparation and characterisation of fly ash based geopolymer mortars, Constr. Build. Mater. 24(10) (2010) 1906-1910.

Chapter 5 – Conclusions and Future Work

Thesis outcomes

In this body of study an assessment of the test methodologies commonly applied in the previous studies for both OPC and AA concretes subjected to sulphuric acid attack has been provided. The assessment has identified the influence of test methodologies on macroscopic degradation rate and microstructural performance. It is shown that wetting and drying cycling and brushing has an influence on macroscopic degradation rate, but not significant. Only the specimens subjected to increased acid concentration undergo significantly accelerated degradation compared to the standard test approach.

Having established that increase acid concentration is the most effective degradation test method, the indicators of susceptibility to corrosion (acid consumption, change of mass, change of length, change in compressive strength, and change of cross-section) have then been assessed. Through the investigation on the long-term behaviour of OPC and AA concretes subjected to 1% sulphuric acid for 18 months in comparison with the test subjected to 3% sulphuric acid for 4 months, the evaluation of the measurements taken reveals that there is no single universal indicator (acid consumption, , change of mass, change of length, and change of cross-section) of resistance to sulphuric acid that could be applied as a simple test technique for the comparison of the degradation performance of different materials.

Through the assessments of the test methodologies and indicators of susceptibility to corrosion, it has been shown that equivalent reductions in compressive strength can be observed within shorter period in higher concentration solution to that of longer period in lower concentration solution, demonstrating that a test procedure to indicate the susceptibility of concretes can be performed within a reasonable time frame for standard testing. It is envisaged that this work will provide the basis for further development of a unified test methodology to indicate the susceptibility of a wide range of cementitious materials to sulphuric acid attack.

This thesis also details the degradation mechanism of OPC based and AA cementitious materials under sulphuric acid attack in terms of chemical reaction and scale of manufacture. Addressing the contradictions identified in previous studies, an improved degradation mechanism of OPC and AA paste has been provided. Importantly, through a quantitative analysis performed at regular intervals from the surface and into the unaffected pastes, how the

degradation proceeds with depth into a specimen has been well established. OPC paste degradation is characterised by a small penetration depth, but narrow transition zone from degraded to non-degraded material. Whereas AA paste degradation involves a large depth of ingress, but with a gradual changing of properties with depth.

Having established the degradation mechanism of OPC and AA paste under sulphuric acid attack in terms of chemical reaction, the influence of scale of manufacture has then been investigated. Through the observation from microscopic to macroscopic measurements, the influence of aggregate type and the interfacial transition zone (ITZ) on the degradation mechanism of mortar and concrete has been well established. The presence of fine aggregate and ITZ between the paste and fine aggregate causes change in porosity of the mortar, affecting the resistance of mortar to sulphuric acid. The chemical composition of coarse aggregate also has a significant influence on the degradation mechanism of concrete.

Having established the degradation mechanism of cementitious materials in paste, mortar and concrete levels, it has been shown that only through the multiscale approach applied in this research in terms of scale of manufacture (paste to mortar to concrete) and in levels of observation from microscopic to macroscopic measurements can the degradation mechanism of a cementitious material be comprehensively understood. It is envisaged that this work will provide the basis for further development of a unified test methodology to understand the degradation mechanism of cementitious materials under sulphuric acid attack in paste, mortar and concrete levels.

Scope for future work

1. In the concrete test, the choice of concrete mix susceptible to corrosion was made in order to ensure that degradation was observed within the duration of PhD program. The behaviour of well-designed concrete mix under sulphuric acid attack should be investigated.
2. Having understand the degradation mechanism of cementitious materials in terms of chemical reaction and scale of manufacture and assessed the behaviour of cementitious materials influenced by different test methodologies, the macroscopic behaviour of cementitious materials influenced by the size of manufacture should be investigated to provide the basis for further development of a unified test methodology.

3. Test methodologies for specific field conditions should be developed via comparing the laboratory test and in-situ test. The biogenic simulation chamber test should be conducted when investigating the field conditions involving biogenic activities.
4. Test methodologies for other aggressive environments should be considered based on the approaches developed in this research.
5. The degradation modelling of cementitious materials subjected to sulphuric acid attack should be developed based on the understanding of the degradation mechanism of cementitious materials in paste, mortar and concrete levels.